BONE TISSUE ENGINEERING APPLICATION WITH THE VASCULOGENESIS INDUCING BIPHASIC SCAFFOLD

by

Nergis Abay Akar

Submitted to Graduate School of Natural and Applied Sciences
in Partial Fulfillment of the Requirements
for the Degree of Doctor of Philosophy in
Biotechnology

Yeditepe University
2018

BONE TISSUE ENGINEERING APPLICATION WITH THE VASCULOGENESIS
INDUCING BIPHASIC SCAFFOLD

APPROVED BY:

Prof. Dr. Gamze Torun Köse ....
(Thesis Supervisor)

Assoc. Prof. Dr. Fatih Kocabaş ....

Assoc. Prof. Dr. Fatma Neşe Kök ....

Assoc. Prof. Dr. Halime Kenar ....

Assist. Prof. Dr. Alev Cumbul ....

DATE OF APPROVAL: ..../..../2018

This thesis is dedicated to my family

and my husband…

ACKNOWLEDGEMENTS

I would like to thank to my thesis advisor Prof. Gamze Torun Köse for giving me support, enthusiasm, guidance and helping me with great patience during all my laboratory work. I would like to offer my thanks to Assoc. Prof. Alev Cumbul for her valuable contributions and experiences to this study. I would also like to express my great gratitude to my friends Görke Gürel Peközer and Ezgi İrem Bektaş for their valuable advices and supports. I also deeply thank to my dear family Esra Abay, Günay Abay, my dear sister Serra Abay, my dear husband Aydın Doğu Akar, my dear uncles Can Akcan, Hasan Akcan and my dear grandfather Zekai Akcan for their intensive support, understanding, encouragement, patience and giving a boost to my morale during all my science life.

ABSTRACT

BONE TISSUE ENGINEERING APPLICATION WITH THE VASCULOGENESIS INDUCING BIPHASIC SCAFFOLD

Bone has a self-healing capacity regenerating itself without leaving a scar. However, critical size defects due to trauma, tumor, disease or infection require bone graft surgeries in which complication rate is high. Bone tissue engineering is thought to be as an alternative for grafting. On the other hand, upon implantation, bone tissue engineering constructs or the grafts generally fail due to insufficient vascularization. Vasculogenesis is important in bone fracture healing which supplies the requirements of the oxygen and nutrient, direct inflammatory signals and cells to the wound site. Vasculogenesis occurs through migration of endothelial cells to the defect site by sensing the signals for inadequate vascularization. One of the strategies to provide vasculogenesis in tissue engineering constructs is to employ environments or angiogenic factors to induce cells to migrate to the defect site. In this strategy a bone tissue engineering scaffold should be designed appropriately by allowing the endothelial cell migration to form vessels. In addition, correct choice of angiogenic factors and their correct combination is also an important step for this strategy. Vascular endothelial growth factor (VEGF) can be used to induce vasculogenesis in tissue engineering constructs. Due to the short half life of those growth factors, sustained release systems or gene therapy methods can be used for the delivery of angiogenic factors. In this study, a fibrous bone tissue engineering scaffold was produced using poly(lactic acid-co-glycolic acid) (PLGA) and rat bone marrow-derived mesenchymal stem cells (rBMSCs) were seeded on it. PLGA and poly(ethylene glycol) (PEG) based hydrogel polymerized around PLGA scaffold, and was used for the sustained release of VEGF activator GS4012. Designed scaffold and sustained release system were tested *in vitro* conditions with endothelial cells isolated from rat peripheral blood (rPBECs) for their migration and microvessel formation ability. After that, the designed system was used to engineer a vascularized bone on critical sized defects on rat crania. This study showed that the usage of VEGF inducer GS4012 facilitated the migration of endothelial cells and led to the occurrance of vasculogenesis that also help the formation of new bone tissue.

ÖZET

DAMARLANMAYI ARTTIRICI ÇİFT FAZLI DOKU İSKELESİ İLE KEMİK DOKU MÜHENDİSLİĞİ UYGULAMASI

Kemik, yara izi bırakmadan kendini tamir etme yeteneğine sahip bir dokudur. Ancak, travma, hastalık veya enfeksiyon sonucu oluşabilecek kritik boyutlu kemik hasarları, komplikasyon riskinin yüksek olduğu greft ameliyatları gerektirmektedir. Kemik doku mühendisliği, kemik greftlerine bir alternatif olarak ortaya çıkar. Öte yandan, hem greftler hem de kemik doku mühendisliği ile oluşturulmuş yapılar implantasyondan sonra genellikle yetersiz damarlanmaya bağlı olarak başarısız olurlar. Damarlanma, dokunun hem besin ve oksijen gereksinimi hem de yara iyileşmesi için enflamatuvar hücre ve faktörlerin bölgeye taşınması açısından kritik önemdedir. Damarlanma, endotel hücrelerin yetersiz damarlanmaya bağlı sinyalleri alarak bölgeye göç etmesiyle gerçekleşir. Doku mühendisliğinde damarlanmayı desteklemek için kullanılan yöntemlerden biri endotel hücrelerin bölgeye göç etmesini sağlayıcı ortam ve faktörler kullanmaktır. Bu yöntemde, endotel hücrelerin göç edebilmesine imkan vererek damar oluşumunu sağlayacak bir doku mühendisliği iskelesi tasarlamak gerekmektedir. Ayrıca endotel hücrelerin göç etmesini sağlayacak faktörlerin seçimi önemli noktalardandır. Vasküler endotel büyüme faktörü (VEGF) damarlanmayı desteklemek için kullanılmaktadır. Büyüme faktörlerinin kısa yarı ömürleri, kullanımlarını sınırlamaktadır. Bu sebeple, bu faktörlerin verilmesinde sürekli salım ya da gen terapisi yöntemleri kullanılabilir. Bu çalışmada, üzerine sıçan kemik iliği mezenkimal kök hücrelerinin (rBMSC) ekildiği fibröz yapılı bir poli(laktik asit-ko-glikolik asit) (PLGA) doku iskelesi üretilmiş ve etrafı bir VEGF aktivatörü olan GS4012'nin sürekli salımını sağlayan PLGA ve poli(etilen glikol) (PEG) tabanlı bir hidrojel ile kaplanmıştır. Tasarlanan sistem, önce *in vitro* ortamda sıçan kanından izole edilmiş peripheral kan endotel hücrelerinin (rPBECs) göç etmesi ve damar oluşturma kapasiteleri açısından test edilmiş, daha sonra ise kranial bölgede kritik boyutlu kemik hasarları açılmış sıçanlarda damarlanmış bir kemik dokusu oluşturulması denenmiştir. Bu çalışma, VEGF indükleyicisi GS4012'nin kullanımının, endotel hücrelerin göçünü kolaylaştırdığını ve yeni kemik dokusu oluşumuna da yardım eden damarlanmanın ortaya çıkmasına yol açtığını göstermiştir.

TABLE OF CONTENTS

LIST OF FIGURES

LIST OF TABLES

LIST OF SYMBOLS/ABBREVITIONS

ALP	Alkaline phosphatase
BM	Bone marrow
BMPs	Bone morphogenetic proteins
BMPR-I	Bone morphogenetic protein receptor-I
Col1	Collagen type 1
DPBS	Dulbecco's Phosphate Buffer Saline
ECM	Extracellular matrix
ELISA	Enzyme-linked immune-sorbent assay
ERK	Extracellular signal-regulated kinase
ET1	Vasoconstrictor endothelin-1
FAK	Focal adhesion kinase
FBS	Fetal Bovine serum
FDA	Food and Drug Administration
FGF	Fibroblast growth factor
GFs	Growth factors
GS4012	VEGF Inducer
GTP	Guanosine triphosphate
HIF	Hypoxia-inducible factors
HUVEC	Human umbilical vein endothelial cell
IGF-I	Insulin like growth factor I
IL-1	Interleukin-1
LDL	Low density lipoprotein
µl	Microliters
mM	Milimolar
MAPK	Mitogen activated protein kinase cascade
MEM α	Minimum Essential Medium α
MSC	Mesenchymal stem cell
MMP	Matrix metalloproteinase
MTS	(3-(4,5-dimethylthiazol-2-yl)-5-(3-carboxymethoxyphenyl)-2-(4-sulfophenyl)-2H-tetrazolium)

OCN	Osteocalcin
OM	Osteogenic media
PCR	Polymerase chain reaction
PDK-1	Phosphoinositide-dependent kinase-1
PEG	Polyethylene glycol
PGA	Poly-glycolic acid
pH	Negative log of hydrogen ion concentration
PI3K	Phosphoinositide 3-kinase
PIP3	Phosphatidylinositol (3, 4, 5)-trisphosphate
PLA	Poly-lactic acid
PLGA	Copolymer of PLA and PGA
RANK	Receptor activator of nuclear factor kappa-B
RANKL	Receptor activator of nuclear factor kappa-B ligand
rBMSCs	Rat bone mesenchymal stem cells
RIPA	Radio immunoprecipitation assay
rPBECs	Rat peripheral blood endothelial cells
Runx2	Runt-related transcription factor 2
TGF-β	Transforming growth factor-β
VEGF	Vascular endothelial growth factor

1. INTRODUCTION

A scaffold design is very crucial for the cells in tissue engineering. The main building blocks of tissue engineering are scaffolds, cells and biochemical signals. These can result in the repair or formation of tissue. Biomaterials are non-viable materials that intend to interact with biological systems. These are preferable due to their 3D formation that is known as scaffolds to get cell attachment, proliferation, differentiation and growth for the formation of new tissue. They can also stimulate cellular response, possess mechanical strength and dimensional stability. Besides, scaffolds should be biocompatible and have porous interconnected network to get an easy vascularization of newly formed tissue.

As an option for grafting, bone tissue engineering is preferred to be used for the healing of critical size defects due to its ability to supply remarkable vascularization. In this system, endothelial cells can migrate to the defect site to eliminate inadequate vascularization and proliferate to obtain new blood vessels [1, 2, 3]. Angiogenic factors are one of the most important strategies for the induction of cells to migrate through the defect site. Vascular endothelial growth factor (VEGF) is generally preferred for the stimulation of vasculogenesis in tissue engineering constructs. However, use of growth factors can be problematic since they have short half life. Thus, sustained release systems are used to deliver angiogenic factors for the development of vasculogenesis [3].

1.1. BONE PHYSIOLOGY

Bone is described as the specialized configuration of connective tissue that is composed of matrix, mineral and osteogenic cell (Figure 1.1). The matrix that is responsible for the regulation of bone mineralization, and also osteogenic cells consist of osteoblasts and osteocytes, are made of proteoglycans and collagen.

Osteon is known as a fundamental unit of bone. Each osteon is comprised of concentric lamellae of compact bone which encloses a central canal (Haversian canal). Also, the structure which is called interstitial lamellae, is made from osteon remnants.
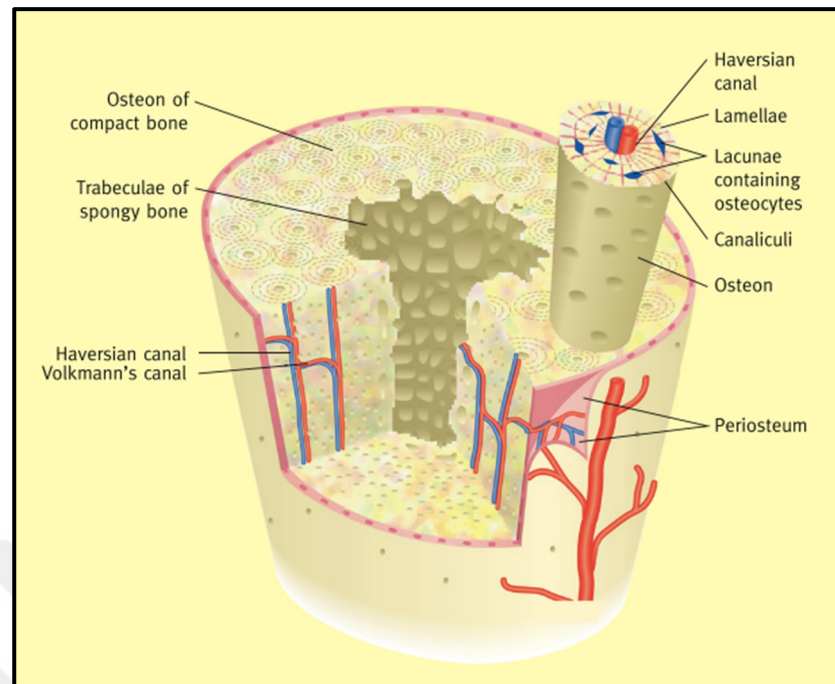
Figure 1.1. Bone structure [2].

In the structure of bone, the hard outer layer is described as cortical bone that is composed of dense and solid configuration. The marrow space is also surrounded by this cortical bone [1, 2]. Mature bone is known as lamellar bone which is formed from both cortical bone and cancellous bone. Parallel arrangement of their collagen structure is formed to get a strong model. A larger surface area of cancellous bone that is seen at the end of long bones, provides some benefits for the metabolic demands. Therefore, activation and remodeling of cancellous bone is at high levels. However, woven bone exhibits a disorganized configuration during healing of fracture and may cause a damage since its structure is not strong enough.

In the structure of lamellar bone, two types of matrices are observed. These are known as organic matrix and mineral matrix. The majority of the organic matrices is composed of the type I collagen that provides bone to be resistant against the tensile forces.

The remaining part of the organic matrix is made from proteoglycans and non collagenous proteins, such as osteonectin, osteocalcin and osteopontin. Also, mineral matrix which mostly includes calcium and phosphate ions as hydroxyapatite crystals, comprises two-thirds of the total bone matrix. The other part of the mineral matrix has magnesium, sodium, potassium, and fluoride. They supply resistancy to the bone under compressive forces [2].

1.2. BONE DEFECTS AND TREATMENTS

Bone defects are generated by disease, injury, and surgical interventions. The process of healing can be induced to make the original state of new tissue. The healing cascade process is composed of inflammation, repair and remodeling states (Figure 1.2). Briefly, in the inflammation step, hematoma formation is obtained due to the movement of fibroblasts and immune cells into the injury site. In the repair step, the combination of collagen fibers and mineralized osteoid is occupied for the formation of callus. After that, formation of woven bone is observed by the ossification of callus structure. As a final step, remodeling of bone begins [3].
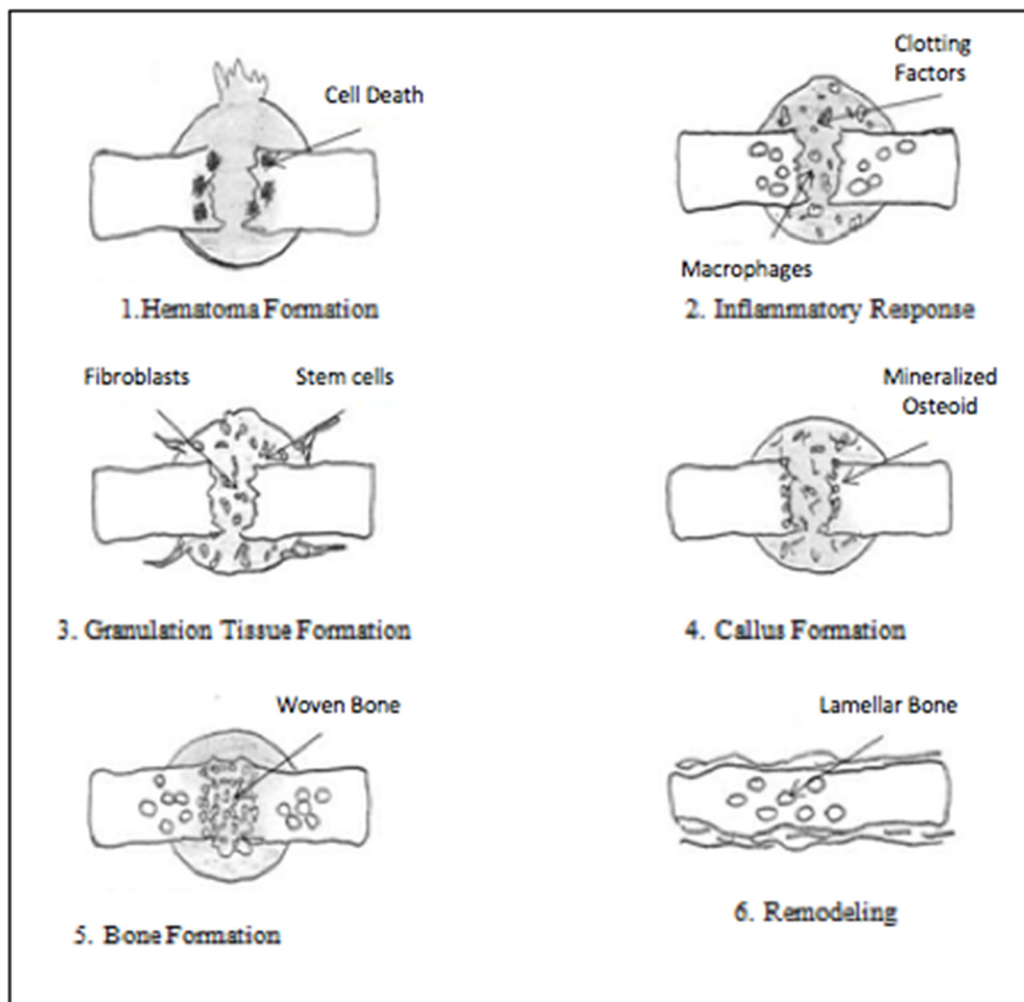
Figure 1.2. Bone repair mechanism [3].

Remodeling of bone is involved for the maintanence of adult bone homeostasis. If there is a problem with balance between bone formation and resorption, the bone mass density and bone homeostasis cannot be preserved. The situation of unbalance can result in various bone diseases [4].

Large bone defects are formed due to trauma, neoplasm, congenital defects, infection and failed arthroplasty. Treatment of these bone defects can be made by orthopaedic surgeon. And also, osteoporosis can be occurred due to the decrease in bone density. Some techniques are used for the reconstruction of bone defects such as grafting techniques and tissue engineering studies [5].

Generally, in a bone surgery, four parameters should be examined. These are known as the length of bone defect, condition of the soft tissue bed in terms of infection and vascularity, competency of soft tissue cover and function in the defected area [6].

In the grafting, allografts, xenografts or autografts, can be used. In autograft techniques, osteoblasts and endosteal osteoprogenitor cells are required for the synthesis of new bone, and a structural matrix that acts as a scaffold. This technique is generally preferred for the reconstruction of bone [7, 8]. Autogenic grafts can be used for the filling of bone defects to heal. They are known as tissues that are harvested from one site and transplanted in or on the body of the same individual. However, a second surgical operation is needed by autogenic grafts for the isolation of the tissue with a limited supply and the donor-site morbidity of autograft can also be observed in a high ratio [9].

Allografts are the tissues obtained from one individual and transplanted to another individual of the same species and can be used in any forms. For the removal of large bone defects, demineralized bone matrix, cortical grafts, osteochondral graft and whole bone segments can be utilized as allografts. Allogenic grafts are unlimited in supply but risks of disease transmission, immunological rejection and donor shortage of allogenic grafts can be observed. Mechanical strength can be provided by allografts to the construct. However, merging of allografts in the host site may take a time. There can be a risk of fracture at the graft-host site because of incomplete healing [6, 9].

Xenografts can also be preferred as an alternative of bone grafting techniques that play a major role in bone healing and regenerative medicine. In this technique, the harvested part from the animal is transferred to the defected site of human body [10]. However, the usage of xenografts can display more disadvantages compared to the autografts and allografts because of the high resorption rate of xenografts. Also, inflammatory response can cause a negative impact on bone healing. The other thing is that various illnessess such as bovine spongiform encephalitis, rabies, Epstein-Barr virus can spread from animals to humans in patching with xenografts to the defected area [11]. Although several harmful effects of xenografts are appeared on humans, these are still preferrable compared to the autografts and allografts due to their availability and lower cost [12].

Nowadays, treatments of bone graft such as xenografting, allografting or autografting are favored to replace or repair damaged bone tissue. The usage of xenografts can show the immunogenicity problems. Allografts have some harmful impacts, such as donor shortages and risks of infections. Autografts suppress development of main complications that are related with transfection and rejection, but the problems associated with the morbidity in the donor site and chronic donor shortages of autografts can lead to the limitations of their usages. Due to some disadvantages of the grafting techniques discussed above, tissue engineering can be preferred to solve the problems related with the replacement of damaged tissues [13, 14].

1.3. BONE TISSUE ENGINEERING

Bone tissue engineering exploits the body's own regeneration capacity by combining cells, biomaterials and cell-inductive stimuli, such as growth factors (GF) or physical stimuli [15]. The main purpose is to restore bone function in critical-sized bone defects that are too large for the body to restore through its own regeneration capacity [16].

Approaches in bone tissue engineering can be described in two main categories: The first is that tissue-engineered constructs with cells and biomaterial scaffolds generated *in vitro* following *in vivo* transplantation, and the second is that scaffolds implanted *in situ* without addition of cells in the constructs [15].

Various sources, including embryonic stem cells and somatic adult cells, can be used to obtain cells. However, the potential of adult somatic cells in tissue engineering can cause some problems due to their low proliferation capability, loss of phenotype and dedifferentiation in the culture. Mesenchymal stem cells (MSCs) can also exhibit great potential as a source of cell in bone tissue engineering because of their use as an abundant autologous cell source for patients [15]. In this technique, small number of cells should be harvested from the patient. The cells are seeded into a scaffold that will be degraded completely and it leads removal of foreign body at the implantation site. Finally, the usage of autologous cells eliminates the rejection problems. Also, the formation of scaffolds such as ceramics, metals, natural polymers, synthetic polymers, and composites can be made by using biomaterials [13, 14].

1.4. BIOMATERIALS AS SCAFFOLDS

Scaffolds that are made of biomaterials are known as the non-living component of tissue engineering. Natural polymers, synthetic polymers, metals, ceramics and composites are used for the formation of scaffolds. They can be used in many areas such as, drug delivery systems, tissue cultures, synthetic blood vessels and dental and maxillofacial applications that interact with the biological systems in the suitable combination of chemical, mechanical, physical and biological characteristics [17].

To engineer the functional tissues and organs, different ways are utilized for the fabrication of scaffolds to facilitate the cell distribution and supply the guidance of cells into three-dimensional space for their growth. The basic methods for scaffold fabrication are solvent casting, electrospinning, particle leaching, rapid prototyping and wet spinning [18].

Biomaterials are very important in tissue engineering applications because of their 3D formation that is known as graft substitutes, or scaffolds, or matrices for cellular attachment and growth causing the formation of new tissue [19]. Three main components that are cell, scaffold and chemical signaling molecules have been utilized for the formation of cellular environments for tissue regeneration [20].

Biomaterials should exhibit some special characteristics while they are designed for tissue engineering studies. They should have a suitable surface for the cell adhesion and the maintanence of cell functions. These materials should be designed to develop cell growth. Moreover, biocompatibility and biodegradability of the scaffolds are very important. They should have lack of immunogenic response and appropriate pore size. Adequate space should be provided for the adhesion of cells onto the surface of biomaterials and also, the spread of cells should be guided throughout the scaffold by the formation of interporosity. Capillary ingrowth and cell-matrix interactions are needed microporosity with pore sizes less than 10 μm. Also, gathering nutrient and the removal of the waste of cells that are grown on the scaffold require macroporosity with pore sizes of 150-900 μm. While biomaterial is processed, the aim should be obtaining suitable three-dimensional structure [21].

Materials from every biomaterial group should have some important properties in bone applications. They should be nontoxic, biocompatible, chemically inert and have an adequate fatique life, proper weight and density. Also, they should be reproducible, easy to fabricate and process on a large scale. Besides, mechanical properties are extremely important to select suitable biomaterials for the repairment of damaged tissue [22].

1.4.1. Polymers

Biomaterials are utilized as temporary matrices for the enhancement of bone tissue. Biodegradable polymers are one type of these materials. There are two types of biodegradable polymers that are known as natural or synthetic polymers.

Natural biomaterials can be used for their good osteoconductive properties. However, they are not mechanically stable, compared to the natural bone tissue. Thus, these materials cannot be available to be used in every occasion. These polymers consists of polysaccharides such as derivatives of hyaluronic acid, chitosan and alginate; or proteins that are known as type-I collagen and fibrin gels [13, 23].

Synthetic biodegradable polymers such as polycaprolactones, polyanhydrides, polylactide, polyglycolide, and copolymers (polylactide-co-glycolide) are preferred to be used in tissue engineering applications [13]. For the fabrication of synthetic polymers, controlled conditions are required.

When these polymers are prepared under controlled conditions, their properties such as Young's modulus, and degradation rate may be modulated for the tissue specific applications.

Since the purity of the materials can be controlled, these materials have an advantage. The risk of toxicity, immunogenicity and infections are not in a high level for pure synthetic polymers. Moreover, synthetic polymers can be favored due to their easy processability, their degradation rates, mechanical and physical properties. However, bulk erosion that leads to the failure of scaffolds can be seen on these polymers [23].

Poly(lactide-co-glycolide) (PLGA) copolymers are the most well-known synthetic polymers that are also known as biocompatible and biodegradable. PLGA that is also referred to as co-polymers of lactide (PLA) and glycolide (PGA), can be used for the fabrication of devices in bone tissue engineering studies because of their great biocompatibility, biodegradability, mechanical properties and nontoxicity for the healing of bone defects [24, 25]. These are also called as saturated poly-α-hydroxy esters. Hydrolytic degradation of these polymers is obtained through de-esterification and the breaking of the components of lactic and glycolic acids into CO_2 and H_2O [23].

Physico-chemical properties of PLGA depend on different factors which include monomer's molecular weight, lactic acid to glycolic acid ratio and the exposure time to water. Its erosion time or degradation rates can show differences by the increase of its molecular weight. The molar ratio of lactic acid and glycolic acid in the polymer chain can also be important to decide the rate of degradation of PLGA copolymers [26, 27].

PLGA with a higher ratio of lactic acid has shown the characteristics of less hydrophilicity, so that less water absorption and slower degradation rate. The methyl side groups in the content of PLA causes it to be more hydrophobic than PGA. Also, the degree of crystallinity is higly important factor due to the impact on the mechanical strength, swelling behavior, rate of hydrolysis and biodegradation of PLGA.

Because of the lack of methyl side group of PGA, it is highly crystalline, but as an exception, its crystallinity is rapidly lost in the form of 50:50 ratio of PLGA copolymers and its degradation rate becomes more rapid, compared to either PGA or PLA [9,10,11].

Glass transition temperature (Tg) of this copolymer is also above 37 °C. The ratio of LA content or molecular weight affects the Tg value. Decrease of their ratios in the copolymer causes the decrease in Tg value [28, 29].

PLGA copolymers can be transformed into fibers by using wet-spinning technique that is a simple and inexpensive method to fabricate wet-spun PLGA monofilament fibers. These fibers are strong, elastic, and suitable as a tissue-engineering scaffolds [30]. Although electrospinning is more widely used to get a fiber formation, wetspinning are preferable due to the higher intrinsic porosity and larger pore size with relatively thick fibers [31]. Also, the scaffolds fabricated with wetspinning show a higher porosity than the ones fabricated with dry electrospinning since they are deposited in a solution [32]. Thus, adhesion and penetration of cells can be facilitated into the scaffold [33].

Dry spinning and wet spinning are known as the types of solution spinning methods. These are generally used for polymers which do not have the ability of melting. In these methods, fiber structure is formed when the polymer solution is passed through a spinneret and then, coagulation bath solution [34]. In dry spinning, thermal evaporation removes the solvents while in wet spinning the polymer coagulation is executed in another fluid that fullfills the requirements of the spinning solvent. However, it is not acceptable as a solvent for the polymer [35, 36].

1.4.2. Hydrogels

Hydrogels are known as aqueous three-dimensional networks. They do not have the ability to be dissolved in water. These are made of hydrophilic polymers that are cross-linked by covalent bonds or physical interactions.

They are also biocompatible and biodegradable and their hydrophilic surface has a low interfacial free energy which lead to a low tendency for cells to attach onto the surfaces of hydrogels.

The holding capacity of water and its permeability are known as the most important features of a hydrogel. Hydrogels swell in water absorbing at least 10 to 20 per cent of their weight in water [37].

Hydrogels can also be stimuli sensitive and reply the small changes in temperature, pH and electric field. Temperature-sensitive hydrogels are also called as thermogels. They persist liquid at room temperature, but when they are in body temperature, a high viscous gel is obtained. The formation of gel supplies the local effect and can lead to the sustainable release of the drug/biomolecule up to a longer duration [38].

Co-injecting progenitor cells or growth factors can be used to increase the functional effects of hydrogels. The beneficial effects of hydrogel-mediated vascular endothelial growth factor (VEGF) delivery can be enhanced by controlled release of VEGF from the biomaterial. Conjugation of VEGF to the gel can supply the sustained local release that lead to prolong activity of protein and angiogenesis [39]. Also, hydrogel integrated with growth factor can behave directly to encourage the development and differentiation of cells in the newly formed tissues and are usually favourable to promote migration of cell, high water content, and quick nutrient diffusion [40].

1.4.2.1. PLGA - PEG - PLGA Copolymers

PLGA - PEG - PLGA block copolymers are a type of temperature-responsive copolymers. Hydrophobic PLGA segments and hydrophilic PEG segment that allows the copolymer molecules stay in the aqueous solution are the components of these copolymers [41]. Also, these triblock copolymers are known as the most biodegradable thermo-gelling polymers [38].

Poly (ethyleneglycol) (PEG) is not biodegradable although it is a hydrophilic and highly biocompatible polymer that has been approved by FDA for its application to the human body by pharmacological applications. However, degradation problem can be solved by copolymerizing PEG with biomaterials such as hydrophobic biodegradable poly (lactic acid), poly (lactide-co-glycolide) and poly (caprolactone). Biocompatibility should be considered in the selection of biodegradable material in which PEG is copolymerized [38].

PEG based copolymers play an important role as a biomedical material because they are biocompatible, biodegradable, thermosensitive and easily controllable. The integration of the PEG within hydrophobic polyesters lead to the improvement of biocompatibility of the carrier, due to the hydrophilicity of the biological environment in nature.

In aqueous solution, self arranged micelle formation is demonstrated by these amphiphilic copolymers due to hydrophobic interactions. These micelles with small size have low toxicity and high stability and therefore, can be preferred to be used in the researches [38].

Depending on the features of temperature-responsive copolymers, lower temperatures lead to the dissolution in water due to the strong hydrogen bonds of hydrophilic PEG segments with water. When an increase in temperature is occurred, weaker hydrogen bonding is observed and sol–gel transition is obtained due to strong hydrophobic forces among the PLGA segments [41]. Copolymer solutions exhibit sol-to-gel transition between 30–37 °C and gel-to-sol transition between 40–70 °C (Figure 1.3) and this is used for drug/biomolecule delivery [42].
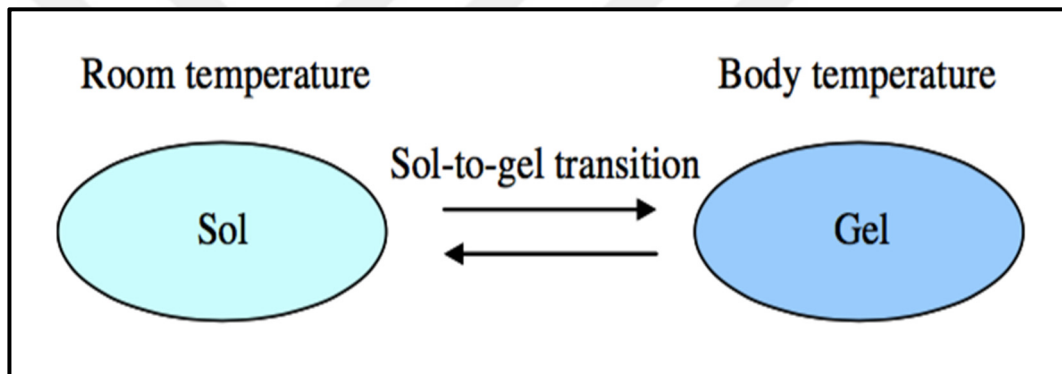
Figure 1.3. Sol-to-gel transition diagram [42].

Rising of the molar ratio of DL-lactide/glycolide in the PLGA segment can also lead to an increase of the hydrophobicity of the copolymer since DL-lactide moiety is more hydrophobic than glycolide. More stable hydrogels can be formed by the copolymer with higher DL- lactide/glycolide molar ratio due to the stronger hydrophobic interactions among the copolymer molecules [41].

The features of PLGA–PEG–PLGA can be modulated by the structures of PLGA with changes in LA/GA ratio. Different chemical structures with an altered hydrophobicity and hydrophilicity affect the copolymer micellization and also the formation of hydrogels [42].

1.5. CELL TYPES USED IN BONE TISSUE ENGINEERING

The selection of cell source is considerably important for the achievement of tissue engineering. Cells that are available in this area may be classified into three groups, such as autologous, allogenic and xenogenic. Autologous cells are the most suitable ones because of their high activity. Allogenic and xenogenic cells are known as immunogenic [43].

An osteocyte, a star shaped cell, is the most commonly found cell in mature bone. Almost 90 per cent to 95 per cent of all bone cells consist of osteocytes that are derived from osteoprogenitors in adult bone. Osteocytes cause bone remodeling through regulation of both osteoclast and osteoblast activity [44]. They are also responsible for providing a support of bone structures and do not divide, but some of them can show the features of differentiation into active osteoblasts.

The synthesis of new bone matrix are supplied by osteoblasts. Preosteoblasts which are appeared near functional osteoblasts in the bone remodeling unit are easily recognized due to their alkaline phosphatase expression. Additionally, they also have an important role for the secretion of type I collagen and other matrix proteins [1].

Osteoclasts, multinucleated cells, are responsible for the catabolic activity that are required for bone resorption, because of their capability of degradation of mineralized matrices such as bone and cartilage. In addition to the ability of osteoclasts for the degradation of the inorganic calcium matrix, they also play a role in the degradation of the organic collagen matrix [45]. Together with bone resorption, osteoclasts can also induce bone formation by the osteoblasts.

Preosteoblasts, preosteoclasts and chondroprogenitors lead to the production of VEGF that induces differentiation into osteoblasts/osteocytes, osteoclasts and chondrocytes, respectively (Figure 1.4). Bone maintenance and bone fracture repair are governed by these cells. VEGF also drives endothelial cell migration, proliferation and tube formation to get a new blood vessels, together with the bone cells, to heal bone defect [46].
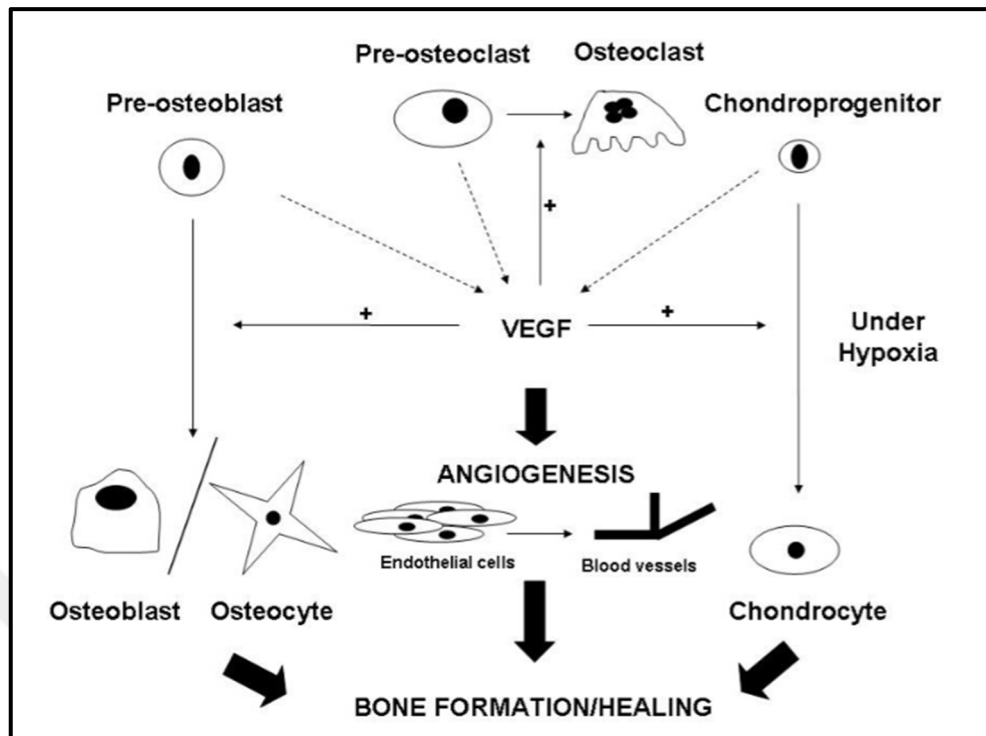
Figure 1.4. Cells required in angiognesis and bone formation [46].

Stem cells are suitable source for bone tissue engineering because of their ability for high proliferation, capacity of self-renewal, features of multilineage differentiation and, thus, regeneration of tissue [47]. Mesenchymal stem cells (MSC) that are located in the bone marrow, is used for the regeneration of bone, cartilage tissue etc. However, stem cells that are isolated from bone marrow can demonstrate the problem of high heterogeneity of whole bone marrow cultures. To overcome this problem, the gradient centrifugation is used to separate MSCs from the culture. In addition to that, adult stem cells or embryonic stem cells can also be used for bone tissue engineering but they have limited usage potential due to their ethical concerns [47].

Furthermore, there are various factors that affect differentiation of MSCs to osteoblasts. One of them is the usage of the osteogenic environment that is responsible for the induction of MSCs to form matrix with high level of collagen type I. The other one is the activation of alkaline phosphatase (ALP) that leads to the occurrence of mineralization. Besides, osteocalcin, Runx2 and bone morphogenetic proteins (BMPs) are also known as the other factors that play roles in the osteoblast differentiation [48].

1.5.1. Co-culture of Cells

Natural or synthetic interactions between cell populations are investigated by using co-culture set-up, especially in tissue enginering applications (Figure 1.5). Sometimes, monoculturing of cells cannot be desired for *in vitro* studies. The two types of cell population can improve the success of culturing. It can also influence the cellular activity in a positive manner. Besides, volume of co-cultures, relative cell numbers and type of populations can change the features of co-cultures [49].
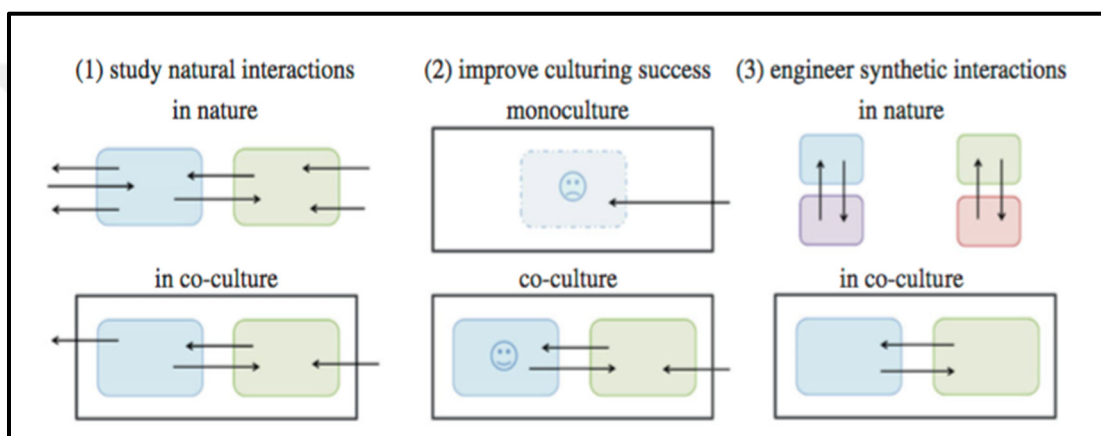
Figure 1.5. Definition and success of co-culture systems [49].

Generally, transwells are preferred for co-culturing systems (Figure 1.6). Hydrogels, scaffolds or microarrays can also be used to construct a co-culturing system [49].
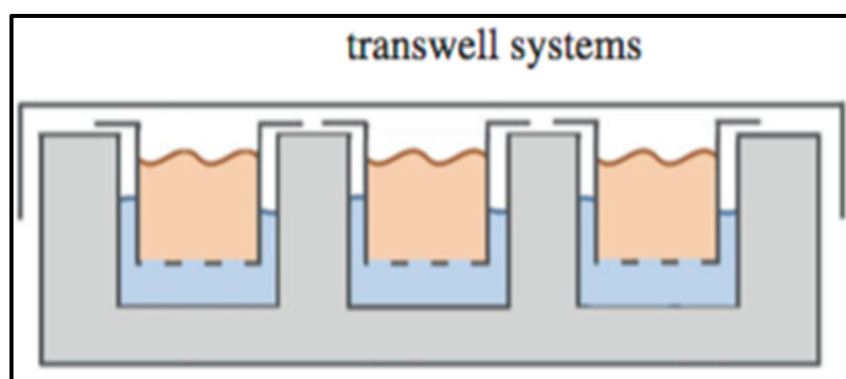
Figure 1.6. Transwell systems in co-culturing studies [49].

In this study, co-culturing of MSCs and endothelial cells was provided by using transwell system. Usage of rat bone marrow derived MSCs (rBMSCs) and rat peripheral blood endothelial cells (rPBECs) was favoured to induce angiogenesis whilst the formation of bone.

Isolation of endothelial cells that is obtained from peripheral blood (PB) does not exhibit morbidity of the donor site, and therefore, it is preferable. Also, high cell proliferation and high potential for angiogenesis make it more favourible [50].

1.6. NEOVASCULARIZATION

Tissue engineering has begun to generate very promising results in recent years, due to advances in stem cell research, the development of new and biocompatible biomaterials, and the prolonged release of growth factors in drug delivery systems. However, inadequate vascularization leads to the failure of many tissue engineering applications. It leads to insufficient bone formation, cell death and weak healing capacity. Vascularization is important for the healing of bone tissue in terms of providing nutrient and oxygen demand, removal of waste materials and transport of hormones, inflammatory cells and signals to the defect site [51].

Angiogenesis and vasculogenesis are the fundamental processes that supply new blood vessel formation. Vasculogenesis is defined as the initial formation of vessels by the differentiation of precursor cells whereas angiogenesis is explained as the expansion of vascular network from pre-existing vessels. These are cumulatively defined as neovascularization [52, 53].

Maturation of nascent blood vessels can be explained by angiogenesis. The activation, migration, and proliferation of endothelial cells (EC) are necessary for the major stages of angiogenesis [54]. They are also required for the formation of bone. Thus, activation of endothelial cells are firstly occured since they are in quiescent state prior to angiogenesis. Then, extracellular matrix (ECM) remodeling is required for the developing of vessels. Also, degradation of ECM that leads to the release of factors for the acceleration of the process of angiogenesis is made by matrix metalloproteinases (MMPs) while proliferation and

migration of endothelial cells are observed and tubular structures and new vessels are formed during this process [53].

Angiogenesis is also known as a main factor to get the formation of bone. Growth factors are responsible to organize many cell types to activate, migrate and differentiate for bone formation [51]. In bone regeneration, expedited neovascularization is a crucial consideration within the defect area. Self-generated angiogenesis is not sufficient for the formation of vessel that is required for the cell viability and tissue regeneration. Thus, it should be enhanced.

To enhance neovascularization, many approaches have been investigated. Prevascularization of tissue engineering scaffold can be used to enhance neovascularization either *in vivo* or *in vitro*. In *in vivo* prevascularization, implantation of tissue engineering scaffold is first applied into the body that is a region with an abundant vascular network and is planned to be surrounded with a microvascular network around within a few weeks. Then, the construct is detached and transplantation is performed into the bone defect site. Two separate surgical procedures are necessary for this approach and it causes the risk of donor site morbidity, thus decreased clinical relevance is observed. In *in vitro* prevascularization, a construct is seeded with endothelial cells which can spontaneously lead to the formation of a vessel-like network [55].

Another application is angiogenic growth factor delivery that demands controlled and sustained release of protein. Successful neovascularization starts with the formation of lumen. That is also followed by the stabilization of vessel. Finally, maturation that leads to the formation of a functional and permanent vascular network is obtained.

Growth factors influence the proliferation and migration of cells, besides cell-cell interaction. This is managed by a controlled combination of various factors, including platelet-derived growth factor (PDGF), transforming growth factor beta 1 (TGF-β1), fibroblast growth factor (FGF) and vascular endothelial growth factor (VEGF) [55].

One of the most widely used regulators of this approach is VEGF that is responsible for the development and repair of bone, besides its angiogenic function. Proliferation of endothelial cells, migration and formation of capillary-like arrangement are stimulated by the help of VEGF.

Expression of VEGF is observed before the formation of vessels in developing bones and it has a close association with the osteoblast. PDGF leads to the maturation of vessel by the recruitment of pericytes. FGF-2 induces the proliferation and migration of endothelial cells [51]. TGF-β production can be provided by various types of cells, including fibroblasts and endothelial cells. It can also activate MMPs and prevent endothelial cell proliferation (Figure 1.7) [51, 53].
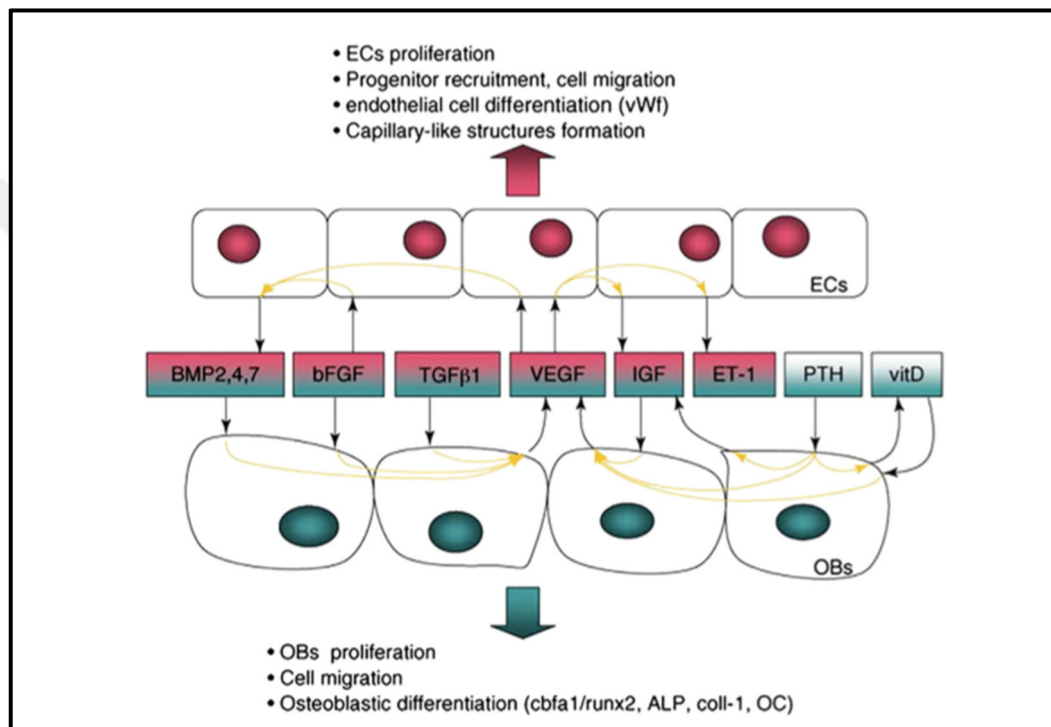
Figure 1.7. Communication between osteoblasts and endothelial cells [51].

In Figure 1.7, red and green arrows show the impacts of growth factors and systemic hormones on the functions of endothelial cells and osteoblasts, respectively. These factors play role to activate particular receptors (black arrows) that induce other proteins' expression after the intracellular signaling pathways activation (orange arrows) [51].

VEGF secreted in the tissue supplies the migration of endothelial cells and the formation of capillary-like structures. However, when VEGF secretion is terminated, the tube-like structures become corrupted by losing their stability. *In vivo,* the effect of VEGF should be continued for 4 weeks in order to ensure the stabilization and persistence of newly formed vessels [51, 56].

Even though it has the ability to form blood vessels, the shortage of its half-life may not be sufficient to ensure the stability and this situation restricts the use of VEGF [51, 56, 57].

The disadvantages of short half life of VEGF can be eliminated by the incorporation of growth factor into an appropriate polymer matrix to achieve its sustained release at the site of action. This leads to the protection of growth factor in the matrix from proteolysis and antibody neutralization. In this way, prolonged retention of the biological activity is obtained *in vivo*. However, growth factor-polymer formulation process with this sustained release system can exhibit denaturation and deactivation of growth factors that can cause the loss of biological activity [56, 57]. For these reasons, in this study, 4-(2-(4-Metoksifenilsüllfanil) ethil) piridin (GS4012) that is a VEGF pathway activator was used instead of VEGF, as an alternative for the induction of vasculogenesis.

Cell transplantation is used as another strategy to enhance vascular formation. The integration of endothelial cells into scaffolds is needed to cause the formation of a vascular network (Figure 1.8). Endothelial cells are responsible for the formation of the lumen of blood vessels. They are also used as a barrier for the transfer of nutrient and provide nonthrombogenic features. Besides, smooth muscle cells are used for providing mechanical strength to the vessels. This approach depends on the anastomosis between endothelial cells that are transplanted and the host cells and formation of a vascular network within the scaffolds. This approach is advantageous due to the reduction of the time required for obtaining the new blood vessel formation [53].
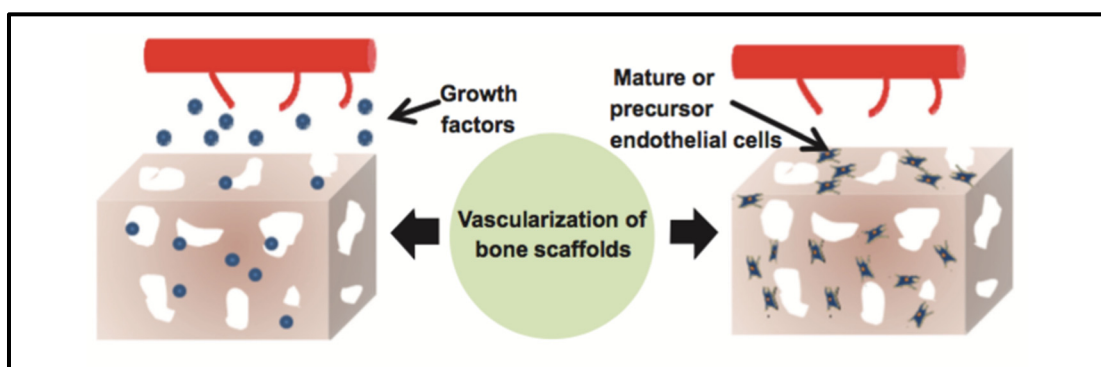
Figure 1.8. Delivery of growth factor and cell transplantation strategies for the induction of vascular growth [53].

MSCs can also be used in cell transplantation approaches since they provide the development of vasculature and new bone inside the scaffolds [53].

This process can be preferable due to its ability to supply the controlled delivery of various factors. However, the low viability of the transplanted cells is known as a major problem. In addition, the limited anastomosis and integration between the transplanted endothelial cells and host cells, and also, a limited control for the development of blood vessel in scaffolds can lead to unsuccessful results [53].

Moreover, hypoxic-condition can be used to provide the release of angiogenic growth factors. Due to damage to the local vasculature that causes the loss of bone, low oxygen level is observed around bone defect site that requires a scaffolds for the promotion of healing [53]. Hypoxia-inducible factors (HIFs) are responsible for the stimulation of angiogenesis in ischemic tissue. It is also involved in the recruitment of angiogenic cells and important in vascular remodeling.

HIF-1 is responsible for the regulation of various human genes, such as VEGF, bFGF, TGF- and PDGF. The expression of these molecules can be increased by HIF-1 activity [53, 58, 59]. Also, secretion of a cocktail of angiogenic factors is authorized by hypoxia (HIF-1) since release of a single factor does not exhibit the development of sufficient vascularization. For example, when endothelial and smooth muscle cells are co-cultured, decrease of the effect of VEGF on endothelial cells is observed. However, its combination with selected factors can induce the stimulation of vessel formation [53, 60].

Furthermore, microscale technologies can be used for vascularization of biomaterials. These techniques are favoured for the formation of vessel-like structures. Microfluidics and bioprinting are the most widely preferred ones [53]. For example, layer-by-layer microfluidics technology creates three dimensional microscale tissue-like structure by using different types of cells in each layer to mimic the structure existed *in vivo* [53, 61]. Computer aided bioprinting is another process for the enhancement of microvascular network in three dimentional hydrogels. In this process, cell aggregates are suspended in hydrogel droplets to form vascularized tissue [53].

1.7. EFFECT OF VEGF AND ITS COMBINATION WITH OTHER GROWTH FACTORS ON ANGIOGENESIS AND OSTEOGENESIS

Angiogenesis is important for bone formation. Without angiogenesis, degeneration of bone tissue or even death is observed. Inadequate angiogenesis causes the restrictions to get oxygen and nutrient which lead to death of cells. The formation of successful bone repair therapies can be improved if suitable combinations are created between osteogenic and angiogenic factors for bone tissue engineering [51].

Binding of VEGF ligands to their membrane-bound receptors lead to the induction of VEGF signaling that causes the activation of multiple downstream pathways. These are known as the Ras/MAPK pathway which is responsible for the regulation of cell proliferation and gene expression, the FAK/paxillin pathway which plays role in the reorganization of the cytoskeleton and cell migration, the PI3K/AKT pathway for the arrangement of cell survival and the vascular permeability (Figure 1.9) [62, 63].
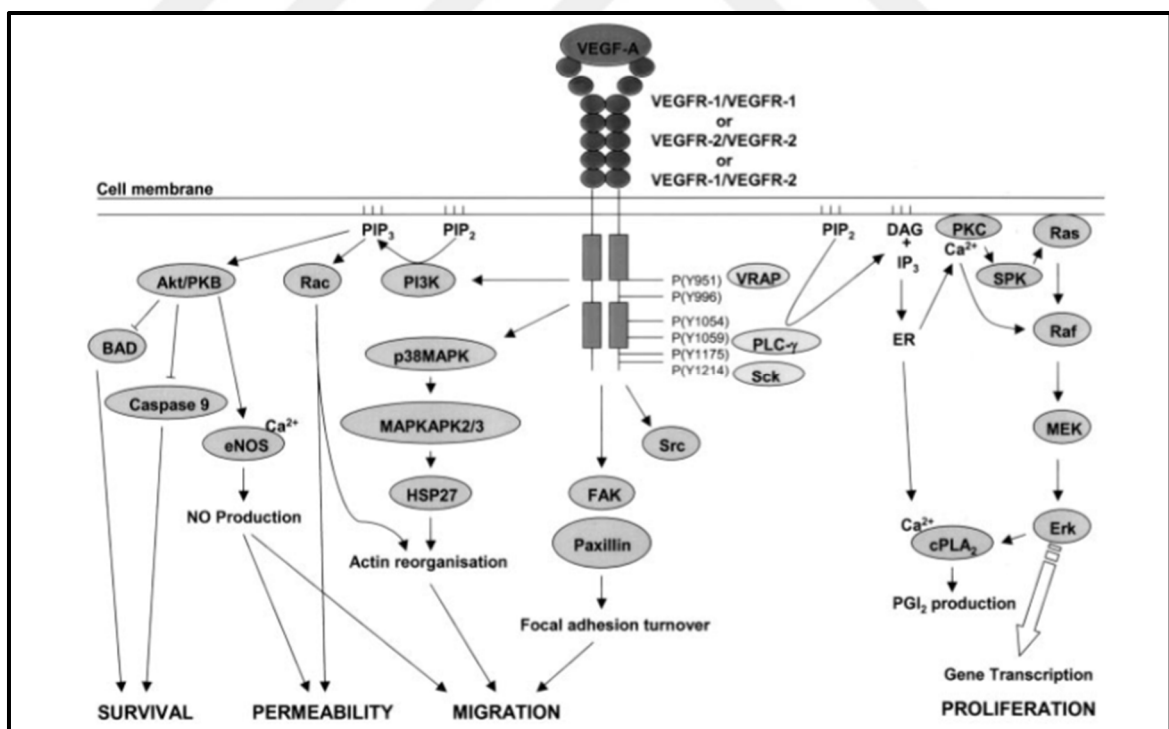
Figure 1.9. VEGF signaling pathway involved in angiogenesis [62].

The RAS proteins are one of the most well known molecules to adjust cell growth due to their position in the signal transduction pathway. They behave as a crucial point to integrate a growth factor signal starting from the membrane through the cytoplasm and into the nucleus with a series of signaling pathways. They are GTP binding proteins. While binding to GTP leads to the activation of Ras proteins, binding to GDP causes inactivation. RAS-GTP binds and provides the activation of the serine/threonine kinase, Raf which is one of the effector proteins causing the activation of the MAPK cascade. The recruitment of Raf to the cell membrane is required for its activation by tyrosine phosphorylation. Raf kinase is called as a MAPKKK. A series of phosphorylation steps is important for enzyme activation to get a MAPK that is called as extracellular signal regulated kinases; ERKs (Figure 1.10) [62, 63].
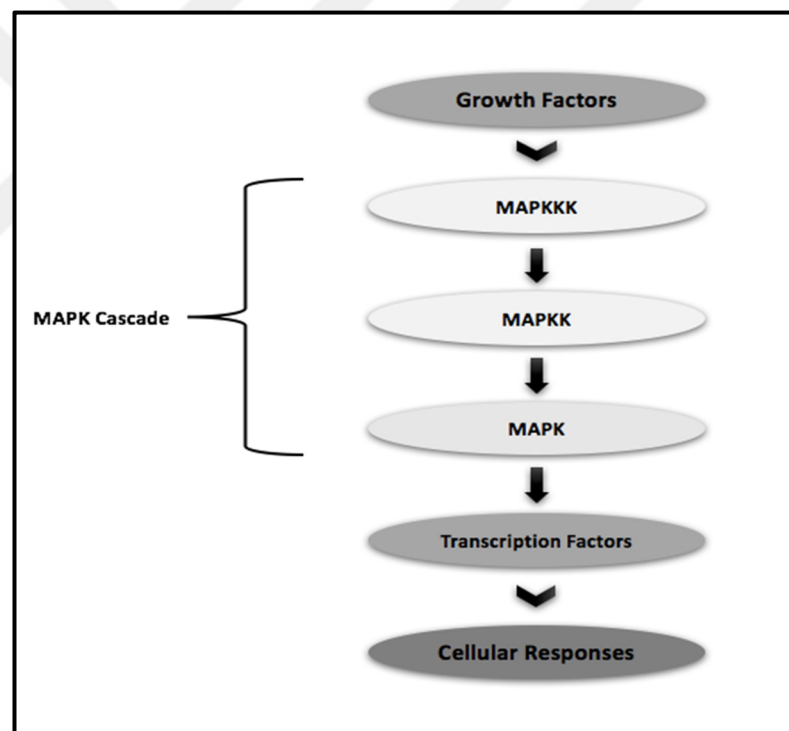
Figure 1.10. Schematic drawing of MAPK activation.

Phosphatidylinositol 3-kinase (PI3K), a lipid kinase, catalyzes the production of the lipid, second messenger, phosphatidylinositol-3,4,5-triphosphate (PIP3) at the cell membrane. The serine/threonine kinase PDK-1 (Phosphoinositide dependent kinase 1) is recruited to the membrane by the production of PIP3. Akt is another serine/threonine kinase. When recruitment of Akt to the membrane is obtained, PDK-1 phosphorylates and activates it.

Then, translocation of activated Akt is observed into the nucleus and nuclear substrates, including transcription factors, are phosphorylated.

In addition to stimulation of cell proliferation, cell signalling can show effects on cellular behaviours. This is due to the intracellular tyrosine kinase, SRC that plays an important role in adhesion, invasion, and motility of cells. SRC contains SH2 and SH3 domains. It also includes a negative-regulatory domain. When phosphorylation of Tyr 530 is exhibited in this domain, it binds to the internal SRC SH2 domain and causes the supression of the kinase domain, thus SRC is not active. It can be activated by receptor tyrosine kinases. The activated kinase is responsible for the phosphorylation of focal adhesion proteins (FAK). These are also important for adhesion and motility. Cell adherence is facilitated by assembly of focal adhesions while disassembly supplies the facilities for cell motility. If SRC is activated, disassembly of focal adhesions is created and increased motility is observed [62, 63].

According to the previous studies, both endothelial cells and osteoblasts are responsible for the production of growth factors that affect the proliferation, migration and differentiation of these cell types [64]. Growth factors that are produced by endothelial cells contain bone morphogenetic protein-2 (BMP-2), insulin-like growth factor (IGF), vasoconstrictor endothelin-1 (ET1). Migration, proliferation and differentiation of osteoblasts are also influenced by these factors [51, 65, 66].

Osteoblasts are able to produce VEGF in high ratios. Existence of VEGF can show various responsibilities. It regulates activity, survival and recruitment of osteoclasts that have the ability for secretion of proteinases to the extracellular matrix for the stimulation of osteoblasts secreted TGF-β, and also, it enhances the life time, proliferation, differentiation and angiogenesis of endothelial cells via activating specific receptors [51].

VEGF behaves as a peacemaker of several factors that are responsible for osteoinduction, including BMP-2, IGF, FGF-2. The expression pattern of VEGF is regulated by these factors. They demonstrate a strong combination and have an interactive effect on osteogenesis and angiogenesis (Figure 1.11).
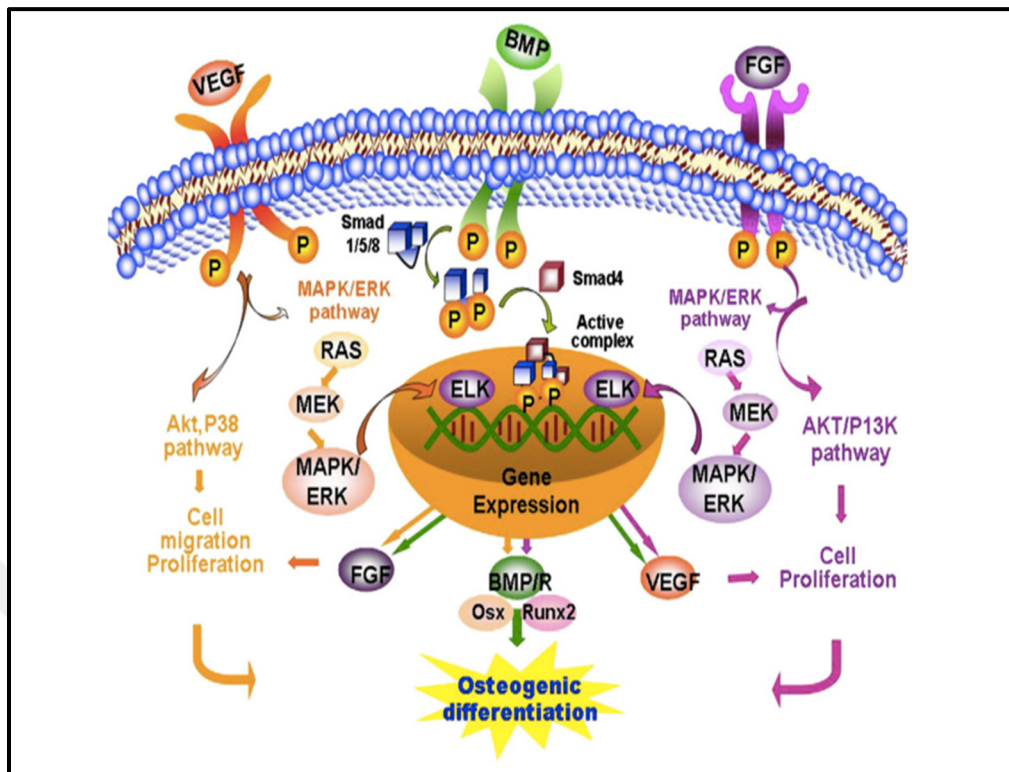
Figure 1.11. Fundamental interactions between growth factors on osteogenic differentiation [51].

Members of FGF family are known as cytokines which are responsible for the stimulation of mitogenesis of various kind of cells, such as endothelial cells, osteoblasts, bone marrow stromal cells, and mesenchymal stem cells. Cells proliferation, migration and differentiation are also regulated by these cytokines. FGF-2 (bFGF) is generally focused on bone formation. It stimulates the formation of angiogenesis and osteogenesis by moving on endothelial cells and osteoblasts, respectively. It is also responsible for the activation of Matrix Metalloproteinases and VEGF fabrication, besides the activation of the proliferation of endothelial cells. In addition, migration of endothelial cells, attraction of pericyte and deposition of matrix in the formation of blood vessels are induced by this growth factor and it leads to the cbfa1/runx2, ALP, type-I collagen expressions [51, 67].

BMP has favourable effects on the formation of bone that is associated with BMP stimulation in vessel formation specifically within bone. Cells can be promoted close to the vascularization site by the help of BMP for the production of angiogenic factors. It stimulates angiogenesis through the generation of VEGF by osteoblasts [51, 68].

Besides, activation of p38 phosphorylation and the smad pathway is supplied by BMP to affect endothelial cell proliferation, migration and formation of tubular structure [69, 70].

IGF-1 is also responsible for promotion of cell proliferation and inhibition of cell apoptosis. It can also serve as an inducer of osteoblasts in response to the production of ECM proteins, like as collagen type 1. In addition, production of IGF and ET-1 are provided by endothelial cells and up-regulation of ALP is stimulated by these growth factors in human osteoblast-like cells [51, 71, 72].

As shown in Figure 1.11, the MAPK/ERK pathway, that influences proliferation of cells and gene expression of FGF and BMP in nucleus, is activated by the VEGF–VEGFRs interaction. This pathway is also activated by FGF–FGFRs interaction and finally, proliferation of cells and gene expression of some growth factors including VEGF, BMP/R, Runx2 are promoted by this interaction. Interaction between BMP–BMPRs can also activate and phosphorylate Smads. After gathering the activated Smads into a heteromeric complex with Smad 4, it is translocated from the cytoplasm to the nucleus and the expressions of bFGF, VEGF and Runx2/Cbfa 1 are regulated.

Growth factors can show different biological effects that are regulated by each other and the connection between these growth factors can change the gene expression and functionality of cell. For the selection of growth factors, type of the reconstituted bones such as compact and spongy bones, is also an important parameter. Combinations of these growth factors for the treatment of different types of bones can display both inductive and repressive effects. For example, combination of BMP and FGF exhibits an interactive effect to heal the critical sized femur defect of a rat, whereas combination of these factors leads to the absorbtion of colloidal gels, thus shows a decrease of bone formation in the femoral defect of a rat [51].

1.8. GROWTH FACTOR RELEASE STRATEGY

Growth factor integration with delivery vehicle leads to develop its effect. The delivery system should be highly biocompatible and biodegradable. It should also have low toxicity and ease of reproducibility. An application of delivery carriers can be influenced by the species of growth factor, physicochemical properties of carrier, and structure of bone defects. The delivery vehicles should ensure a time and dose-controlled release of growth factor.

They also provide a scaffold which causes the enhancement in cell attachment and recruitment. In addition, allocation of voids should be occurred to encourage migration of cells and angiogenesis [51, 73, 74].

Growth factors that show their effects on angiogenesis and bone formation are dose-dependent. The process of sustained release kinetics of growth factors is aimed to keep a therapeutic dose for longer than rapidly releasing scaffolds. In general, lower effective doses are supplied by sustained release of growth factors, compared to single injection [51]. Carrier vehicle which can be three dimensional scaffolds, hydrogels or microparticles, is also important for the required dose of growth factors. The efficient doses should be adjusted since it can affect the promotion of angiogenesis or bone formation. Inefficient dose can cause suppression of vessels and bone formation. For instance, undesirable emergence of hematoma and ectopic bone formation may be occurred due to excess BMP-2 [51, 75, 76]. In addition, excessive dose of VEGF and FGF can cause inhibition of osteogenesis and lead to vascular leakage [77].

The delivery materials can be categorized as natural or synthetic organic materials and inorganic materials. Fibrin, gelatin, collagen, chitosan, hyaluronan, and alginate are known as the common natural materials used as delivery carrier. Most of them are biocompatible and biodegradable, but they have various problems such as the restricted source of natural materials, immunogenicity, and difficulty in process. Moreover, synthetic polymers supply ideal chemical and mechanical properties, compared to natural polymers. Less immunogenicity of synthetic polymers is observed [51, 78, 79].

Release profiles of growth factors from scaffolds can be controlled by several methods. For that reason, growth factor loaded scaffolds are fabricated. Firstly, growth factors can be attached to the polymeric scaffold. This method provides the immobilization of growth factor to the polymer surface via chemical crosslinking, or growth factor adsorption. Secondly, growth factors can be entrapped within scaffolds. In this method, growth factors are directly incorporated within scaffolds during the fabrication process and the polymers are generally mixed with the growth factors prior to process the scaffold (Figure 1.12) [80].
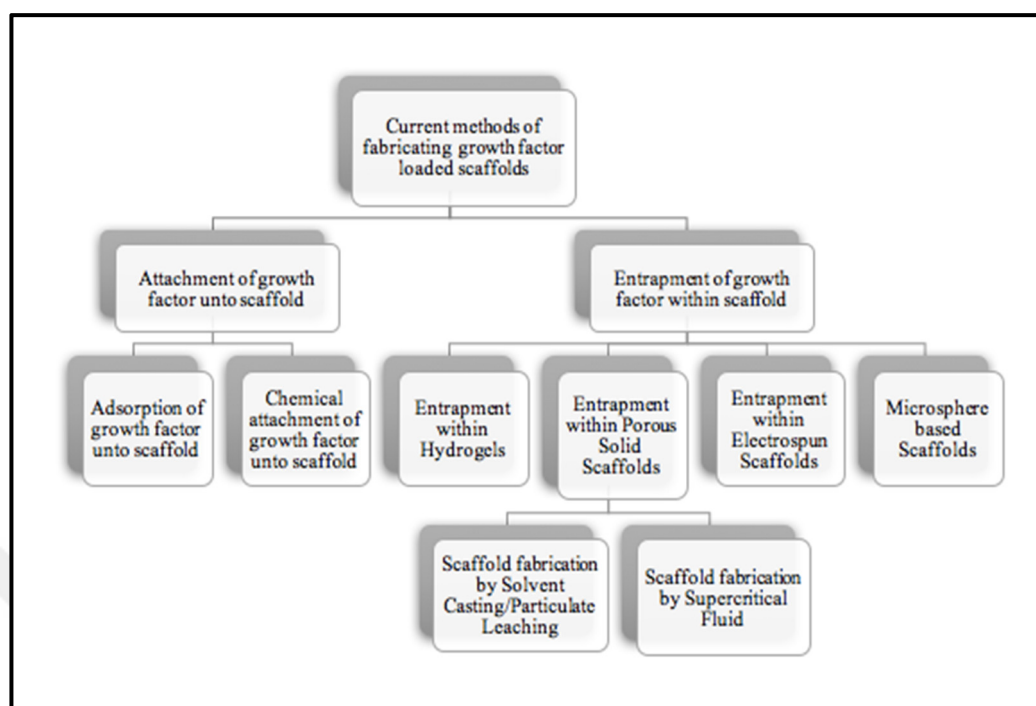
Figure 1.12. Current methods of producing growth factor loaded scaffolds [80].

Direct physical entrapment of biomolecules within hydrogels is the most well-known process for the production of three dimensional release systems to promote bone tissue regeneration. Hydrogels for sustained growth factor release has an advantage for being stimuli-responsive gels, that have the ability to be produced on-demand release systems [81].

Delivery of growth factors from hydrogels depends on the basic mechanism of biomolecule diffusion through the highly hydrophilic scaffold and gel degradation [38]. Sustained release of biomolecule depending on diffusion can be divided into two phases. The first one is a rapid burst phase and the second one is a prolonged diffusion phase. Dose-dumping effect is caused by burst release and it has a damage for patients in clinical trials. Material interaction with drugs/biomolecules, fabrication conditions, and morphology of the sample can cause burst release and its degree can be decreased by several methods. Increasing cross- linking density of the matrix surface, embedding the drug/biomolecule within a polymeric matrix, and loading drug/biomolecule with higher concentrations through the center of the matrix can be used for the reduction of the amount of burst release. However, the prediction of burst release is still problematic [82].

Moreover, the most well-known reactions that happen within hydrogel delivery systems are known as the breaking of polymer chains via hydrolytic or enzymatic degradation.

The surface or bulk erosion of hydrogels controls the rate of growth factor release (Figure 1.13). It depends on the process of diffusion of water into the polymer matrix and its degradation behaviour. When the faster diffusion of water is obtained than the degradation of polymer, bulk erosion of the polymer is observed. However, when the diffusion of water is lower than the degradation of polymers, it goes through the surface erosion. According to the type of erosion, the release rate of growth factors can be influenced [83].
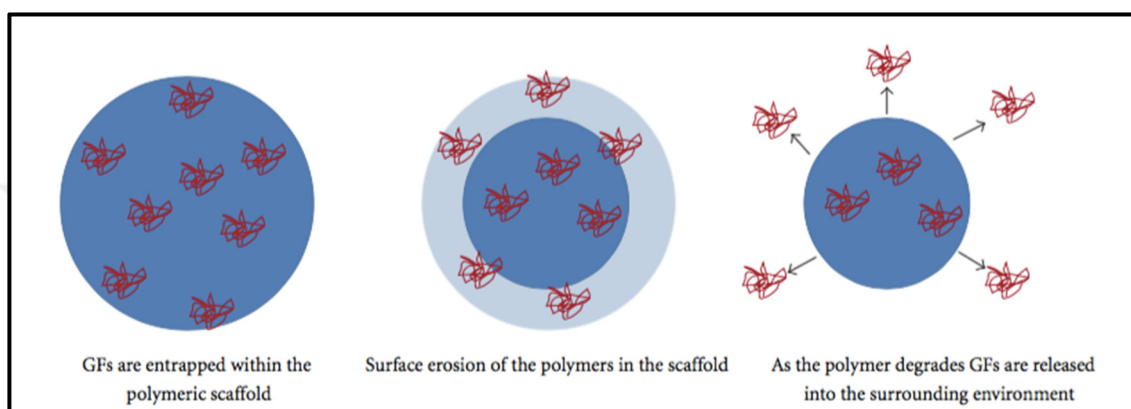
Figure 1.13. The breakdown and release of growth factors from polymeric encapsulation [83].

1.9. EFFECT OF GS4012 ON ANGIOGENESIS

GS4012 is a pyridinyl - thioether compound that upregulates the VEGF passing through the cell membrane. GS4012 has been found to activate the VEGF receptor by inhibiting the ERK pathway [84, 85].

In one study, the effect of GS4012 on vascularization was evaluated. The zebrafish mutation gridlock disrupted aortic blood flow in a region. Because of this mutation, in damaged zebrafish, it was proven that GS4012 caused the formation of vascularization. The expression of vascular endothelial growth factor (VEGF) was upregulated, and the activation of the VEGF pathway was sufficient to suppress the gridlock phenotype. In addition to that, some experiments proved that HUVECs treated with GS4012 created more tubes and produced more VEGF compared to non-treated ones [85].

In this study, the lower cost, stable and durable GS4012 instead of VEGF, was encapsulated into PLGA-PEG-PLGA that can provide sustained release and the activation of VEGF pathway in an efficient manner and extended periods. PLGA-PEG-PLGA hydrogel also served as a reservoir for the released substance.

1.10. OBJECTIVES OF THE STUDY

In this study, a fibrous bone tissue engineering scaffold was produced using poly(lactic-co-glycolic acid) (PLGA) to obtain the first phase of the tissue engineered scaffold by wet spinning technique and mesenchymal stem cells were isolated from rat bone marrow (rBMSCs) to be seeded on these scaffolds for the formation of bone tissue. The first phase of this construct was fibrous PLGA structure that provides mechanical support to the tissue engineered scaffold for the proliferation and differentiation of cells into bone tissue.

Sustained-release hydrogel was used as a second phase of the tissue engineered scaffold. PLGA and poly(ethylene glycol) (PEG) based hydrogel were polymerized around PLGA scaffold and used for the sustained release of VEGF activator GS4012. Designed scaffold and sustained release system were tested *in vitro* on endothelial cells isolated from rat peripheral blood (rPBECs) for their migration and microvessel formation ability. For that reason, rPBECs were seeded onto the porous structural insert that was placed into the wells of the cell culture plates (Figure 1.14).
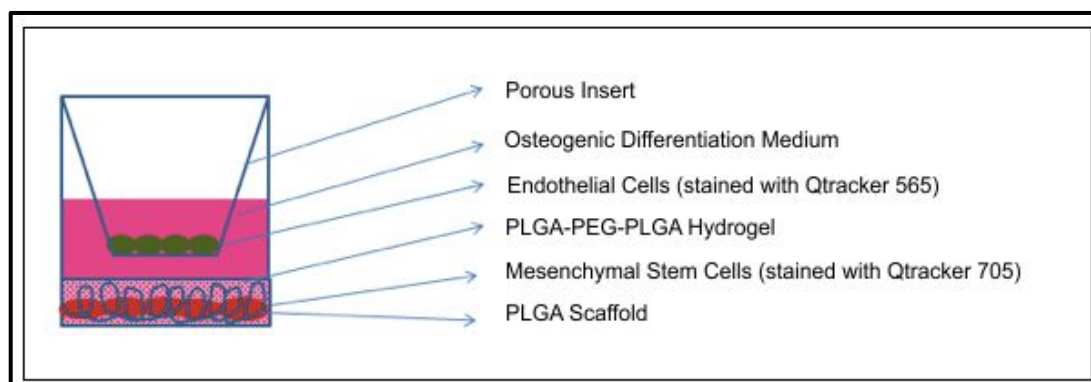
Figure 1.14. Experimental design used in *in vitro* studies.

The strategy proposed in this study can decrease the rate of failure of bone healing due to the insufficient vascularization and shortens the time for post-surgery recovery time of patients by accelerating the process of healing of bone defect.

This study is novel for the use of biphasic tissue engineering scaffold which consists of a fibrous PLGA scaffold base and PLGA-PEG-PLGA hydrogel that make sustained release possible. In literature search, no study was found about the effects of GS4012 on stem cells and its use for tissue engineering strategies. *In vitro* experimental model that was designed to be used in this study is a novel experimental model for tissue engineering strategies that has not been used before. In addition, this tissue engineering design can decrease the demand for implants and prostheses.

2. MATERIALS

2.1. CHEMICALS

- Rat Endothelial Cell Basal Medium (Cell Application, USA)
- Dulbecco's Phosphate Buffer Saline (DPBS) (Gibco, Germany)
- MEM Alpha Medium (1X) (Gibco, Germany)
- Primocin (100 µg/ml) (InvivoGen, USA)
- Trypsin-EDTA (Sigma-Aldrich Corporation, Germany)
- Fetal Bovine Serum (FBS) (Gibco, Germany)
- Penicillin-Streptomycin (Sigma-Aldrich Corporation, Germany)
- Amphotericin (Sigma-Aldrich Corporation, Germany)
- Prolong Gold Antifade Reagent (Invitrogen, USA)
- DAPI Molecular Probes – Invitrogen, USA)
- Dichloromethane (Merck Millipore, USA)
- Isopropanol (Merck Millipore, USA)
- Formaldehyde (Fluka, Switzerland)
- Tween® 20 (AppliChem, Germany)
- Glutaraldehyde (Sigma-Aldrich Corporation, Germany)
- Cacodylic Acid Buffer (Sigma-Aldrich Corporation, Germany)
- Ketamine (Sigma-Aldrich Corporation, Germany)
- Xylazine (Sigma-Aldrich Corporation, Germany)
- Sodium Citrate (Merck Millipore, USA)
- Formic Acid (Merck Millipore, USA)

2.2. KITS

- CellTiter 96® Aqueous One Solution Cell Proliferation Assay Kit (MTS, Promega, USA)
- Alkaline Phosphatase (ALP) Assay Kit (SIGMAFAST^{TM})

- RNA Extraction Kit (GeneJET RNA Purification Kit, Thermo Scientific, USA)

- Sensiscript RT Kit (Qiagen, Germany).

- Maxima SYBR Green/ROX qPCR Master Mix (Thermo Scientific, USA)

- Rat VEGF Picokine^{TM} Elisa Kit (R&D Systems, USA)

- Endothelial Tube Formation Assay (Cell Biolabs, Inc.) Kit

2.3. CD MARKER ANTIBODIES

- CD90 Antibody (BD Pharmingen, USA)

- CD45 Antibody (BD Pharmingen, USA)

- CD29 Antibody (BD Pharmingen, Philippines)

- CD11a Antibody (Abcam, USA)

- CD31 Antibody (Abcam, USA)

2.4. OTHER REAGENTS

- Alizarin Red Staining (Sigma Aldrich, Germany)

- Oil Red O (ScienceCell, USA)

- Sodium Pyruvate (Sigma-Aldrich Corporation, Germany)

- Alcian Blue (American MasterTech, USA)

- von Kossa Staining (Sigma-Aldrich Corporation, Germany)

- Silver Nitrate Solution (500 µl) (Sigma-Aldrich Corporation, Germany)

- Sodium Thiosulfate (Sigma-Aldrich Corporation, Germany)

- Protease Inhibitor (Sigma-Aldrich Corporation, Germany)

- RIPA Lysis Buffer (Santa Cruz, USA)

- PLGA-PEG-PLGA Copolymer (Sigma-Aldrich Corporation, Germany)

- VEGF Inducer, GS4012 (Sigma-Aldrich Corporation, Germany)

- Qtracker® 565 and Qtracker® 705 Cell Labeling Kits (Molecular Probes, USA)

- Poly (D, L-lactide-co-glycolide) (PLGA) (Sigma-Aldrich Corporation, Germany)

- Collagen Type I (Millipore, USA)

- Histopaque 1083 (Sigma-Aldrich Corporation, Germany)

- StemXVivo®Osteogenic Supplement (R&D Systems, Inc., USA)

- StemXVivo®Chondrogenic Supplement (R&D Systems, Inc., USA)

- StemXVivo®Adipogenic Supplement (R&D Systems, Inc., USA)

- Dil-Acetylated-Low Density Lipoprotein (Dil-AcLDL) (Molecular Probes, USA).

- Goat Anti Mouse Secondary Antibody Alexa Fluor 555 (ThermoFisher Scientific, USA)

- CD 31 Mouse Anti Rat Primer Antibody (LifeSpan Biosciences, Inc.)

- Bone-Specific Genes (Collagen Type I, Runx2, ALP, Osteocalcin, VEGF, CD 31) (Macrogen, South Korea)

2.5. INSTRUMENTS

- Laminar Flow Cabinet (ESCO Lab. Culture Class II Biohazard Safety Cabinet 2A, Singapore)

- CO_2 Incubator (Thermo Scientific, USA)

- Fluorescence Microscope (Carl Zeiss, USA)

- Brightfield Microscope (Carl Zeiss, USA)

- Inverted Microscope (Nikon Eclipse TC 100, USA)

- Scanning Electron Microscope (Carl Zeiss EVO, Germany)

- Confocal Microscope (Leica, Germany)

- Centrifuge (Hettich micro 22R and Sigma 2-5 centrifuge, Germany)

- Nanodrop Spectrophotometer (Thermo Scientific, USA)

- pH Meter (Hanna, Germany)

- Hemacytometer (Hausser Bright-Line, USA)

- Vortex (Stuart, UK)

- FACS Calibur (BD Biosciences, USA)

- ELISA Plate Reader (Bio-Tek EL x 800, USA)

- CFX96 Touch™ Sequence Detection System (Bio-Rad, USA)

- Sputter Coater (Bal-tec SCD 005, Germany)

- Confocal Microscope (Leica, Germany)

- Microtome (Leica RM 2245 model; Leica Instruments, Germany)

- 8.0 µm ThinCert™ Inserts (Greiner Bio One, Germany)
- 12 Deep Well Cell Culture Plates (ThinCert ™ Multiwell Plates, Greiner Bio One, Germany).

3. METHODS

3.1. PREPARATION OF FIBROUS SCAFFOLD BASES

To prepare fibrous scaffolds, the wet spinning setup was established (Figure 3.1). It is composed of syringe pump fixed in vertical plane and turntable in the horizontal plane. Syringe pump has the ability to fix the flow rate of PLGA/dichloromethane solution and turntable can help to rotate coagulation bath in the horizontal plane. The flow rate of solutions was fixed at 15 μl/min via syringe pump.

Figure 3.1. Wet spinning setup.

Different concentrations (4, 8, 12, 15, 20, 25 and 30 per cent) of PLGA (PLA:PGA 75:25) (M_w=66,000-107,000) were prepared by using different concentrations of isopropanol – dH$_2$O coagulation baths (75:25, 60:40, 50:50, 40:60, 25:75) by using wet-spinning technique. The PLGA was dissolved in dichloromethane at concentrations of 4, 8, 12, 15, 20, 25 and 30 per cent and the solutions were coagulated in IP:DW coagulation baths via syringe and syringe pump for the construction of the tissue engineering scaffold in the fibrous structure.

After wet-spinning, these samples were incubated in coagulation bath at 4 °C overnight. Then, they were frozen at -80 °C for 6 hours and freeze-dried for 2 days. Then, they were cut into equal circular pieces to be used for *in vitro* studies.

3.2. CHARACTERIZATION OF FIBROUS PLGA SCAFFOLDS

3.2.1. Scanning Electron Microscopy

After the preparation of different concentrations of PLGA scaffolds in coagulation baths, they were coated with gold by sputter coater and samples were analyzed with scanning electron microscope to determine their surface characteristics.

3.2.2. Contact Angle Analysis

According to the results of SEM, PLGA samples at 20, 25 and 30 per cent concentrations were determined to be used with 75:25, 60:40, 50:50 IP:DW coagulation baths. For the measurement of the contact angles on smooth surfaces, different concentrations (20, 25 and 30 per cent) of PLGA solutions were prepared, poured onto 1 x 1 cm lamella, and dried at room temperature and expected to form a film. After that, each of the prepared samples were incubated in coagulation baths with a composition of 75:25, 60:40, 50:50 (IP: DW) at 4 °C overnight. Then, they were washed with distilled water and allowed to dry and used for contact angle measurement.

3.2.3. Degradation of PLGA Scaffolds

According to the results of SEM, the concentrations of PLGA in different coagulation baths in which the best fiber formation was observed, were selected and degradation studies were carried on by using these selected PLGA concentrations. After the preparation of fibers, they were cut into small pieces and weighed. Then, they were dipped into 5 mL of 0.09 per cent sodium azide in phosphate buffered saline solution (0.0095 M PO_4, pH: 7.5) in the sterile centrifuge tubes and they were placed into the shaking water bath at 37 °C. After 7, 15, 30, 60, 90 and 120 days of incubation, pH of phosphate buffered saline

solution was measured for the observation of the decrease of pH values due to the degradation of PLGA scaffolds. After that, PLGA scaffolds were lyophilised and measurements of their weights were also recorded. According to that, the rate of degradation of PLGA scaffolds was evaluated.

3.2.4. Scanning Electron Microscopy of Wet Spun PLGA Scaffolds After The Degradation Analysis

The degraded PLGA scaffolds that were examined to evaluate the changes in their pH values, and their weights, were dried and covered with 10 nm gold after 120 days and analyzed by scanning electron microscopy.

3.3. RELEASE PROFILE OF GS4012

For the second phase of the tissue engineered scaffold, a PLGA-PEG-PLGA solution (0,2 g/mL) was prepared by dissolving the copolymer in phosphate buffered saline (PBS) solution and mixed with 100 μg/mL GS4012 VEGF activator [85]. Gel formation was obtained at 37 °C. PBS (100μL) was added onto the hydrogel as a release medium of GS4012. Release of GS4012 from the hydrogel was analyzed by spectrophotometric methods at 1st, 2nd, 3rd, 5th, 7th, 9th, 12th, 15th, 20th and 27th days at 252 nm. The calibration curve was constructed by measuring the absorbance of GS4012 concentrations, prepared at serial dilutions of 10-500 μg/mL, at 252 nm. The slope of the calibration curve was utilized for the calculation of the amount of GS4012 released from the hydrogel.

3.4. *IN VITRO* CELL CULTURE STUDIES

3.4.1. Isolation of Mesenchymal Stem Cells From Rat Bone Marrow (rBMSCs)

Mesenchymal stem cells (MSCs) were obtained from bone marrow of 6-7 weeks old, Sprague-Dawley rats. Briefly, after decapitation of the rats, the femurs and tibias were taken out.

The femurs and tibias were washed with complete medium which contains minimum essential medium (α MEM) including 1,000 unit/mL penicillin-streptomycin-amphotericin, and then bone marrow in the femoral and tibial bones was transferred to the centrifuge tubes by washing inside of the bones with complete medium using the sterile syringe and centrifuged at 2,000 rpm for 5 minutes. Then, the pellet was dissolved in complete medium, transferred into T25 culture flask and incubated in CO_2 incubator at 37 °C, in 5 per cent CO_2 and 90 per cent humidity. The medium on the bone marrow-derived mesenchymal stem cells (rBMSCs) was replenished twice a week until confluency was reached.

3.4.2. Isolation of Endothelial Cells From Rat Peripheral Blood (rPBECs)

Endothelial cells were isolated from peripheral blood of 6-7 weeks old, Sprague- Dawley rats. Briefly, histopaque 1083 was used to get peripheral blood mononuclear cells. It (15 mL) was added into centrifuge tubes and whole blood (15 mL) was layered onto the histopaque 1083 surface carefully. They were centrifuged at 400xg for exactly 30 minutes at room temperature. After centrifugation, the opaque interface layer containing the mononuclear cells was transferred into a clean 50 mL conical centrifuge tube. Then, PBS (15 mL) was added into tube and it was centrifuged at 250xg for 10 minutes. The supernatant was discarded and the cell pellet was resuspended in 4-5 mL of PBS and they were centrifuged at 250xg for 10 minutes. The supernatant was discarded and washing steps were applied to remove histopaque 1083 from the mononuclear cells. After the washing step, the cells were resuspended in cell culture medium. Then, they were transferred to a T25 flask and incubated at 37 °C, in 5 per cent CO_2 and the medium was changed every other day until confluency was reached.

3.4.3. Qdot® Staining of rBMSCs and rPBECs

Positively charged slides were sterilized in 70 per cent ethanol for an hour, then washed with PBS and air dried. rPBECs ($1x10^5$) in endothelial cell growth medium and rBMSCs ($1x10^5$) in α MEM were seeded onto the slides. The next day, Qtracker® 565 and Qtracker® 705 Cell Labeling Kits were applied on the slides. For this analysis, the mixture of component A (1.5 µL) and component B (1.5 µL) of staining kit was prepared both in 200 µL endothelial

cell growth medium and in 200 µL α MEM. Media on the slides were discarded and the new media containing component A and component B of staining kit were dropped onto the slides. They were incubated for 2 hours and slides were washed with PBS. Cells were fixed with 3.7 per cent formaldehyde for 30 minutes and they were washed with dH_2O and exposed to 1:1,000 diluted DAPI (1 mg /mL) for 15 minutes. Slides were again washed with dH_2O. ProLong Gold Antifade Reagent was added onto the cells. Then, they were covered with coverslip and left in the dark at room temperature overnight. The next day, they were examined under the confocal microscope.

3.4.4. Characterization of rBMSCs

3.4.4.1. Characterization of rBMSCs by Flow Cytometry Analysis

rBMSCs were trypsinized and counted with hemacytometer when they reached to the 3rd passage. Cells ($5x10^5$) for each antibody and negative control were put into FACS tubes. PBS (2 mL) was added into FACS tubes and centrifuged at 2,000 rpm for 5 minutes. Cell pellet was resuspended in 200 µL PBS. Then, they were incubated with the antibodies, CD29, CD45, CD11a, CD90 and CD31 cell surface markers at 4 °C for an hour. No antibodies was added to the negative control tube. Then, cells were washed with 2 mL physiological saline solution (PBS) and centrifuged at 2,000 rpm for 5 minutes to remove excess antibodies. After centrifugation, they were resuspended in 400 µL PBS and samples were analyzed in a flow cytometer (FACSCalibur, Becton Dickinson, USA).

3.4.4.2. Characterization of rBMSCs

To prove that the cells isolated from bone marrow were mesenchymal stem cells, $2x10^4$ cells/well were seeded onto the cell culture plate. Growth medium (GM) included 10 per cent fetal bovine serum and 1 per cent penicillin and streptomycin in α MEM medium was added onto the cells and incubated for 3 days. Then, the medium of each wells was refreshed with either growth medium as control group or differentiation medium that was either osteogenic, chondrogenic or adipogenic medium required for rBMSCs differentiation. For the preparation of osteogenic, chondrogenic and adipogenic mediums, osteogenic

supplement in 1:20 dilution, chondrogenic supplement in 1:100 dilution and adipogenic supplement in 1:100 dilution were used, respectively, in 50 mL α MEM included 10 per cent FBS, 1 per cent penicillin-streptomycin.

3.4.4.2.1. Osteogenic Differentiation

Von Kossa staining was performed for the determination of mineralized nodules after 7, 14 and 21 days from the initiation of bone differentiation. Cells were fixed with 3.7 per cent formaldehyde for 45 minutes. Then, they were washed with dH_2O and 5 per cent silver nitrate solution was added onto the cells and they were left under UV light for 1 hour. Then, the wells were washed 2 times with dH_2O and the reaction was stopped with 5 per cent sodium thiosulfate solution that was followed by the washing step with dH_2O. After the reaction was stopped, cells were stained with nuclear fast red dye for 5 minutes. The wells were photographed and the mineralized areas were examined under the inverted microscope.

Moreover, alizarin red staining was performed at days 7, 14 and 21 for the determination of mineralized nodules. For this staining, cells were fixed with 3.7 per cent formaldehyde and waited for 45 minutes at room temperature. Then, they were washed twice with dH_2O. Alizarin red solution was added and kept in the dark for 45 minutes at room temperature. After washing steps, the stained cells were photographed under the inverted microscope.

3.4.4.2.2. Chondrogenic Differentiation

Alcian blue staining was applied at days 7, 14 and 21. Alcian Blue PAS Stain Kit was used after the fixation of cells with 3.7 per cent formaldehyde. Then, the wells were washed with dH_2O and alcian blue was added. It was waited for an hour at room temperature. After an hour, they were washed twice with dH_2O and then 1 per cent periodic acid solution was added and incubated for 10 minutes at room temperature. After washing steps, Schiff reagent was put into the wells and waited for 10 minutes at room temperature. After washing steps with hot tap water for 2 minutes, haemalum mayer solution was added to stain the nucleus of the cell and washed after 30 seconds. Then, they were washed with tap water for a while. Finally, the photos of the wells were taken and the stained areas were examined under the inverted microscope.

3.4.4.2.3. Adipogenic Differentiation

After 7, 14 and 21 days of adipogenic differentiation, Oil Red O staining was performed to observe the fat storage of the cells. For that reason, cells were fixed with 3.7 per cent formaldehyde for 45 minutes. After washing step with dH_2O, the cells were incubated in 60 per cent isopropanol for 5 min. After the extraction of isopropanol, the wells were allowed to dry. The Oil Red O dye, which was dissolved in isopropanol at a concentration of 3 mg / mL, was then added to the wells by mixing with a 3:2 ratio of water and left in the dark for 30 minutes at room temperature. After washing steps, the stained areas were examined under the inverted microscope.

3.4.5. Characterization of rPBECs

3.4.5.1. Characterization of rPBECs by DiI-Acetylated-low density lipoprotein (DiI-AcLDL)

Endothelial cells were characterized by their capacity to uptake Dil-acetylated-low density lipoprotein (Dil-AcLDL). To observe this metabolism, acetylated-low density lipoprotein (Ac-LDL) labeled with1,1'-dioctadecyl-3,3,3',3'-tetramethly-indocarbocyanine perchlorate fluorescent probe was used in Dil-Ac-LDL form. Dil-Ac-LDL (10 µg/mL) was put into the cell culture plates and incubation was started at 37 °C for 4 hours. Then, it was analyzed under the fluorescence microscope.

3.4.5.2. In vitro Angiogenesis Assay

For the characterization of isolated endothelial cells, endothelial tube formation assay (Cell Biolabs, Inc.) kit was used. For this process, ECM gel solution secreted by Engelbreth-Holm-Swarm (EHS) tumor cells was used. Gel material, which is in liquid state at low temperatures, was added to 96-well cell culture plates and gelled at 37 °C for 30 minutes. After that, endothelial cells were seeded onto the gels, and then incubated at 37 °C for 18 hours.

Then, Calcein AM stain was added into each well and incubated for 30 minutes at 37 °C. After washing steps, cells were visualized under the fluorescence microscope to observe tube formation.

3.4.5.3. Indirect Immunofluorescence of CD31 (PECAM-1)

rPBECs ($5x10^5$) were seeded onto the positively charged slides. After 2 days, slides were washed with PBS, and they were fixed with 3.7 per cent formaldehyde for 15 minutes. After fixation, absolute methanol was added and waited at -20°C for 10 minutes. Then, the samples were washed with PBS and exposed to 0.1 per cent Triton X 100 for 10 minutes. After that, blocking solution (1 per cent BSA and 0.1 per cent Tween 20 in PBS) was used to incubate cells for an hour. Mouse anti rat primer antibody was diluted at a ratio 1:500 with 0.1 per cent Tween 20 in PBS. Then, diluted antibody (100 µL) was added and samples were incubated overnight. After incubation, goat anti mouse secondary antibody Alexa Fluor 555 (100 µL) was diluted at 1:200 with 0.1 per cent Tween 20 in PBS and added onto the slides and waited for an hour. Then, the slides were exposed to washing step with PBS and DAPI diluted at 1:1,000 was added onto the slides for 15 minutes. Then, they were washed again. The ProLong Gold Antifade Reagent was added onto cells and covered with coverslip and left in the dark at room temperature overnight. The next day, it was examined by using confocal microscope.

3.4.5.4. Migration of rPBECs

For this analysis, rPBECs (100,000 cells/well) were seeded onto the insert that was placed into the wells of cell culture plates and growth media was added onto these cells. In order to test the effect of GS4012, the medium containing 5 µg / mL GS4012 was added into the wells [85]. In addition, the medium containing 30 ng / mL VEGF was added into the wells as a positive control and the growth medium was added into the wells as a negative control. The cells were allowed to migrate for 72 hours. Then, the cells on the insert were fixed and stained with crystal violet dye. After that, the cells at the top of the insert were wiped off with a cotton swab and the cells passing under the bottom of the insert were observed by using brightfield microscopy.

3.5. *IN VITRO* CELL – MATERIAL INTERACTIONS

3.5.1. Preparation of Biphasic Scaffold with rBMSCs and rPBECs

Previously prepared PLGA fibers were put into 12-well plates and sterilized with 70 per cent ethanol. After washing the scaffolds with PBS, they were dried under the laminar flow cabinet. Next, rBMSCs and rPBECs were detached from the flasks by trypsinization and counted by hemacytometer. After the optimal cell density was determined, rBMSCs were seeded on PLGA scaffolds in 12 deep well cell culture plates. After the attachment of rBMSCs, they were stained with Qtracker 705. Also, rPBECs were seeded into the insert that were placed into the wells of the cell culture plates. After rPBECs attachment, they were stained with Qtracker 565. Then, PLGA- PEG- PLGA solution was added onto rBMSCs seeded PLGA scaffold and polymerization was achieved at 37 °C. After the polymerization, the insert seeded with rPBECs was transferred and placed into 12 deep well cell culture plates in which PLGA scaffolds were seeded with rBMSCs.

3.5.2. Determination of Cell Proliferation on Wet Spun PLGA Scaffolds by MTS Assay

CellTiter 96® AQueous One Solution Cell Proliferation Assay (MTS) was applied onto samples (20-60-40, 25-60-40, 30-60-40, 30-75-25 and 25-75-25) to determine the cell density inside these scaffolds. Briefly, the selected samples were sterilized with 70 per cent ethanol for 2 hours. Then, they were washed with PBS and left in CO_2 incubator at 37 °C, 5 per cent CO_2 and 90 per cent humidity in complete medium. The next day, rBMSCs (20,000 cells/well) were seeded onto PLGA scaffolds. Cells were incubated at 37 °C, 5 per cent CO_2 and 90 per cent humidity throughout 21 days on these scaffolds. At days 7, 14 and 21, MTS reagent diluted with α MEM at 1:6 ratio was added onto each scaffolds and they were incubated at 37 °C in CO_2 incubator for 2.5 hours. Then, their absorbance values were obtained at 490 nm by using Elisa Plate Reader and cell numbers were also calculated using calibration curve of rBMSCs.

3.5.3. Investigation of Cell – Scaffold Interaction by Scanning Electron Microscopy

The selected scaffolds were washed with PBS and left in an incubator at 37 °C in complete medium. The next day, rBMSCs (20,000 cells/scaffold) were seeded onto them and incubated throughout 21 days of incubation. At days 14 and 21, the scaffolds were washed with cacodylic acid buffer and fixed with 2.5 per cent glutaraldehyde solution for 1 hour at room temperature. After that, they were washed again with a solution of cacodylic acid buffer. Then, the samples were dried at room temperature before SEM analysis and coated with 10 nm gold. Gold coated specimens were examined by scanning electron microscope and evaluated for cell attachment.

3.5.4. Confocal Microscopy Analysis of Cell Seeded 20-60-40 PLGA Scaffolds

Migration of rPBECs through the scaffold was observed by confocal microscopy at days 7, 14 and 21. For this analysis, rPBEC cells (100,000) were seeded into the insert having 8.0 μm pores and placed inside the wells of the cell culture plates. After the cell attachment, they were stained with Qtracker 565. Also, rBMSC (100,000) were seeded in PLGA scaffolds in 12 deep well cell culture plates. After the attachment of rBMSCs, they were stained with Qtracker 705. In order to test the effect of GS4012 on cell migration, PLGA- PEG- PLGA solution mixed with GS4012 (5μg/mL / day) was added onto the cell seeded PLGA scaffolds [85]. In addition, PLGA- PEG- PLGA solution containing 30 ng / mL VEGF was added as a positive control and PLGA- PEG- PLGA solution without GS4012 or VEGF was added as a negative control. After the addition of PLGA- PEG- PLGA solutions onto the rBMSCs seeded PLGA scaffold, the polymerization of the hydrogel was achieved at 37 °C within 15 minutes. Then, the porous insert seeded with rPBECs was placed into 12 deep well cell culture plates in which PLGA scaffolds were seeded with rBMSCs. After 7, 14 and 21 days of incubation, cells in the wells were incubated for 30 minutes at room temperature with 3.7 per cent formaldehyde for fixation. Then, the cells were washed with dH_2O and stained with DAPI (1 mg / mL) diluted at 1:1,000 and waited for 15 minutes. The cells were washed again and Prolong Gold Antifade reagent was added. Then, the cells were covered with coverslip and left in the dark at room temperature overnight. The next day, it was examined in a confocal microscope.

3.5.5. Scanning Electron Microscopy Analysis of Cell Seeded 20-60-40 PLGA Scaffolds

Wet spun PLGA scaffolds (20-60-40) were washed with PBS and left in an incubator at 37 °C, 5 per cent CO_2 and 90 per cent humidity in complete medium. The next day, rBMSCs (100,000) were seeded onto these scaffolds and incubated at 37 °C, 5 per cent CO_2 and 90 per cent humidity throughout 20 days of incubation. At days 10 and 20, cells were washed with cacodylic acid buffer solution and fixed with 2.5 per cent glutaraldehyde solution for 1 hour at room temperature. After that, they were washed again with a solution of cacodylic acid buffer. Then, the samples were dried at room temperature before SEM analysis and coated with 10 nm gold. Gold coated specimens were examined by scanning electron microscope and evaluated for cell attachment.

3.5.6. Cell Differentiation on Wet Spun 20-60-40 PLGA Scaffolds

3.5.6.1. Osteogenic Differentiation of rBMSCs on PLGA Scaffolds

After cell seeding, osteogenic differentiation medium (α MEM with 1 per cent penicillin streptomycin, 10 per cent FBS, 1:20 StemXVivo^{TM} osteogenic supplement) was added, and the plates were incubated in the CO_2 incubator for 21 days. The medium was replenished twice a week.

3.5.6.2. Cell Proliferation on PLGA Scaffold by MTS Assay

In this analysis, 20-60-40 samples were cut into small pieces and put into 24-well cell culture plates and sterilized for 2 hours. Then, the scaffolds were washed with PBS and left in incubator at 37 °C, 5 per cent CO_2 and 90 per cent humidity in complete medium. The next day, rBMSCs (50,000) were seeded onto these scaffolds and complete medium was added. Cells were incubated on PLGA scaffolds for 21 days of incubation at 37 °C, 5 per cent CO_2 and 90 per cent humidity. At day 3, the medium was changed with osteogenic medium. At days 4, 7, 14 and 21, MTS reagent diluted with α MEM at a ratio 1:6 was added onto each scaffold and incubated at 37 °C, 5 per cent CO_2 incubator for 2,5 hours and their absorbances

were measured at 490 nm using Elisa Plate Reader. Cell numbers were calculated using calibration curve of rBMSCs.

3.5.6.3. Alkaline Phosphatase Assay

Alkaline phosphatase assay was used to measure the conversion of p-nitrophenyl phosphate to p-nitrophenol in the presence of alkaline phopshatase by using Elisa Plate Reader. ALP assay was applied at 4, 7, 14 and 21 days after the PLGA scaffolds were seeded with rBMSCs. For this analysis, 20-60-40 samples were cut into small pieces and sterilized for 2 hours in 24-well cell culture plates. After sterilization, they were washed with PBS and incubated overnight in complete medium in CO_2 incubator. The next day, rBMSCs (50,000) were seeded onto 20-60-40 PLGA scaffolds and complete medium was added. Cells were incubated on these scaffolds throughout 21 days of incubation at 37 °C, 5 per cent CO_2 and 90 per cent humidity. After day 3, osteogenic medium was added.

After 4, 7, 14 and 21 days of incubations, cells were washed with PBS. p-Nitrophenyl Phosphate (pNPP) Tablet (silver foil) and Tris Buffer Tablet (gold foil) were dropped into an appropriate container containing 20 ml of water. The solution was vortexed until the complete dissolution of tablets was achieved. pNPP substrate solution (1 mL) was added to each well and incubated in the dark for approximately 45 minutes at room temperature. After the incubation period, absorbance values were measured at 405 nm. Then, the amount of total protein isolated by using RIPA solution from the cells in which ALP activity was measured, was analyzed at 562 nm with Smart™ micro BCA protein assay kit to calculate the normalized values.

3.5.6.4. von Kossa Staining

The 20-60-40 samples were prepared and rBMSCs were seeded as described in section 3.5.6.3. At day 3, osteogenic medium was added onto the samples. At days 7, 14 and 21, von Kossa staining was applied for the determination of mineralized nodules. For this analysis, cells were fixed with 3.7 per cent formaldehyde for 45 minutes. Then, they were washed with dH_2O and silver nitrate solution was added onto the cells. They were left under UV light for 1 hour and the wells were washed twice with dH_2O.

The reaction was stopped with 5 per cent sodium thiosulfate solution. Then, the wells were again washed with dH$_2$O. Cells were stained with nuclear fast red dye for 5 minutes and the mineralized areas were photographed.

3.5.6.5. Real Time PCR Analysis

For this analysis, biphasic scaffold design was prepared with rPBECs and rBMSCs. rBMSCs (100,000) were seeded on PLGA scaffolds in 12 deep well cell culture plates and rPBEC (100,000) were seeded onto the insert having 8.0 μm pores that was placed into the cell culture plate. Then, the PLGA- PEG- PLGA solution mixed with GS4012 (5 μg/mL /day) and PLGA- PEG- PLGA solution without GS4012 were added onto the rBMSCs seeded PLGA scaffolds in 12 deep well cell culture plates, respectively [85]. After the addition of PLGA- PEG- PLGA solutions onto the cell-seeded PLGA scaffold, polymerization was observed at 37 °C, approximately within 15 minutes. After the polymerization, the porous insert seeded with rPBECs was placed into 12 deep well cell culture plates in which PLGA scaffolds were seeded with rBMSCs. At day 3, osteogenic medium was added onto the scaffolds. On the other hand, in the transwells, α MEM was used during 21 days of incubation period. After 7, 14 and 21 days of incubation, the expression levels of bone-specific genes (Collagen Type I, Runx2, ALP, Osteocalcin, VEGF, CD 31) were determined by Real Time PCR analysis. Briefly, total RNA was isolated from the cells on the scaffolds using RNA extraction kit (Thermo Scientific, USA) and then cDNA was produced from total mRNA using the Sensiscript RT Kit. Then, Real-Time PCR was performed using primers for bone-specific genes (Table 3.1) and Maxima SYBR Green Master Mix in CFX96 Touch^{TM} Real-Time PCR Detection System. The Real Time PCR results were normalized using the housekeeping gene, beta-actin. At the end of this study, the value of the expression results of the experimental group containing PLGA-PEG-PLGA hydrogel with GS4012 was divided into the value of the expression results of the control group containing PLGA-PEG-PLGA hydrogel without GS4012 and the graphs of fold change were plotted.

Table 3.1. Sequences of the primers used for the Real Time PCR.

Primers		Sequence (5'→3')
β-actin	F	TGTTGCCCTAGACTTCGAGC
	R	AACGCAGCTCAGTAACAGTCC
VEGF	F	CGACAGAAGGGGAGCAGAAA
	R	GCTGGCTTTGGTGAGGTTTG
ALP	F	CGTCATGCCCCAAAACGTAG
	R	GGTACTGACGGAAGAAGGGG
CD 31	F	CTGGGAGGTATCGAATGGGC
	R	CCCGAGACTGAGGAATGACG
Runx2	F	AACCACAGAACCACAAGTGC
	R	CTGAAGAGGCTGTTTGACGC
Osteocalcin	F	AAGTCCCACACAGCAACTCG
	R	GTCCTGGAAGCCAATGTGGT
Collagen Type I	F	AAACCTCTCTCGCCTCTTGC
	R	CAGGCTGGTGTGATGGGATT

3.5.6.6. Rat VEGF Elisa Assay

In this analysis, biphasic scaffold design was prepared as in the section 3.5.6.5 and incubated for 21 days. At day 3, osteogenic medium was added onto the scaffolds and replenished twice a week. During the replenishment of medium, old media were collected and kept at 20 °C until analyzed for the determination of the amount of secreted VEGF from the cells. After 7, 14 and 21 days, released VEGF amount was measured by Elisa Method.

3.6. *IN VIVO* STUDIES ON RAT MODEL: DETERMINATION OF BONE AND VASCULAR FORMATION

The study was approved by Yeditepe University Experimental Animal Ethics Committee (YÜDHEK). In this study, there were 5 groups (Table 3.2) and 6 rats were used for each group to determine bone and vessel formation. For *in vivo* studies, rBMSCs were grown and seeded (10^6 cells/scaffold) onto 20-60-40 wet-spun PLGA scaffolds (8 mm diameter). Briefly, after the general anesthesia of the rats with ketamine HCL (60 mg/kg) ve Xylazine (5 mg/kg), an 8 mm diameter cranial defect was created. Approximately, an 1.5 – 2 cm incision was made down to the periosteum overlying the calvarium.

Table 3.2. Group names and their features used *in vivo* studies.

Group No	Group Name	Group Explanation	The Amount of Rats
1	Only Biphasic Scaffold	PLGA scaffold base + PLGA-PEG-PLGA hydrogel	6
2	Biphasic Scaffold with GS4012	PLGA scaffold base + PLGA-PEG-PLGA hydrogel with GS4012	6
3	Biphasic Scaffold with Cells	PLGA scaffold base seeded with rBMSCs + PLGA-PEG-PLGA hydrogel	6
4	Biphasic Scaffold with Cells and GS4012	PLGA scaffold base seeded with rBMSCs + PLGA-PEG-PLGA hydrogel with GS4012	6
5	Control Group	No treatment	6

Then, PLGA scaffold or rBMSCs seeded PLGA scaffold was placed into the defect site. Then, PLGA-PEG-PLGA hydrogel or PLGA-PEG-PLGA hydrogel with GS4012 was added onto these scaffolds. Gelling of PLGA-PEG-PLGA was observed within 15 minutes. After the experimental groups mentioned above were prepared, the periosteum and the skin was separately sutured.

After 4 and 8 weeks of surgery, 3 rats in each group were sacrified by decapitation. After sacrification, the region of defect sites with surrounding tissue was harvested and prepared for histological evaluation. For the fixation of the tissues, 10 per cent neutral formaldehyde in 0.1 M phosphate buffer (pH 7.4) at 4 °C was used. Morse solution (10 per cent sodium citrate and 22.5 per cent formic acid) was used for decalcification process for 28 days. After rinsing the samples with tap water for 12 hours, dehydration of fixed tissues was carried out in alcohol series. When the samples were embedded into paraffin, they were sliced vertically with a thickness of 10 μm using a rotary microtome and calvaria sections were placed onto the slides that were coated with poly-L-lysine and Masson's Trichrome Staining Technique was applied to stain the slides. For histomorhometric analysis, the Cavalieri principle was used to estimate the volume of the bone and soft tissue.

3.7. STATISTICAL ANALYSIS

For this study, IBM SPSS Statistics 22 for statistical analysis (SPSS IBM, Turkey) programs were used. Kruskal Wallis test (post hoc Mann Whitney U test) was applied for comparison of the parameters in this study. The Mann-Whitney U test was performed to compare the two groups of parameters. Friedman Test (post hoc Wilcoxon sign test) was also used for intra-group comparisons of the parameters. Significance was assessed at $*p<0.05$ level for *in vitro* studies and $**p <0.5$, $***p <0.001$ levels for *in vivo* studies.

4. RESULTS

4.1. PREPARATION OF FIBROUS SCAFFOLD BASES

After wet spinning setup was established, different concentrations (4, 8, 12, 15, and 20 per cent) of PLGA (PLA:PGA 75:25) (M_w=66,000-107,000) were firstly prepared by using 75:25 concentration of isopropanol - dH_2O (IP:DW) coagulation bath by using wet-spinning technique (Figure 4.1).
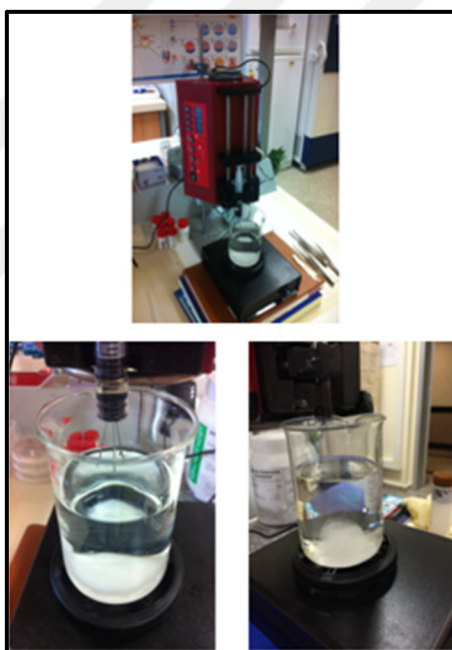
Figure 4.1. Wet spinning setup.

PLGA solutions at concentrations of 4, 8, 12 and 15 per cent had no fibrous structure for 75:25 IP:DW coagulation bath, but PLGA solutions at 20 per cent concentration resulted in the formation of fibers in 75:25 IP:DW coagulation bath with the fixed flow rate of solutions at 15 μl/min via syringe pump. Therefore, PLGA concentrations of 20 per cent or more were tried for further usage. PLGA concentrations (20 , 25 and 30 per cent) were prepared by using different concentrations of IP:DW coagulation baths (75:25, 60:40, 50:50, 40:60, 25:75) to observe the fiber structure. The formation of fiber structures were observed in 75:25, 60:40, 50:50 coagulation baths for 20, 25 and 30 per cent concentrations of PLGA

solutions. However, 40:60 and 25:75 IP:DW coagulation baths didn't work with these PLGA concentrations. These observations were proved by scanning electron microscopy.

4.2. CHARACTERIZATION OF FIBROUS PLGA SCAFFOLDS

4.2.1. Scanning Electron Microscopy

After preparation of different concentrations of PLGA scaffolds in different coagulation baths, they were coated with gold by Sputter Coater and samples were evaluated with scanning electron microscope. The results showed that 4, 8, 12 and 15 per cent PLGA concentrations did not exhibit any fibrous structure in 75-25 IP:DW coagulation baths (Figure 4.2). The images of 4 per cent PLGA concentrations were not obtained. However, the expected fiber structure was obtained with 20 per cent concentration of PLGA in 75-25 IP:DW coagulation baths. Thus, 20 per cent, 25 per cent and 30 per cent concentrations were tried with 75:25, 60:40, 50:50, 40:60 and 25:75 IP:DW coagulation baths. According to the results, no fibrous structure was observed in the 40:60 and 25:75 coagulation baths for all concentrations and further studies were continued with 75:25, 60:40 and 50:50 coagulation baths. PLGA solutions at concentrations of 20, 25 and 30 per cent showed the improved fiber structure in IP:DW coagulation baths with the compositions of 75:25, 60:40, 50:50 and the fixed flow rate of solutions at 15 μl/min via syringe pump (Figures 4.3-4.5). However, 60:40 and 75:25 IP: DW coagulation baths were more successful in wet spinning regardless of the PLGA concentrations. As shown in Figure 4.4a by the arrows in the scanning electron micrographs of 25-50-50 sample, fiber breaks were observed leading to the presence of unsuccessful spinning of 25 per cent PLGA concentration in 50:50 IP:DW coagulation bath. Generally, fibers were continuous except for the sample of 25-50-50.
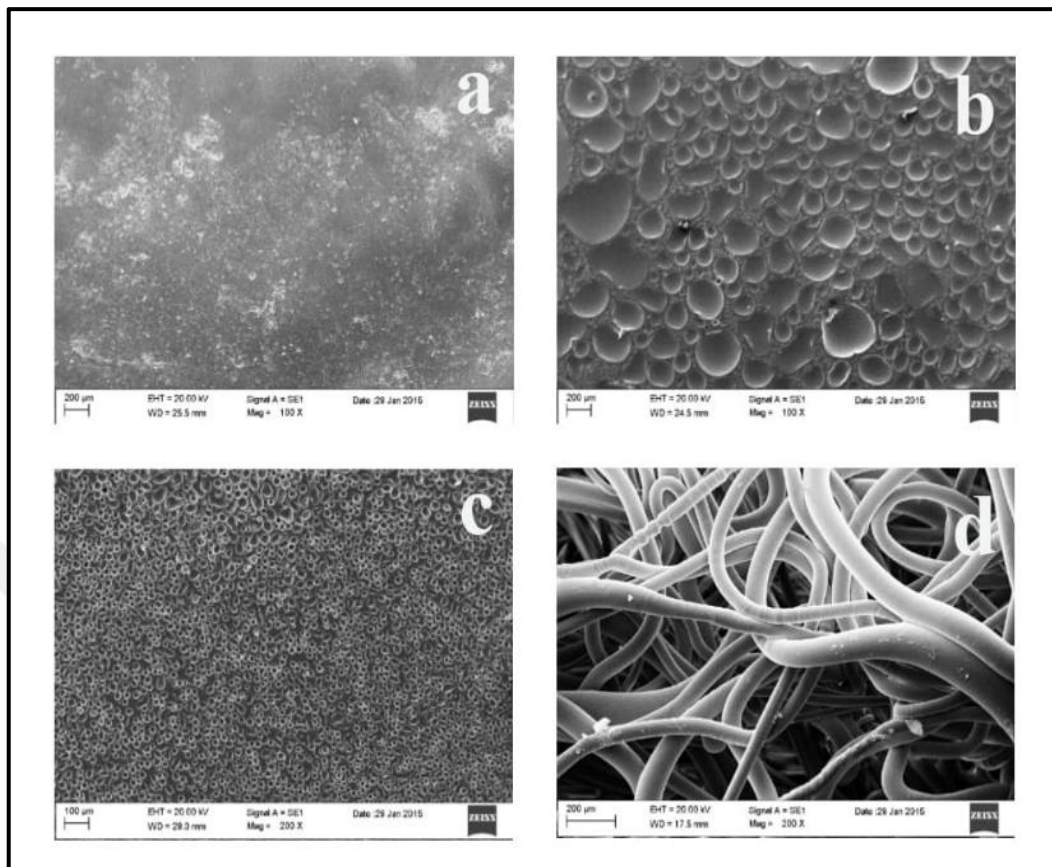
Figure 4.2. Scanning electron micrographs of wet-spun PLGA at different concentrations a) 8 (100X magnification) b) 12 (100X magnification) c) 15 (200X magnification) d) 20 (200X magnfication).
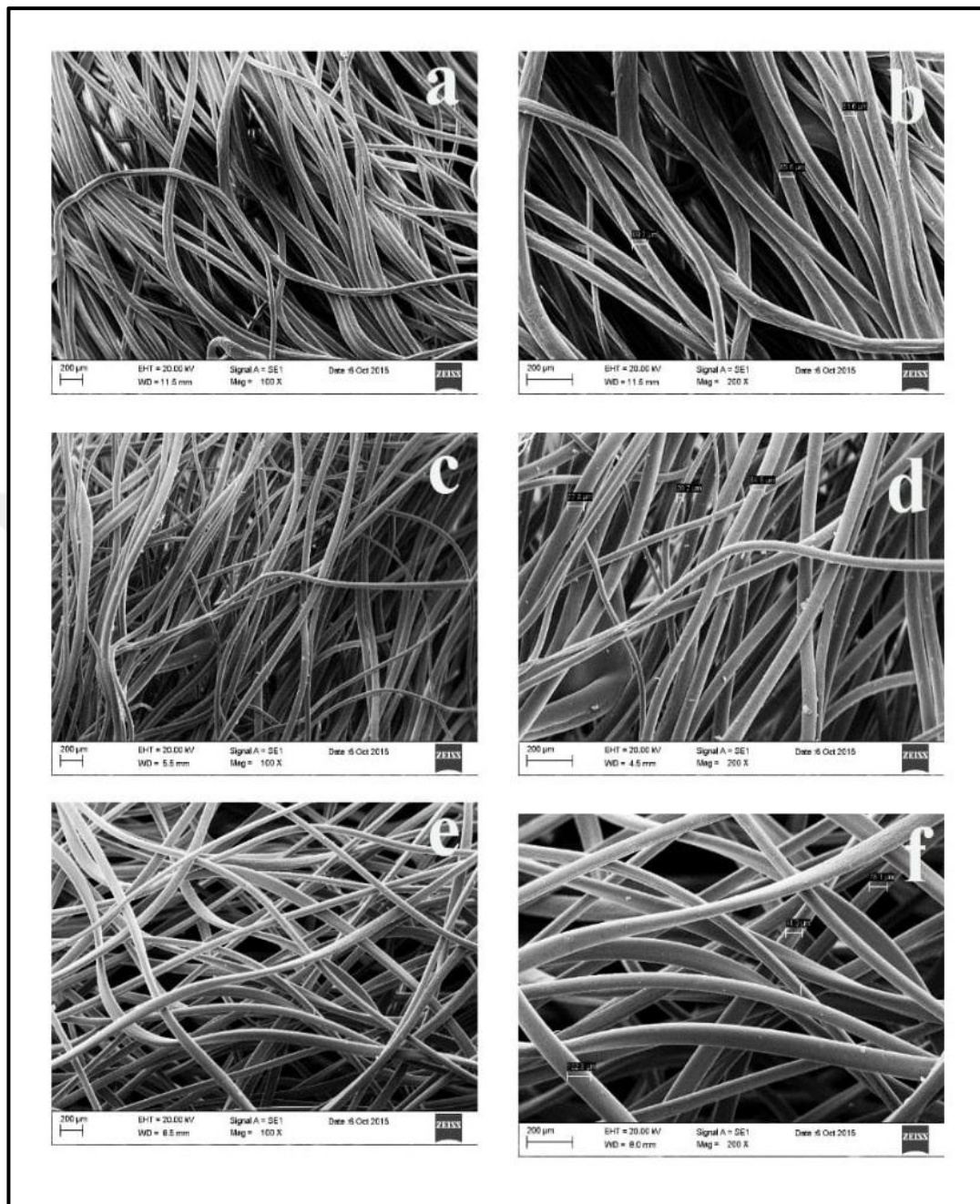
Figure 4.3. Scanning electron micrographs of wet-spun PLGA (20 per cent) in (a, b) 50:50, (c, d) 60:40, (e, f) 75:25 (Isopropanol: dH2O) coagulation baths. (a, c, e) 100X magnification, (b, d, f) 200X magnification.
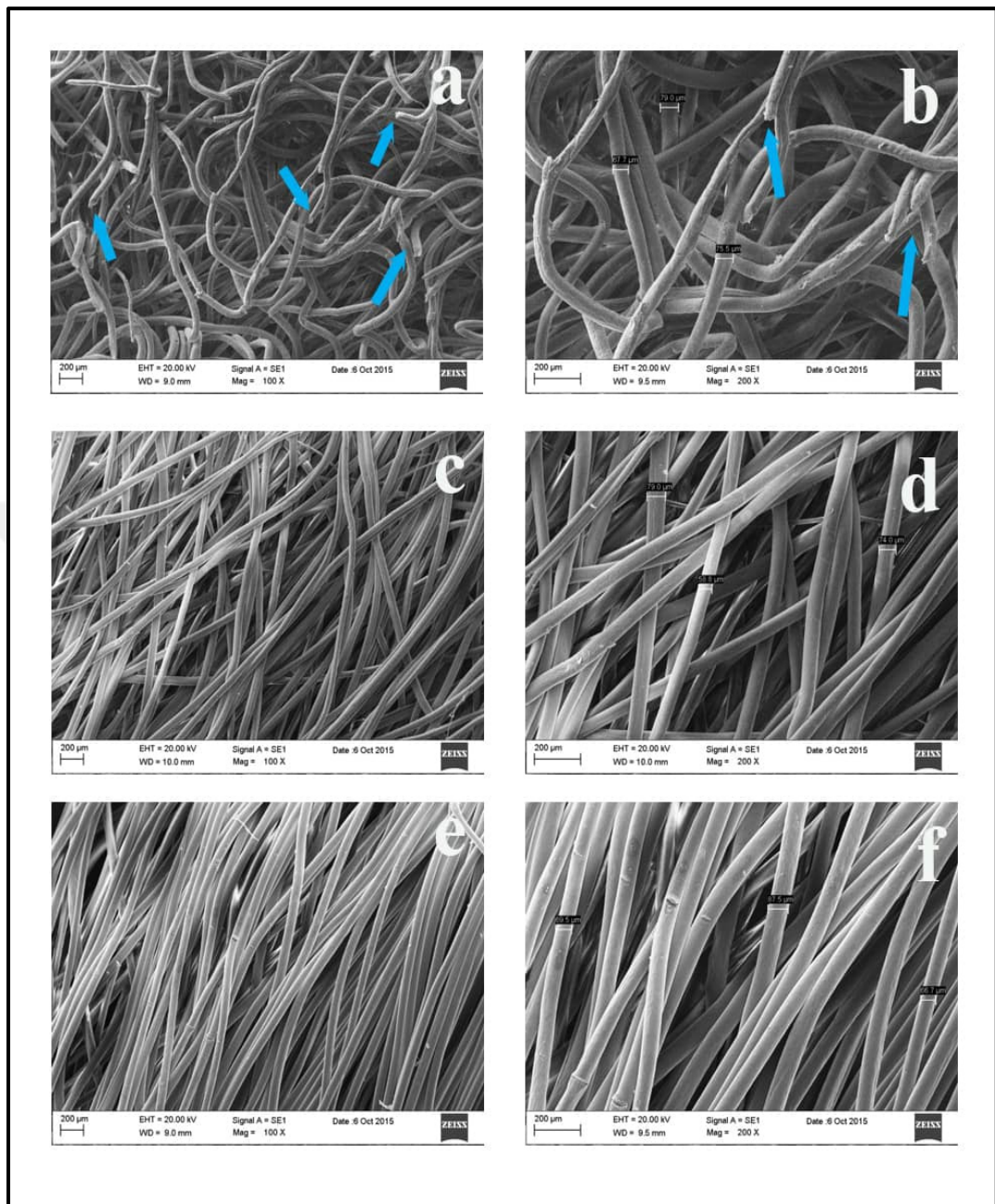
Figure 4.4. Scanning electron micrographs of wet-spun PLGA (25 per cent) in (a, b) 50:50, (c, d) 60:40, (e, f) 75:25 (Isopropanol: dH2O) coagulation baths. (a, c, e) 100X magnification, (b, d, f) 200X magnification.
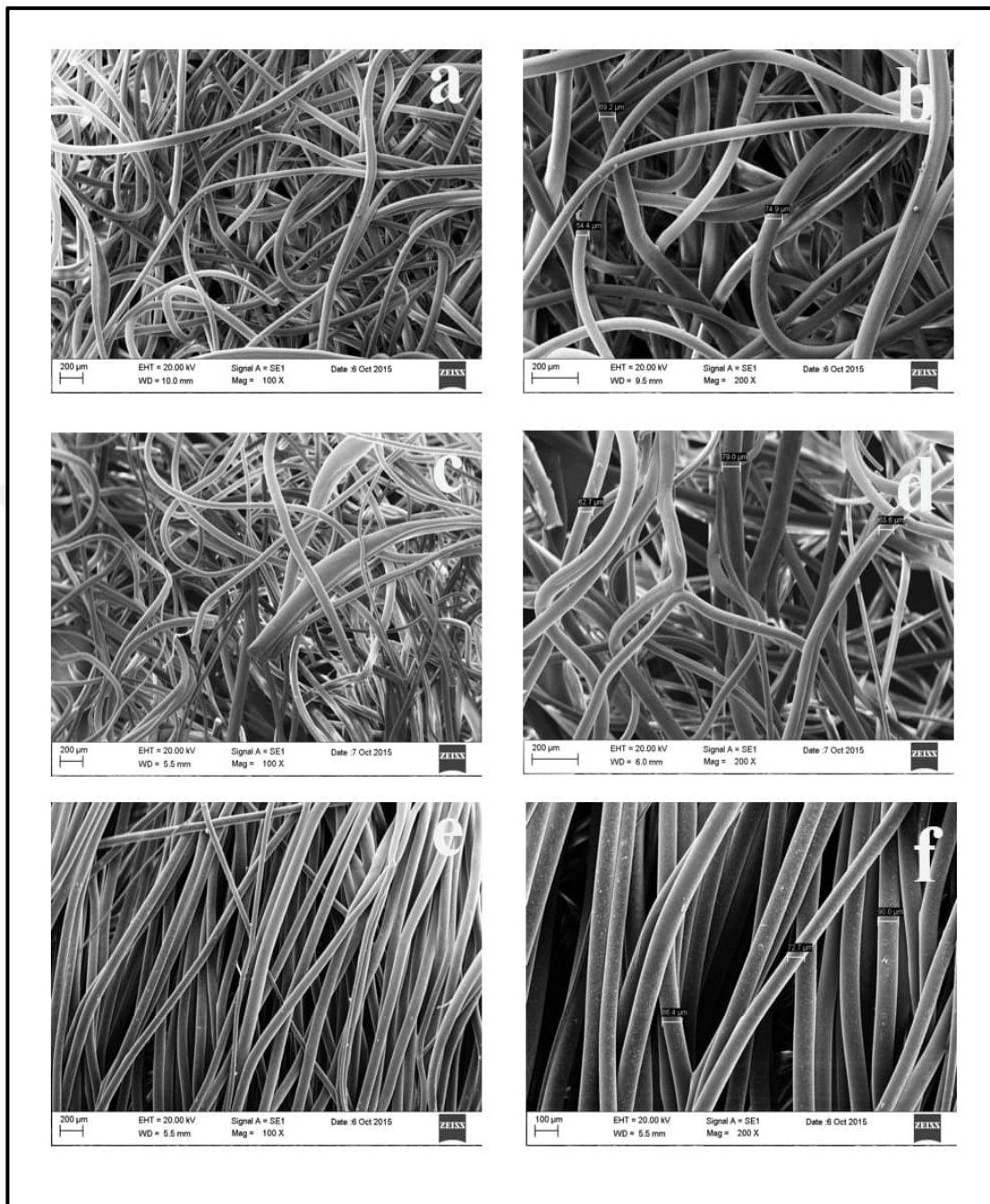
Figure 4.5. Scanning electron micrographs of wet-spun PLGA fibers (30 per cent) in (a, b) 50:50, (c, d) 60:40, (e, f) 75:25 (Isopropanol: dH2O) coagulation baths. (a, c, e) 100X magnification, (b, d, f) 200X magnification.

According to scanning electron microscopy images, the sizes of fibers were between 50-100 μm for all samples and did not change significantly due to the PLGA concentration and the compositions of IP:DW coagulation bath (Figure 4.6). Also, the fibers in 75:25 coagulation bath were thicker than those in other baths and 60:40 and 75:25 coagulation baths were found more successful in wet spinning regardless of the PLGA concentration.
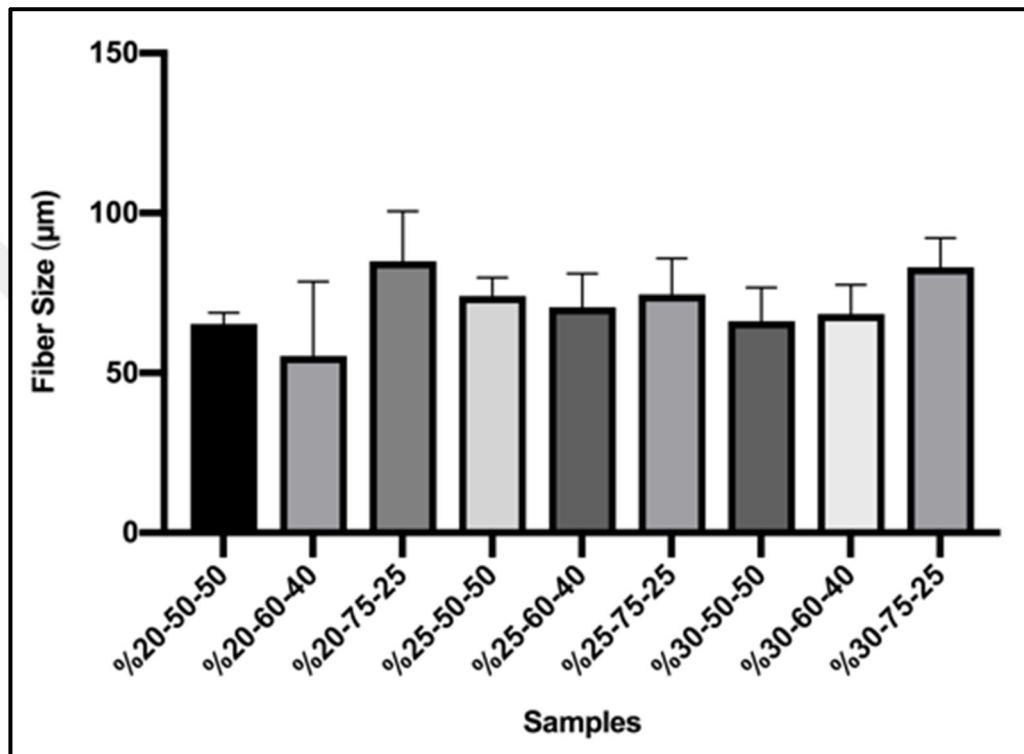
Figure 4.6. Comparison of sizes of wet-spun PLGA fibers at different concentrations.

4.2.2. Contact Angle Analysis

According to the results of scanning electron microscopy, different concentrations (20, 25 and 30 per cent) of PLGA were prepared by using different concentrations of isopropanol – dH_2O coagulation baths (75:25, 60:40, 50:50) by using wet-spinning technique for the analysis of contact angle. Results showed that the contact angle of each sample was below 90 °C (Figure 4.7). Thus, the surfaces were wettable enough and it was observed that the contact angle of the samples was not affected from the PLGA concentrations and the coagulation bath compositions. There was not statistically significant difference in contact angle measurements between these groups.
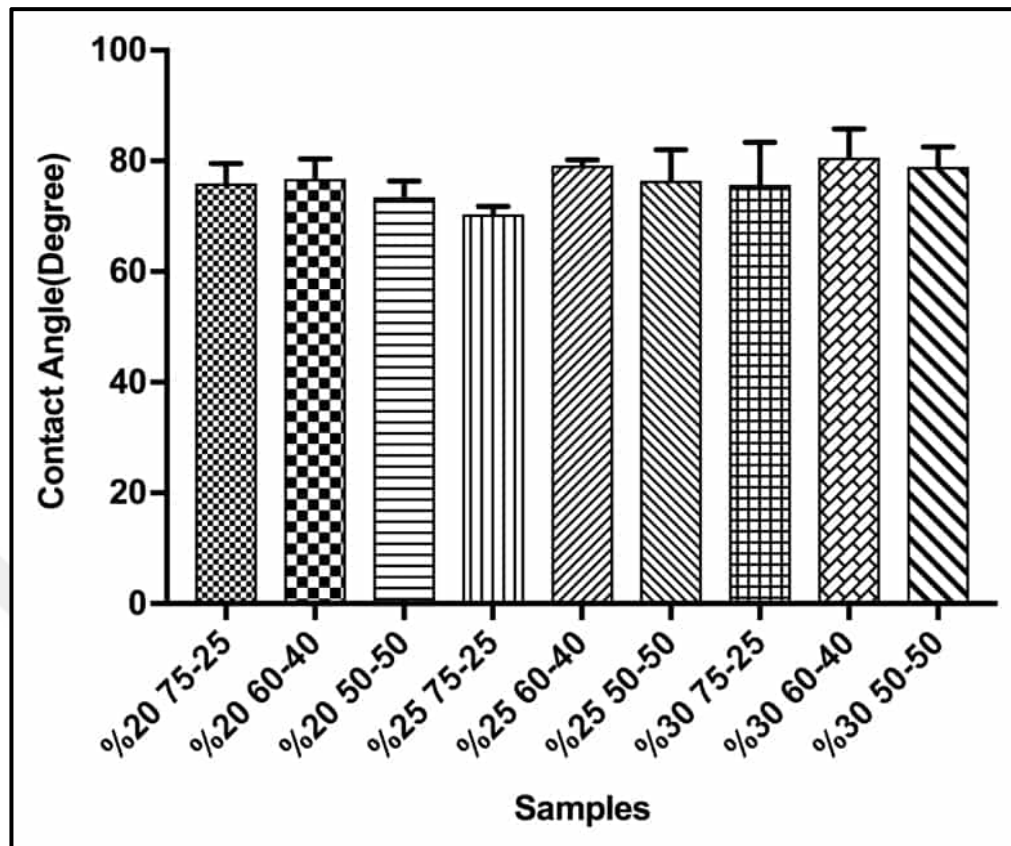
Figure 4.7. Contact angle measurements of PLGA films at different concentrations in different coagulation baths.

4.2.3. Degradation of PLGA Scaffolds

According to the results of SEM, the wet - spun PLGA samples (20-60-40, 25-60-40, 30-60-40, 30-75-25 and 25-75-25) were selected for degradation studies during 120 days. The optimization of the samples of 20-75-25 and 50-50 IP:DW coagulation baths could not be provided. Results showed that they preserved at least 80 per cent of their weight during the first 90 day incubation period, regardless of concentration and coagulation bath composition (Figure 4.8a). However, degradation rate of PLGA scaffold started to increase after day 90, especially for samples of 30-75-25 and 25-75-25 samples and it was observed that PLGA 30-75-25 lost 80 per cent of its weight while PLGA 25-75-25 completely degraded after 120 days of incubation. At day 120, the weight loss of PLGA 25-75-25 was significantly higher than the other groups (*p <0.05). The weight loss of PLGA 30-75-25 was also found significantly higher than the groups of 20-60-40, 25-60-40 and 30-60-40 (*p <0.05).
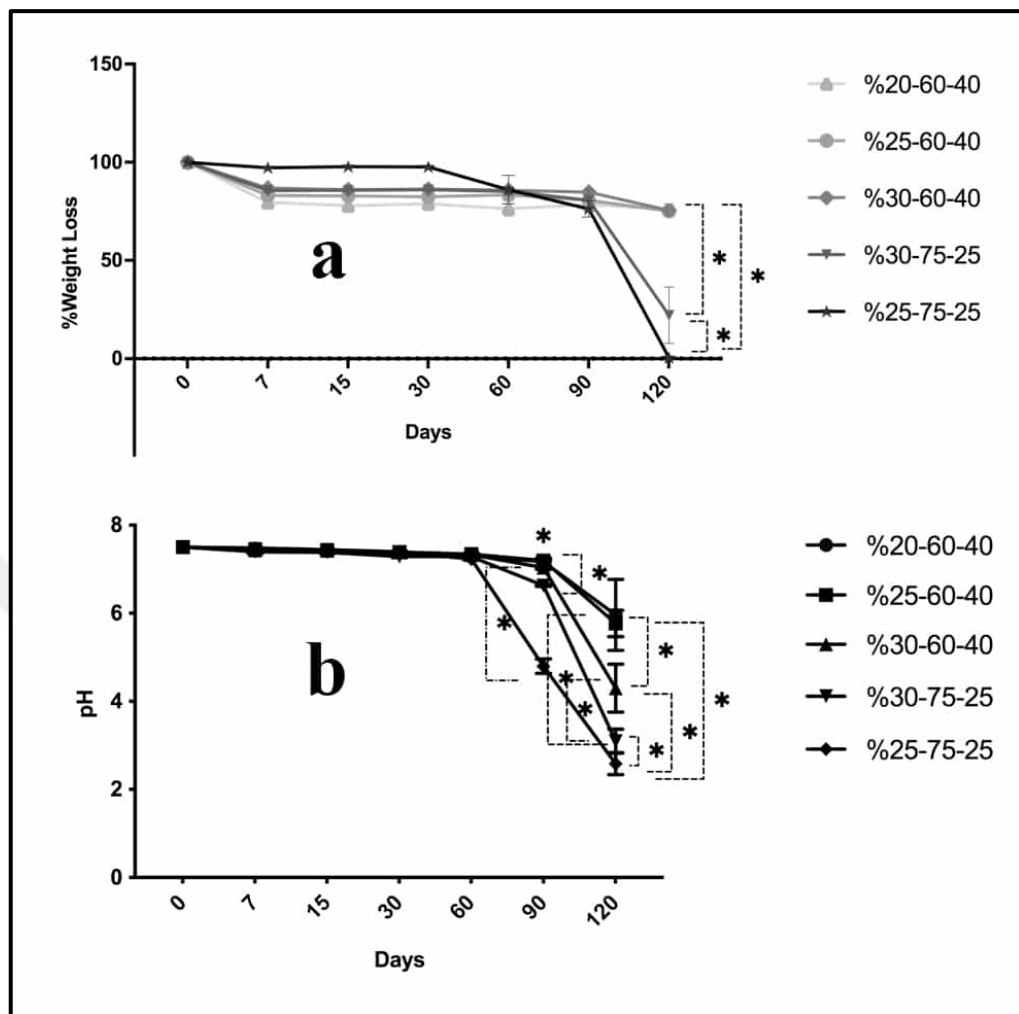
Figure 4.8. The rate of (a) weight loss and (b) pH decreasing as a function of time (day) (*p < 0.05) during biodegradation of fibrous PLGA scaffold.

Also, PLGA fibers did not exhibit too much pH change in the first 90 days except for a 25 per cent PLGA that was spun in a 75:25 water bath composition, parallel to the weight loss graph and the rate of scaffold degradation (Figure 4.8b). At day 90, pH of PLGA 25-75-25 was observed significantly lower than all other groups ($^*p<0.05$). Moreover, a significant decrease in pH of PLGA 30-75-25 was observed compared to 20-60-40, 25-60-40 and 30-60-40. The pH of 30-60-40 was significantly lower than the samples of 20-60-40 and 25-60-40 ($^*p <0.05$). After 90 days of incubation period, decrease in pH of the solution was also seen with increasing incubation period due to degradation of PLGA scaffold. At day 120, the pH of PLGA 25-75-25 was significantly lower than the other groups ($^*p <0.05$) and PLGA 30-75-25 exhibited the lower pH value than PLGA 20-60-40, 25-60-40 and 30-60-40 ($^*p <0.05$).

4.2.4. Scanning Electron Micrographs of Degraded Wet Spun PLGA Scaffolds

After the degraded PLGA scaffolds were dried and covered with 10 nm gold, they were evaluated by scanning electron microscopy. Images of the samples were demonstrated at the end of the 90 day incubation at which the degree of degradation was examined most clearly. At day 120, some samples were completely destroyed and could not be shown here.

According to the scanning electron micrographs of the samples resulting from degradation analysis; the samples of 75-25 coagulation bath were the most clearly degraded ones and the deformation of fibers was also observed clearly (Figure 4.9). During incubation of fibers, they were eroded from the surface, and therefore, some of the fibers were broken. According to the result of SEM of these degraded samples, 20-60-40 was selected to be the least degraded one. These images also supported the results of the loss weight and pH changes in degradation study.
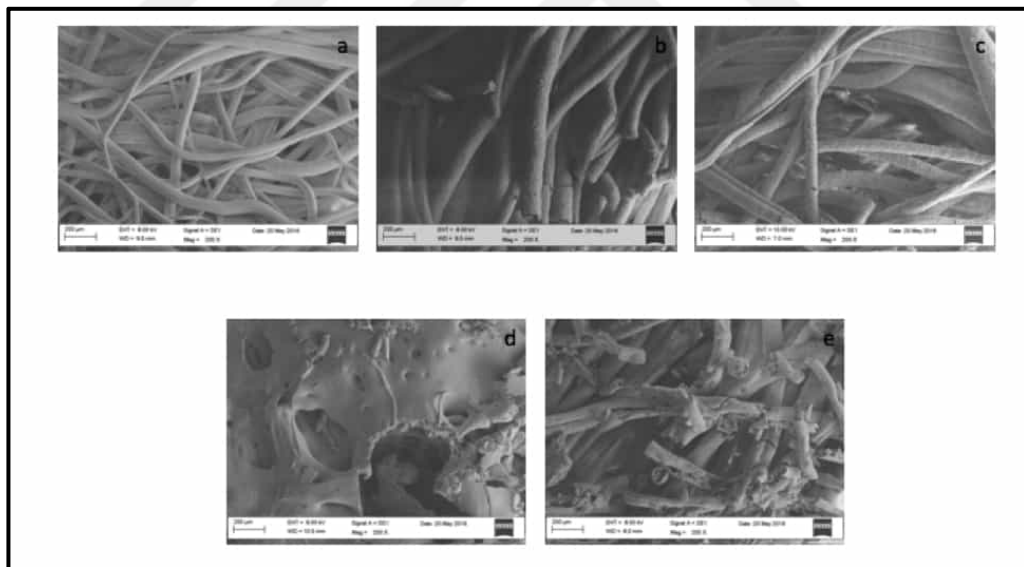
Figure 4.9. Scanning electron micrographs of wet-spun PLGA at the end of 90 days of incubation period; a) 20-60-40, b) 25-60-40, c) 30-60-40, d) 25-75-25, e) 30-75-25.

4.3. RELEASE PROFILE OF GS4012

In this study, PLGA-PEG-PLGA hydrogel was used for a GS4012 delivery (Figure 4.10). GS4012 was released with degradation of the hydrogel. The release of GS4012 from the PLGA-PEG-PLGA hydrogel was high in the first 24 hours than the other days, then stabilized and reached to plateau phase (Figure 4.11). The highest amount of GS4012 release was occurred at the first 24 hours and half of the GS4012 was released at the end of day 7. In the first 24 hours, the release of more GS4012 than the other days was thought to be due to the fact that the GS4012, which was physically adsorbed around the hydrogel surface, passed into the release environment. After day 15, the amount of release was accelerated due to the degradation of the hydrogel.
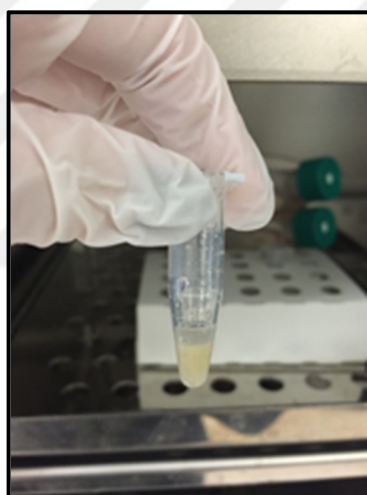
Figure 4.10. PLGA-PEG-PLGA hydrogel that includes GS4012 and GS4012 releasing medium.
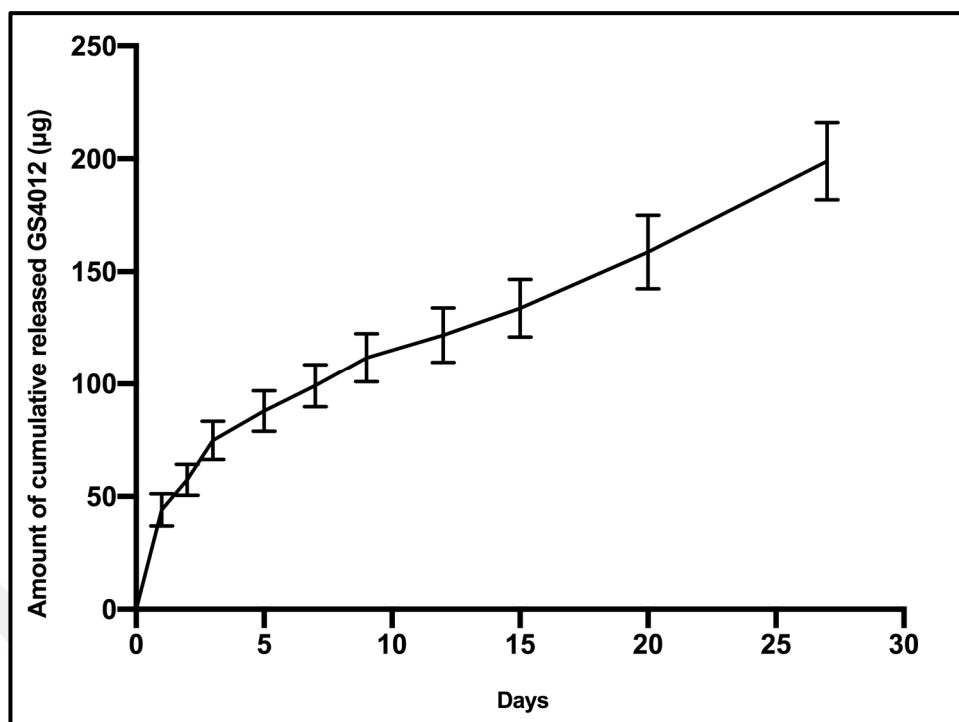
Figure 4.11. GS4012 release from the PLGA-PEG-PLGA hydrogels throughout 27 days of incubation.

4.4. *IN VITRO* CELL CULTURE STUDIES

4.4.1. Isolation of Rat Bone Marrow Stem Cells (rBMSCs)

rBMSCs were isolated from bone-marrow of 6-7 weeks old, Sprague-Dawley rats and their medium was replenished twice a week until confluency was reached. After that, these primary cultures were observed under bright field microscopy (Figure 4.12).
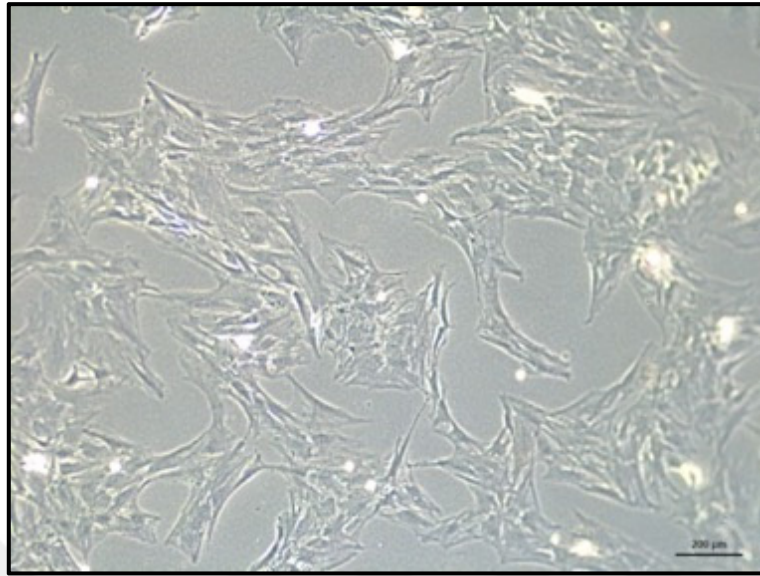
Figure 4.12. Bright field microscope image of rBMSCs with 10X objective.

4.4.2. Isolation of Rat Peripheral Blood Endothelial Cells (rPBECs)

Endothelial cells were isolated from peripheral blood of 6-7 weeks old, Sprague- Dawley rats. Briefly, Histopaque 1083 was used to obtain peripheral blood mononuclear cells. Then, they were cultured and their medium was replenished twice a week until confluency was reached. Primary cells were observed in elongated morphology (Figure 4.13).
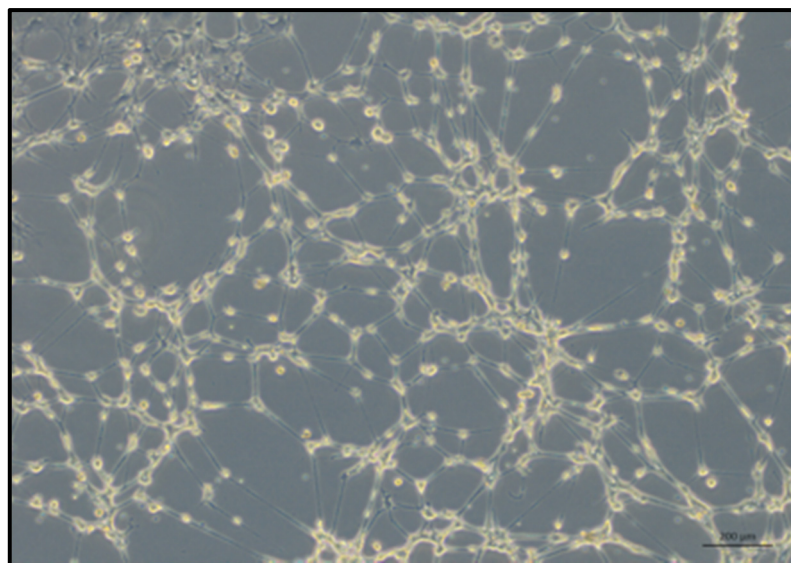
Figure 4.13. Bright field microscope image of rPBECs with 10X objective.

4.4.3. Qdot® Staining of rBMSCs and rPBECs

Qtracker® 565 and Qtracker® 705 Cell Labeling Kits were applied for rPBECs and rBMSCs, respectively and they were also stained with DAPI. Then, confocal images of rPBECs (Figure 4.14a) and rBMSCs (Figure 4.14b) were observed. While rPBECs were seen as green with 565 nm fluorescence, rBMSCs were observed as red with 705 nm fluorescence. Cells have the ability to uptake Qdot® nanocrystals and become fluorescent at designated wavelengths. Nucleus of cells were also stained blue with DAPI.
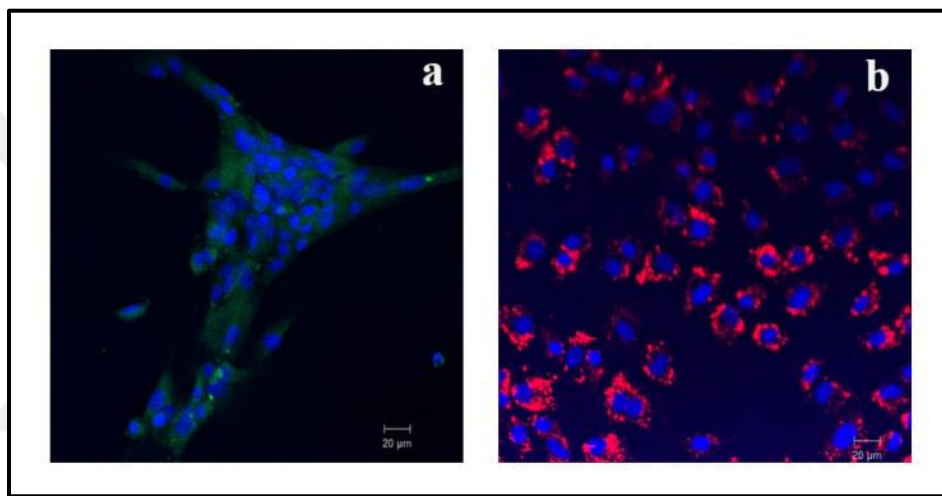
Figure 4.14. Confocal microscope images of (a) rPBECs stained by Qtracker® 565 Cell Labeling Kit and (b) rBMSCs stained by Qtracker® 705 Cell Labeling Kit. (Objective: 20X).

4.4.4. Characterization of rBMSCs

4.4.4.1. Flow Cytometry Analysis

In this analysis, the stem cell properties were determined using flow cytometry via cell surface markers. The results of flow cytometry analysis demonstrated that cells were positive for mesenchymal stem cell surface markers CD29 and CD90, had low expression for hematopoietic stem cell markers CD11A and CD45, and were also negative for an endothelial cell surface marker CD31 (Figure 4.15).

The percentages of positivity of the cells were shown in the Table 4.1 below. According to these results, mesenchymal stem cell properties of rBMSCs were proved by flow cytometry analysis.

Table 4.1. Cell surface antigen expression of rBMSCs.

Surface Antigen	Percentage of positively marked rBMSCs
CD29	99.55
CD90	94.67
CD11A	9.74
CD31	2.38
CD45	5.17
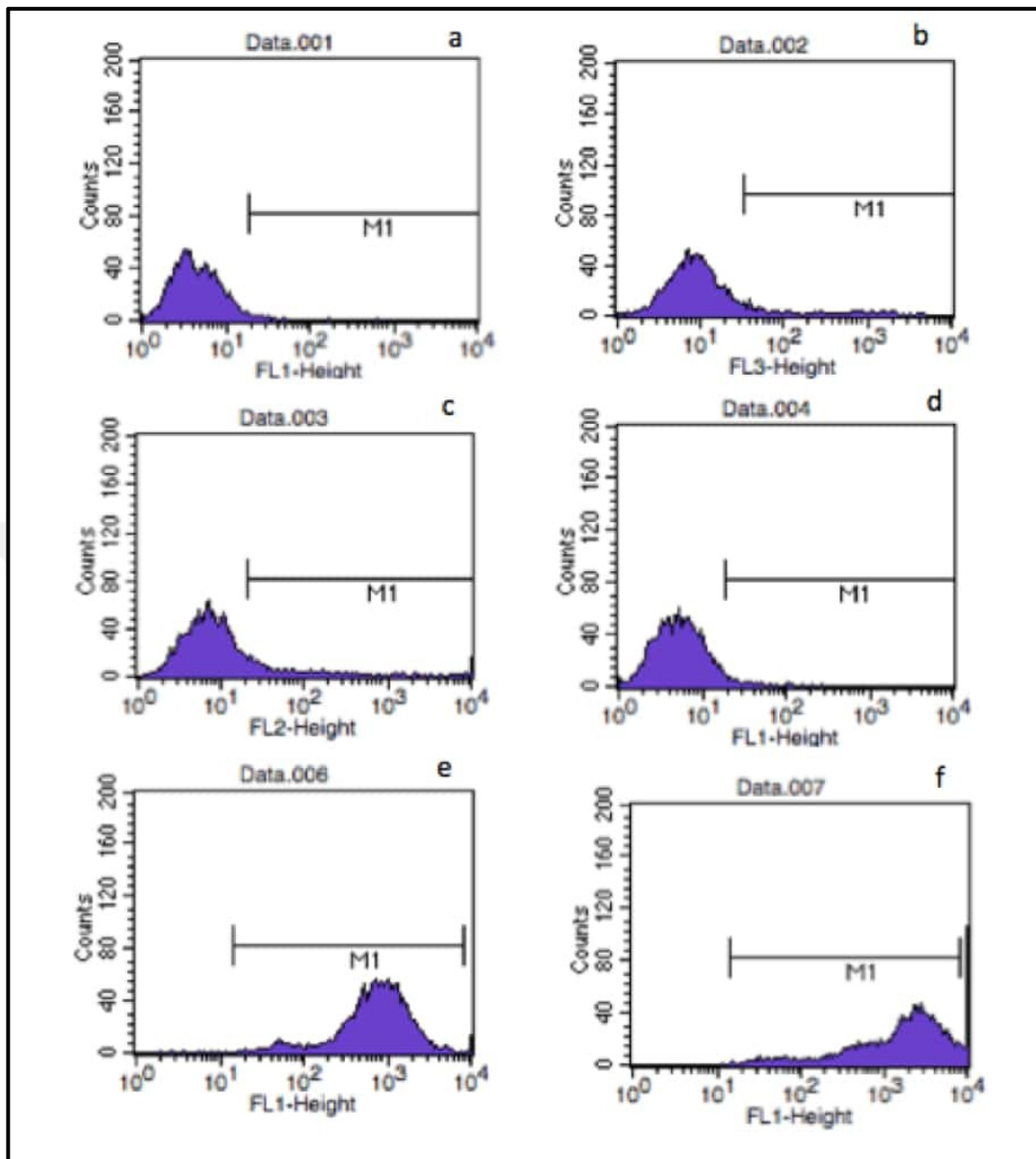
Figure 4.15. Flow cytometry histograms of rBMSCs a) Negative control; labeled with (b) CD45, (c) CD11A, (d) CD31, (e) CD29, (f) CD90 antibodies.

4.4.4.2. Differentiation Tests

To prove that the cells isolated from bone marrow were mesenchymal stem cells; osteogenic, chondrogenic and adipogenic differentiation tests were performed, in addition to flow cytometry analysis.

4.4.4.2.1. Osteogenic Differentiation

von Kossa Staining

von Kossa staining was performed after 7, 14 and 21 days of incubation for the detection of mineralized nodules. In this test, positively charged silver ions reacted with negatively charged phosphates and carbonates in calcium deposits and were then reduced to a brown color under UV light. The microscopic images show that as the time passes, the amount of mineralized nodulus in osteogenic medium containing wells was increased, compared to the mineralized regions in growth medium containing wells (Figure 4.16).

Figure 4.16. Microscopic images of mineralized nodules by von Kossa staining with growth medium at days 7, 14 and 21 (A, C, E) and osteogenic medium at days 7,14 and 21 (B, D, F). Scale: 50 μm.

In this figure, mineralized areas stained with von Kossa and exposed to UV light, appeared to be brown. Cells were pink since they were stained with nuclear fast red.

Alizarin Red Staining

Alizarin red staining was also performed to detect mineralized nodules after 7, 14 and 21 days of incubation. The mineralized areas were stained with alizarin red due to the calcium in the calcium phosphate mineral and appeared as red. From day 7 to day 21, the areas that showed more concentrated stainings, expressed the increase in the amount of bone differentiated cells, especially in the osteogenic medium containing wells (Figure 4.17). According to the microscopic images, it was found that mineralized regions in osteogenic medium was formed more intensively than the ones in growth medium and the increase in the amount of these regions was observed at day 21.
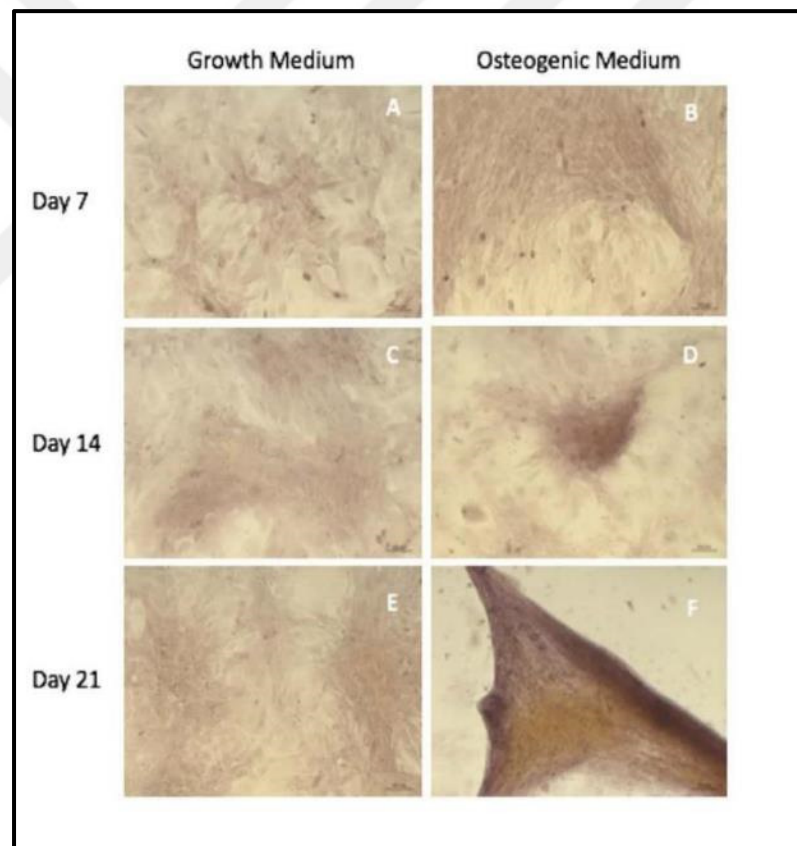
Figure 4.17. Microscopic images of Alizarin Red staining of rBMSCs with growth medium at days 7, 14 and 21 (A, C, E) and osteogenic medium at days 7,14 and 21 (B, D, F). Scale: 100 μm.

4.4.4.2.2. Chondrogenic Differentiation

Alcian Blue Staining

After 7, 14 and 21 days of incubation, alcian blue staining was executed to evaluate cartilage-specific extracellular matrix formation of cells (Figure 4.18).
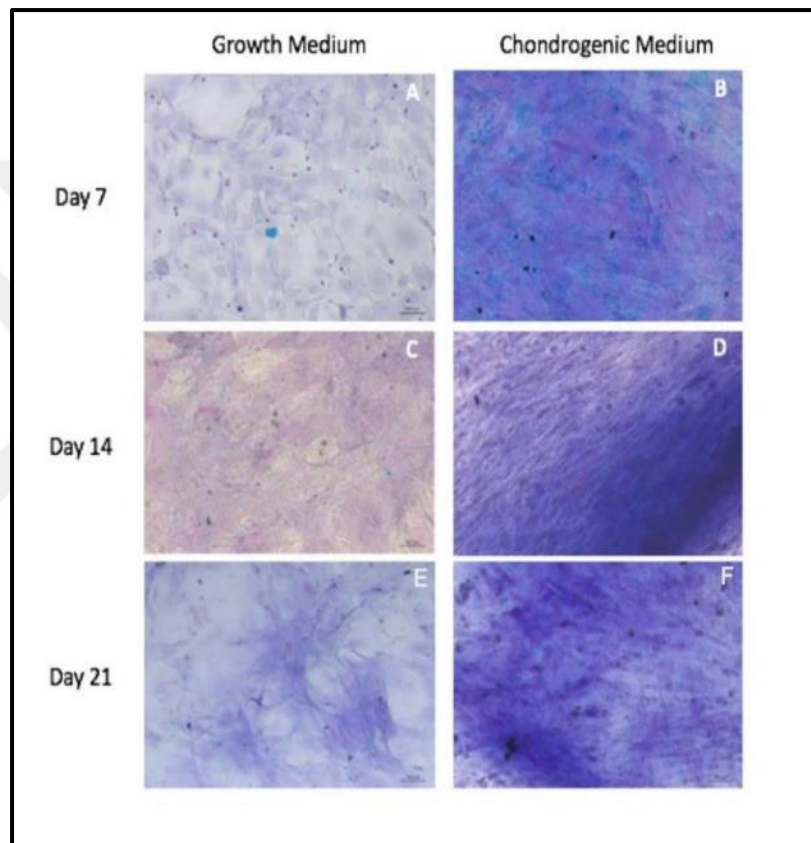
Figure 4.18. Microscopic images of Alcian Blue staining of rBMSCs with growth medium at days 7, 14 and 21 (A, C, E) and osteogenic medium at days 7,14 and 21 (B, D, F). Scale: 200 μm.

Alcian blue (pH:2,5) stained sulphated and carboxylated acid mucopolysaccharides. It was used to show that acid mucin, neutral mucin and nuclei were stained with bright blue, bright magenta, and light blue, respectively.

It was aimed to stain the extracellular matrix secreted by the chondroblasts and to be observed under the light microscope by Alcian blue staining.

According to the microscopic images, it was found that extracellular matrix in chondrogenic medium was formed more intensively than the ones in growth medium and this amount increased at day 21 (Figure 4.18). The mesenchymal stem cells differentiated into the chondroblasts, led to the formation of mature chondrocytes during 21 day of incubation period, and they synthesized an extracellular matrix intensively.

4.4.4.2.3. Adipogenic Differentiation

Oil Red O Staining

After 7, 14 and 21 days of incubation, Oil Red O staining was performed to observe the adipogenic storage of the cells. According to the observations, more adipogenic cells that were exposed to adipogenic medium, were found than that of growth medium and this amount was increased at day 21 (Figure 4.19). Oil droplets deposited inside the cell were seen as red at day 7 and claret red at days 14 and 21 due to the elevated amount of oil droplets.
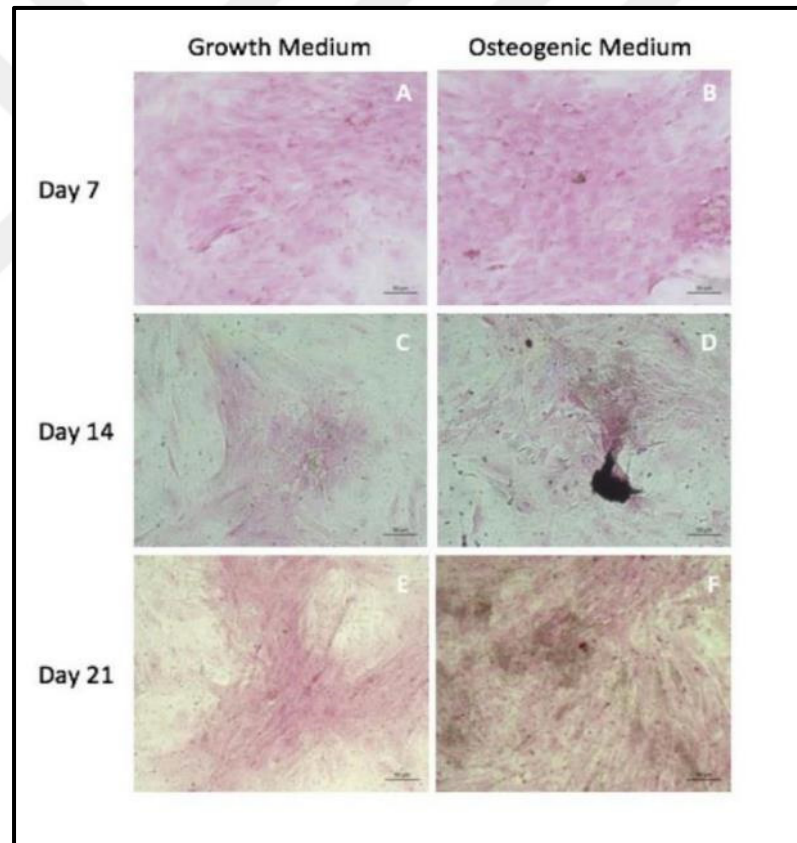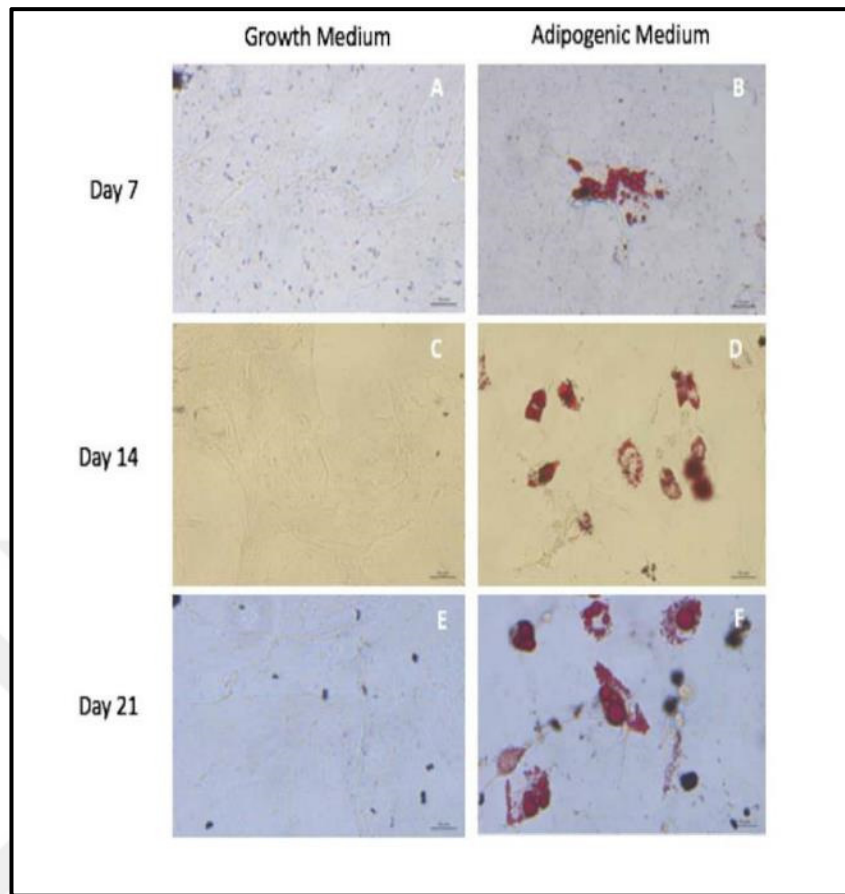
Figure 4.19. Microscopic images of Oil Red O staining of rBMSCs with growth medium at days 7, 14 and 21 (A, C, E) and osteogenic medium at days 7,14 and 21 (B, D, F). Scale: 50 μm.

4.4.5. Characterization of rPBECs

4.4.5.1. LDL Uptake Assay

rPBECs were characterized by their ability to uptake the labeled low density lipoprotein, Dil-Ac-LDL, into the cell. It led us to observe the accumulation of the protein in the cells fluorescently (Figure 4.20).

The fluorescence of the cells containing the LDL can be seen in the Figure 4.20a and the fluorescence and light microscope merged images of the cells are presented in Figure 4.20b.

It was observed that all cells in the bright field microscope emitted fluorescent light. It indicates that all cells in the culture were endothelial cells and there was no cross contamination. If there was a cross contamination, the cells that did not overlap with each other could be observed in the Figure 4.20b. This proved the endothelial characterics of the cells.
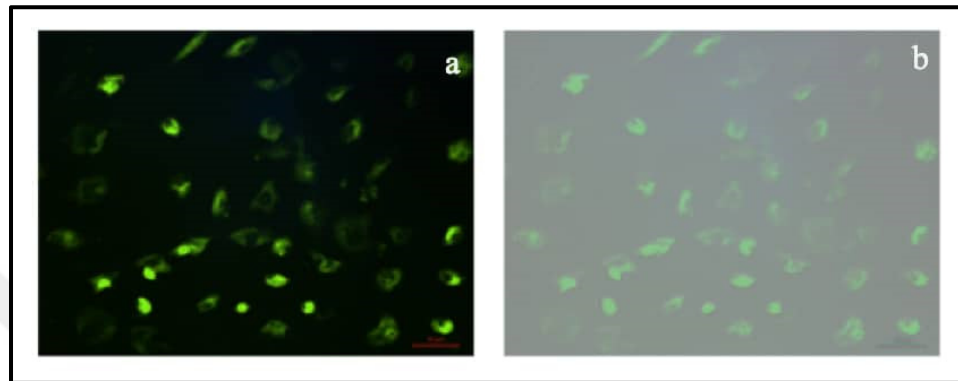
Figure 4.20. After LDL uptake of the cells, fluorescence microscope images of rPBECs (a); merged images of rPBECs by fluorescence microscope and bright field microscope (b) (X20).

4.4.5.2. CD 31 Staining

The characteristics of isolated rPBECs were examined with confocal microscope by labeling CD31 antibody that is a specific surface marker for endothelial cells. CD31 expression was demonstrated in green color and nucleus of cells were observed in blue color. As seen in Figure 4.21, all of the cells were stained with CD31. Thus, cells isolated from peripheral blood were found to exhibit endothelial cell properties.
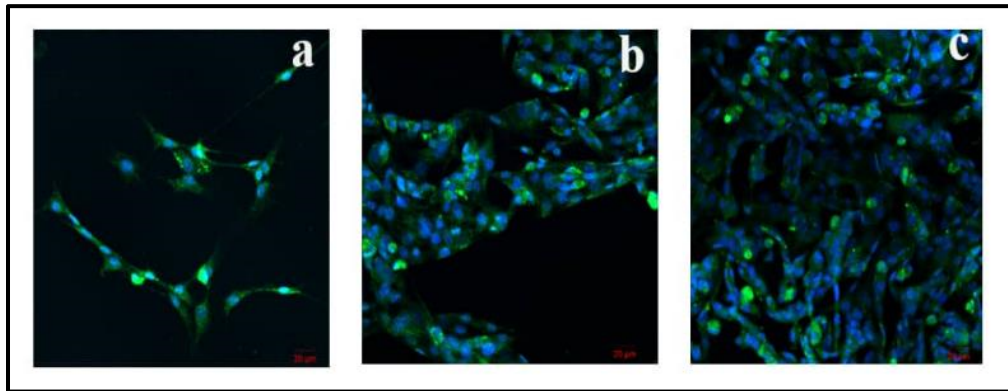
Figure 4.21. Confocal microscopy images of rPBECs labeled with CD31 (a, b, c). Scale: 20 µm. Green: CD31, Blue: DAPI.

4.4.5.3. In vitro Angiogenesis Assay

Endothelial cells are capable of forming 3 dimensional tubular structures on either collagen-coated culture dishes or ECM gel material. In this study, ECM gel solution secreted by Engelbreth-Holm-Swarm (EHS) tumor cells was used. After the cells were stained with Calcein AM, they were visualized by fluorescence microscopy. According to the images, isolated rPBECs on ECM gel material, exhibited the formation of tubular structure as shown in Figure 4.22 a, b, c. *In vitro* tube formation of rPBECs proved that they were endothelial cells.
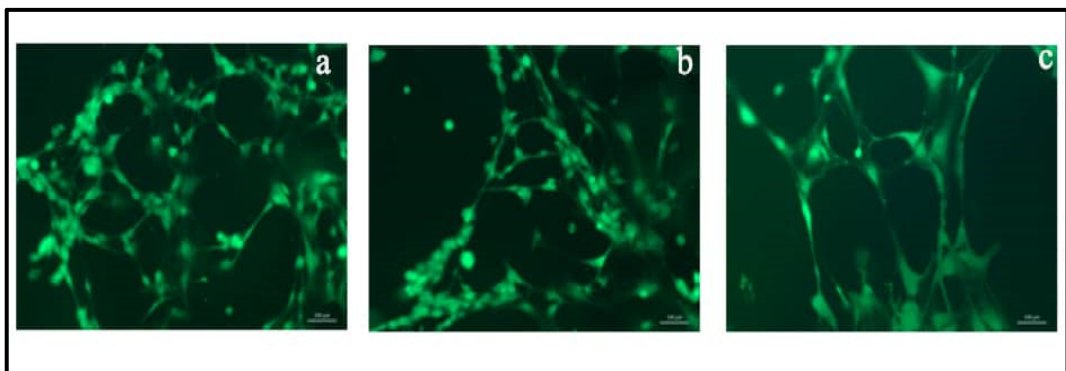
Figure 4.22. Fluorescence microscope images of rPBECs (a, b, c) stained with Calcein AM on the ECM gel material. Scale: 100 µm. (X10).

4.4.5.4. *Migration of rPBECs*

This study was conducted to understand the effect of GS4012 on migration of rPBECs. After the cells seeded onto the insert were fixed and stained with crystal violet, the cells passing through the bottom of the insert were examined under bright field microscopy. According to the results, when the cell densities at the bottom of the insert were compared, the cells migrated from the pores to the bottom of the insert in the wells containing growth medium (Figure 4.23c), but it was found that they did not go to the wells of the cell culture dish. In the wells containing VEGF (Figure 4.23a) and GS4012 (Figure 4.23b), it was observed that the cells did not only migrate to the bottom of the insert, but also migrated to the cell culture dish from the bottom of the insert when they were checked under the microscope. GS4012 was more successful for the migration of cells to the wells of cell culture plates than that of VEGF.
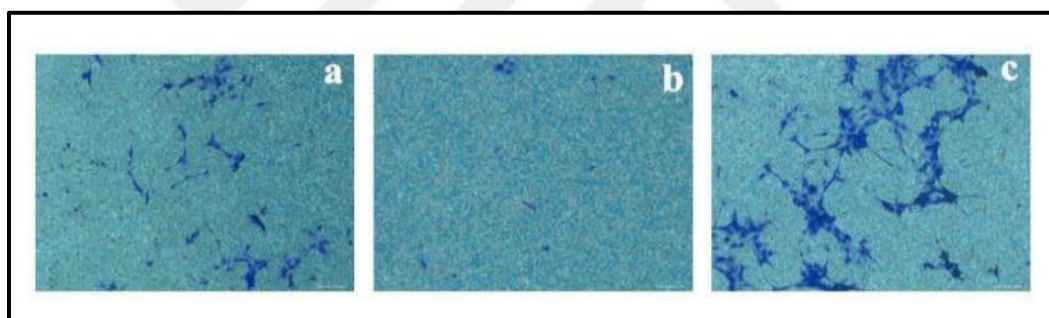
Figure 4.23. Light microscope images of crystal violet-stained endothelial cells migrating to the bottom of the insert a) VEGF-added medium, b) GS4012- added medium, c) Growth medium. Scale: 200 μm.

4.6. *IN VITRO* CELL – MATERIAL INTERACTIONS

4.6.1. Examination of Cells on Wet Spun PLGA Scaffolds by Scanning Electron Microscopy

Scanning electron micrographs of rBMSCs seeded scaffolds were obtained at days 14 and 21 with 1000 X magnification. It could be observed in Figure 4.24 that cells attached on the

surfaces of all scaffolds and the highest attachment of rBMSCs was achieved onto the sample of 20-60-40.
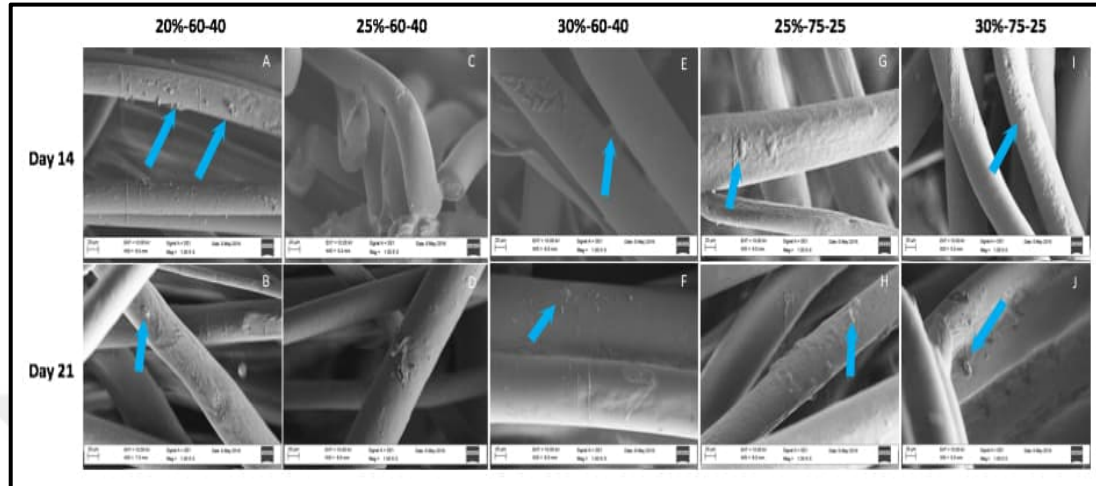
Figure 4.24. Scanning electron micrographs of rBMSCs seeded PLGA scaffolds with 1000X magnification. (A, B) 20-60-40 at days 14 and 21, (C, D) 25-60-40 at days 14 and 21, (E, F) 30-60-40 at days 14 and 21, (G, H) 25-75-25 at days 14 and 21, (I, J) 30-75-25 at days 14 and 21. Arrow shows the cell.

4.6.2. Determination of Cell Proliferation on the Scaffolds by MTS Assay

According to the results of degradation tests, CellTiter 96® AQueous One Solution Cell Proliferation Assay (MTS) were applied for the selected samples (20-60-40, 25-60-40, 30-60-40, 30-75-25, 25-75-25) to observe the viability of rBMSCs on different PLGA scaffolds.

The results of MTS assay showed that seeded cells were attached to all selected PLGA scaffolds, but cell proliferation was obtained in the samples of 20-60-40 and 30-75-25 better than the others throughout 21 days of incubation (Figure 4.25). At day 7, cell proliferation in the samples of 30-75-25 and 25-60-40 was significantly lower than the ones in the samples of 25-75-25 and 30-60-40 (*p <0.05). At day 14, cell proliferation in the samples of 20-60-40 was significantly higher than the ones in the samples of 30-60-40 and 30-75-25 (*p<0.05). At day 21, cell proliferation in the samples of 30-75-25 was also significantly higher than the ones in the samples of 25-60-40, 25-75-25 and 30-60-40 (*p <0.05).

Also, in the sample of 25-60-40, the cell proliferation was significantly lower than the one in the samples of 20-60-40, 25-75-25 (*p <0.05). Moreover, in the sample of 30-75-25; there was a statistically significant difference in cell proliferation (*p<0.05) between the 7, 14, 21 days of incubation. The amount of cell at day 7 was significantly lower than the ones at days 14 and 21 (*p <0.05) and the cell number at day 14 was significantly lower than the one at day 21 (*p <0.05). Therefore, sample of 20-60-40 was chosen as the best sample according to the results of MTS cell proliferation assay, and degradation analysis. For the rest of the experiments, PLGA 20-60-40 scaffolds were prepared and PLGA-PEG-PLGA hydrogel with or without GS4012 was added onto it.
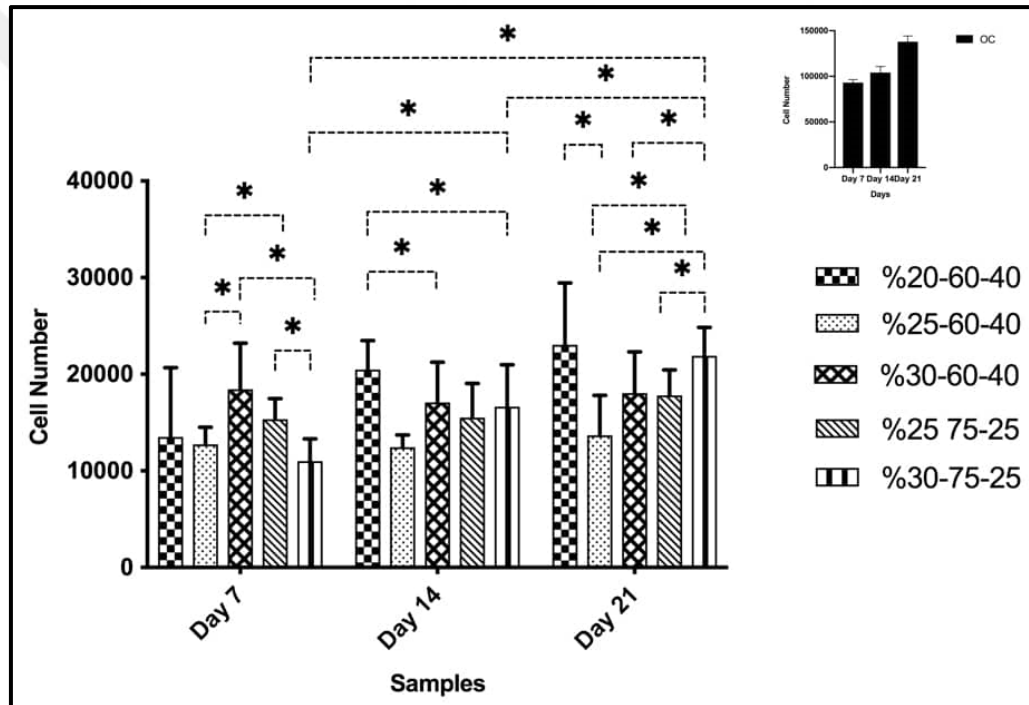
Figure 4.25. Cell proliferation on different PLGA scaffolds (20-60-40, 25-60-40, 25-75-25, 30-60-40 and 30-75-25) after 7, 14 and 21 days of incubation. Initial cell seeding density was 2x10^4 cells/sample (*p < 0.05). Indent on the top right corner shows the cell proliferation on Tissue Culture Plate (TCP) and OC stands for the cells seeded into wells of the tissue culture plate (only cell).

4.6.3. Confocal Microscopy Analysis of 20-60-40 Cell-Seeded Scaffolds

In this analysis, migration of rPBECs was obviously observed by confocal microscopy during 21 days of incubation period from the porous insert to the wells containing rBMSCs seeded PLGA scaffolds with GS4012 or VEGF added PLGA-PEG-PLGA hydrogel (Figure 4.26). According to the images, migration of endothelial cells to the wells containing PLGA-PEG-PLGA with VEGF or GS4012 was observed from day 7 to day 21. It clearly demonstrated the success of GS4012, the VEGF activator, on the ability of endothelial cells to migrate.
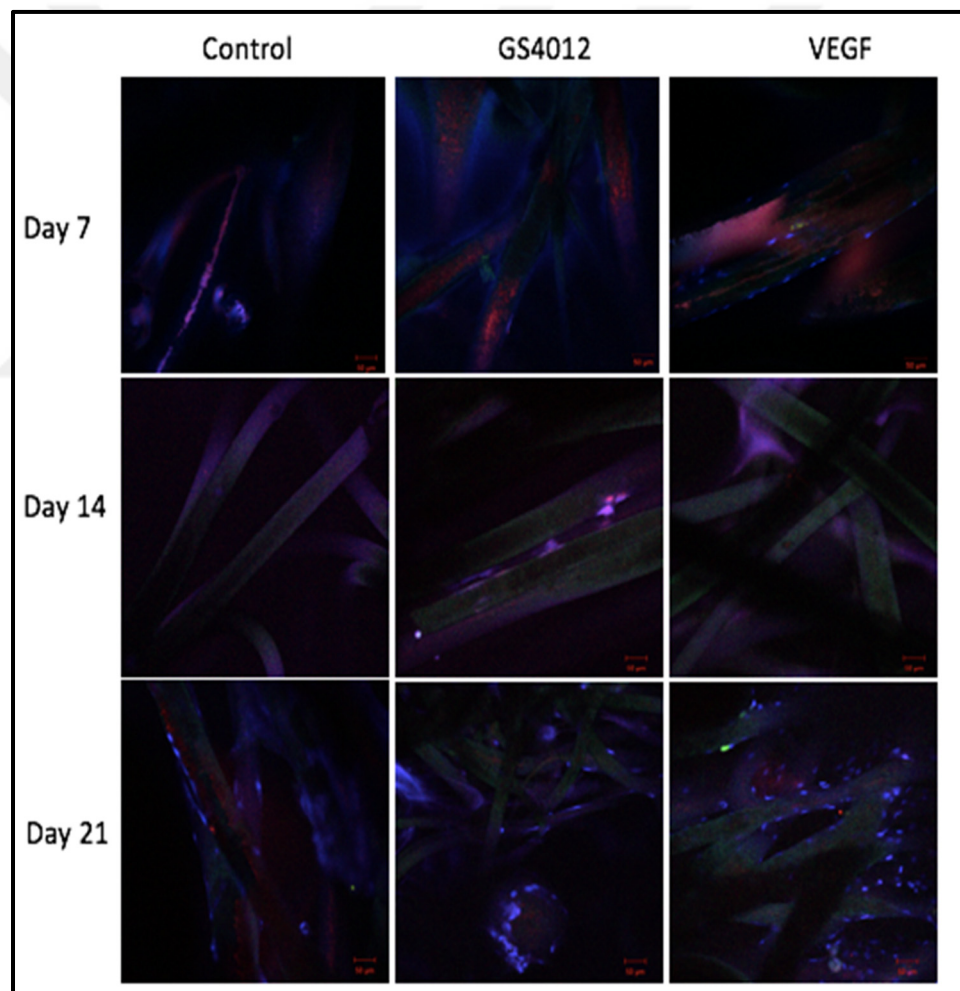
Figure 4.26. Determination of migration of endothelial cells by confocal microscopy after 7, 14 and 21 days of incubation. DAPI: Blue, rBMSCs: Red (stained with Qtracker 705), rPBECs: Green (stained with Qtracker 565) (x10).

4.6.4. Scanning Electron Microscopy of Cell Seeded 20-60-40 PLGA Scaffolds

Gold-coated, cell seeded 20-60-40 PLGA scaffolds were examined in a scanning electron microscope and they were evaluated in terms of cell adhesion (Figure 4.27). At day 10, cell spreading and proliferation were observed on this scaffold, and the cells completely covered the scaffold at day 20. Throughout 20 days of incubation, we observed the best cell attachment and spreading. It showed that 20-60-40 PLGA scaffolds were suitable to get a cellular viability.
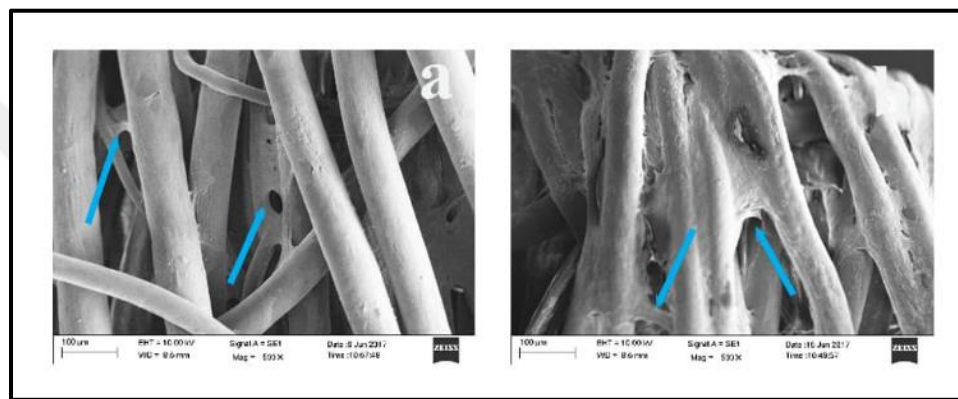
Figure 4.27. Scanning electron micrographs of MSCs seeded onto PLGA fibers (20-60-40) at days 10 (a) and 20 (b). Magnification: 200X.

4.7. CELL DIFFERENTIATION ON 20-60-40 WET SPUN PLGA SCAFFOLDS

4.7.1. Determination of Cell Proliferation by MTS assay

Cell viability and proliferation of rBMSCs on 20-60-40 wet spun PLGA fiber were determined by using MTS cell proliferation assay after 4, 7, 14 and 21 days of incubation (Figure 4.28). In this part of the study, the effect of 20-60-40 wet spun PLGA fiber on the proliferation of rBMSCs after addition of differentiation medium was investigated for bone regeneration. According to the results, increase in rBMSC number was significantly achieved during the first 14 days (Figure 4.28) (*p<0.05). Then, significant decrease in cell number was obtained from day 14 to day 21 (*p<0.05).
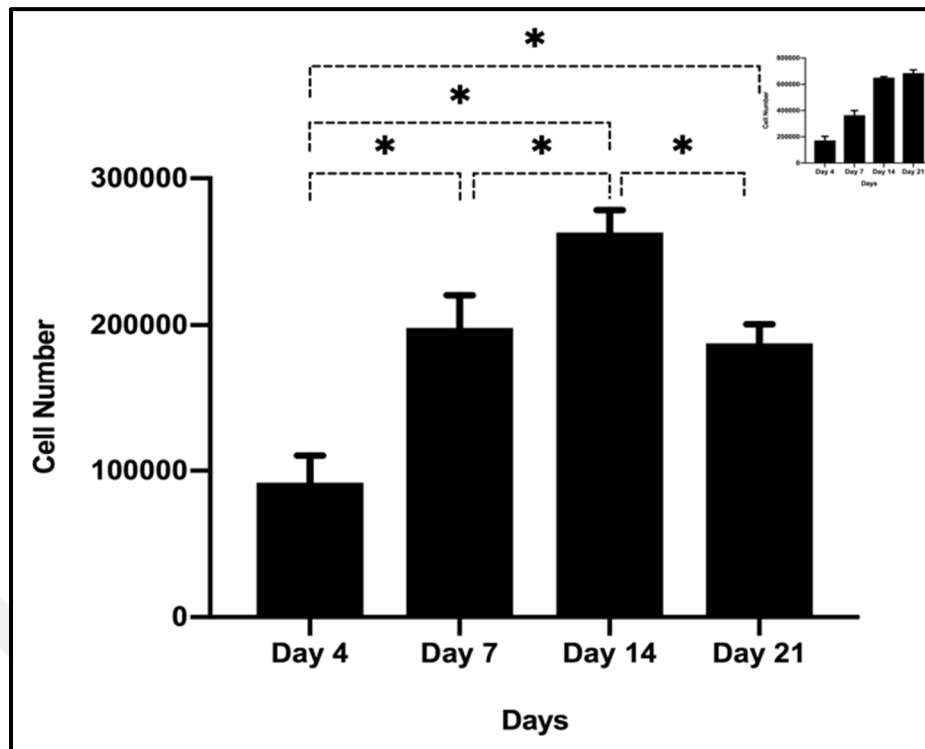
Figure 4.28. Cell proliferation on 20-60-40 PLGA scaffolds after 4, 7, 14 and 21 days of incubation. Initial cell seeding density was 5×10^4 cells/sample (*p < 0.05). Indent on the top right corner shows the cell proliferation on Tissue Culture Plate (TCP) and OC stands for the cells seeded into wells of the tissue culture plate (only cell).

4.7.2. Alkaline Phosphatase Assay

Alkaline phosphatase activity of rBMSCs on 20-60-40 PLGA fiber was investigated at days 4, 7, 14 and 21. Alkaline phosphatase assay was applied to measure the conversion of p-nitrophenyl phosphate to p-nitrophenol in the presence of alkaline phopshatase at 405 nm. In this study, the amount of alkaline phosphatase (ALP), one of the early markers of bone differentiation, was determined by an enzymatic method using ALP kit. Results showed that cells seeded on both tissue culture plates and scaffolds exhibited high levels of ALP activity after day 4 (Figure 4.29). While ALP activity of the cells grown in the tissue culture plates did not show too much increase or decrease from day 4 to day 21, cells seeded on PLGA scaffold showed the significant increase in ALP activity from day 4 to day 7 (*p<0.05). Although ALP activity was still high at day 14, no significant increase has been observed from day 7 to day 14.

From day 14 to day 21, the significant increase in ALP activity was observed again (*$p<0.05$).
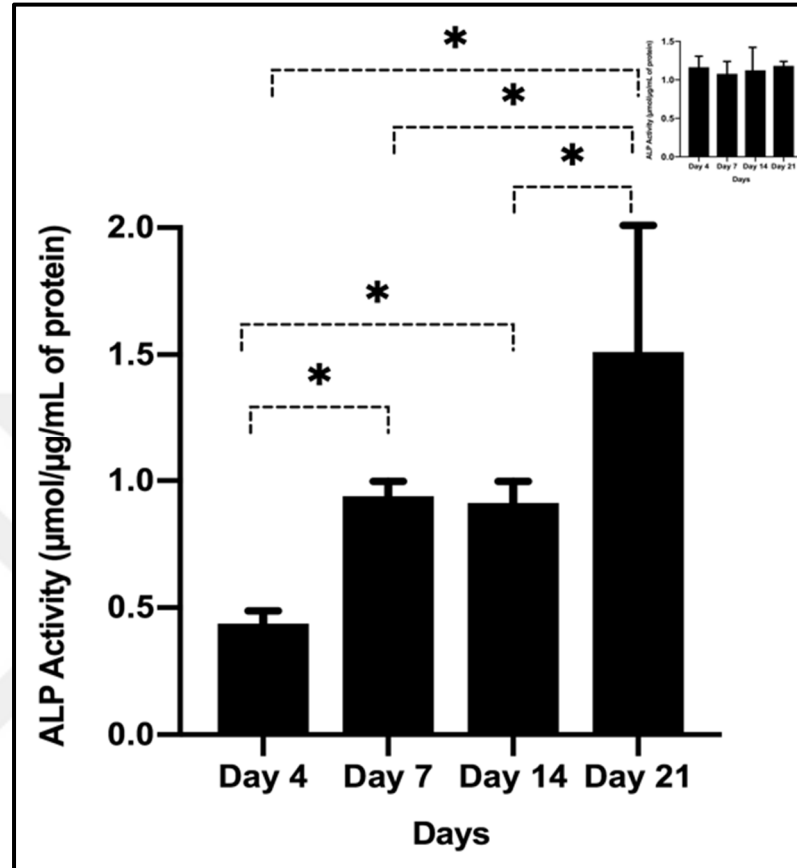
Figure 4.29. ALP activity analysis on 20-60-40 PLGA scaffolds after 4, 7, 14 and 21 days of incubation (*$p < 0.05$). Indent on the top right corner shows the ALP Activity on Tissue Culture Plate (TCP) and OC stands for the cells seeded into wells of the tissue culture plate (only cell).

4.7.3. von Kossa Staining

von Kossa staining was applied to determine mineralization on 20-60-40 PLGA scaffolds after 7, 14, and 21 days of incubation. Mineralization is also known as a late marker of osteoblast formation and mineralized nodules are shown by the brown regions in Figures 4.30 and 4.31. According to these images, mineral deposition of cells were identified by these brown regions from the 7th day of incubation period and also the increase in the intensity of brown regions was observed throughout 21 days of incubation (Figure 4.31).

On TCP, at day 7, red regions showing the presence of cells were obtained more than brown regions. However, reduction of red areas was appeared at the end of 21 days of incubation due to the mineralization (Figure 4.30).
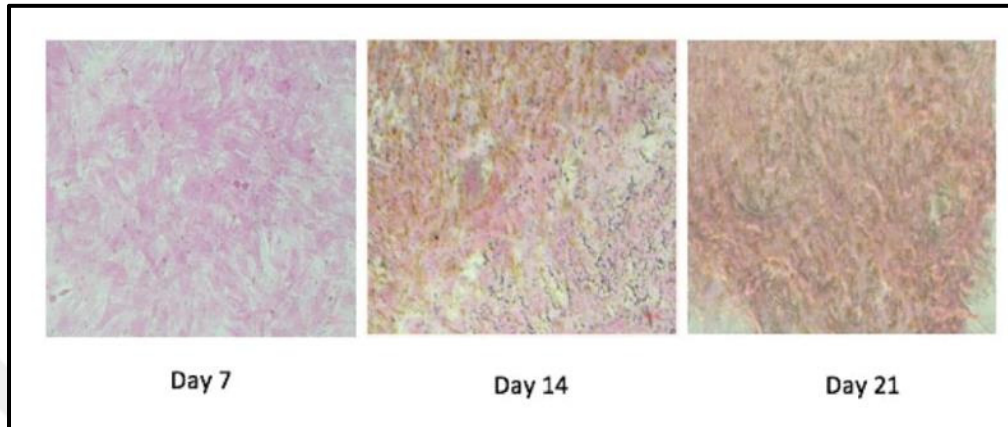
Figure 4.30. Microscope images of mineralization of rBMSCs seeded on TCP at the end of 7, 14 and 21 days of incubation by von Kossa staining (20X).
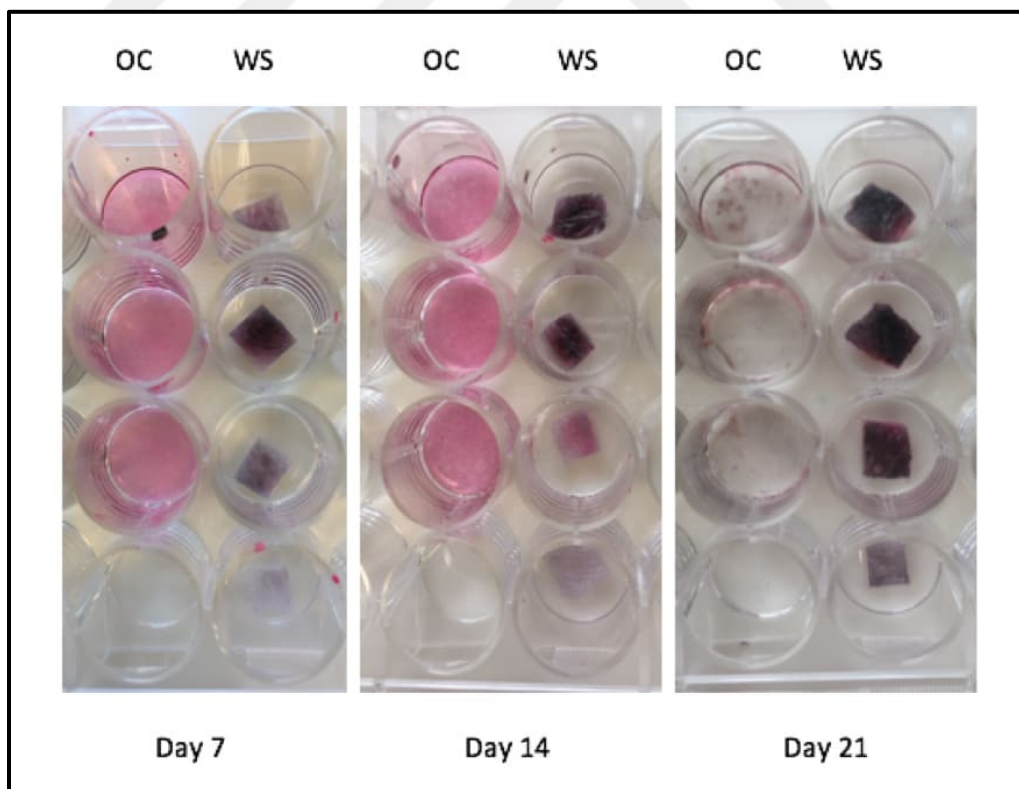
Figure 4.31. Mineralization images of rBMSCs seeded on wet spun PLGA fiber at the end of 7, 14 and 21 days of incubation by von Kossa staining (OC: Only Cell; WS: Wet Spun Scaffolds).

4.7.4. Real Time PCR

In this analysis, RNA was isolated from the cells that were cultured for the measurement of bone differentiation. Then, isolated RNA was transcribed into cDNA. The optimization of primers were performed before Real Time PCR. Then, the expression levels of VEGF, CD31, ALP, Runx2, osteocalcin and collagen type I were determined using Real Time PCR technique.

According to the results, at day 7, approximately 1.3-fold difference in VEGF expression was found between the experimental group and control group (Figure 4.32A). This indicates that rBMSCs expressed 1.3 fold VEGF compared to the control group. At day 14, decrease of VEGF expression was observed. At day 21, the amount of VEGF expressed by rBMSCs in the group containing GS4012, was increased again and the fold change was found as 2.6 between the experimental group and control group (Figure 4.32A).
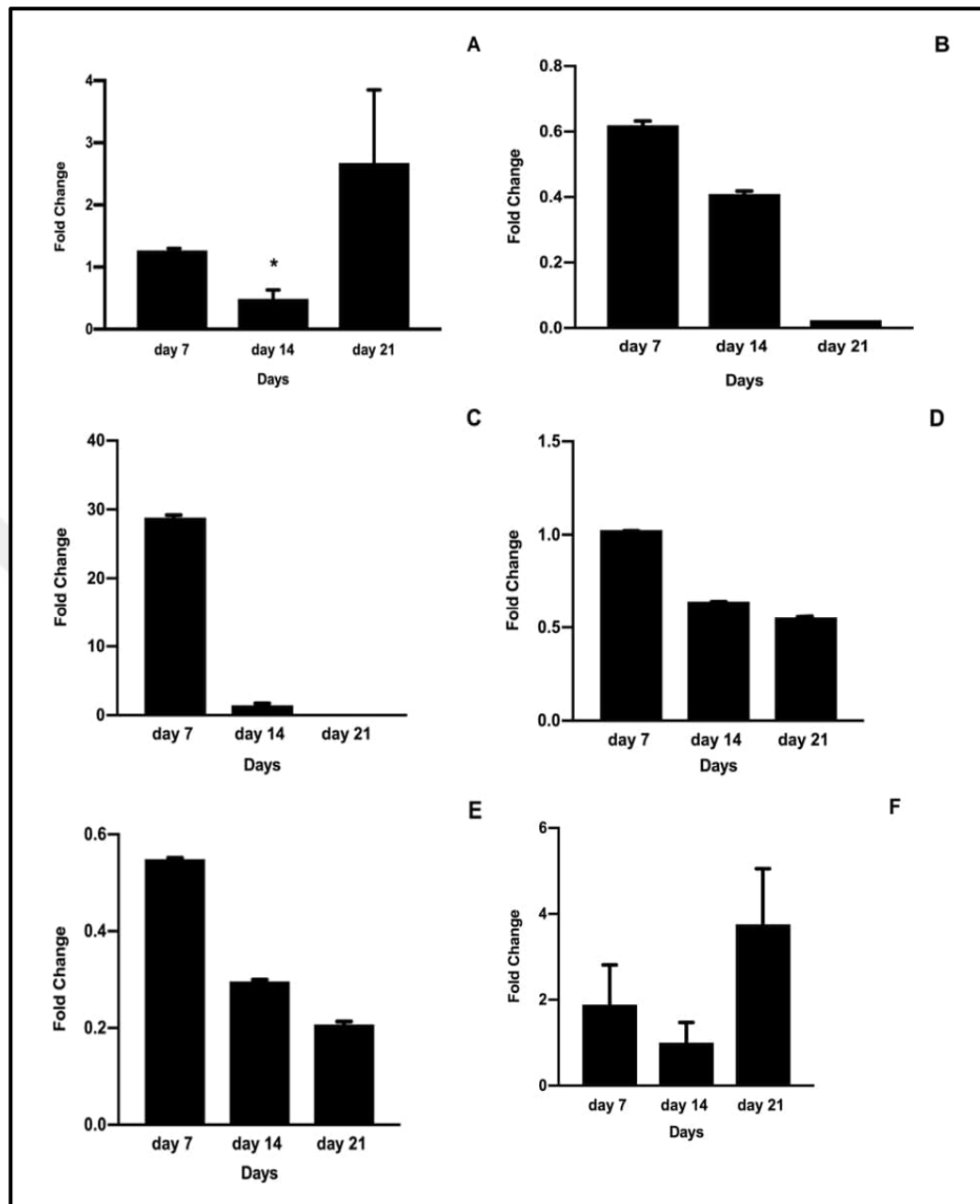
Figure 4.32. Expression levels of A) VEGF, B) CD31, C) Alkaline phosphatase (ALP), D) Runx2, E) Osteocalcin, F) Collagen type I (Col I) after 7, 14 and 21 days of incubation periods (*p<0.05). * shows the statistical significance between the experimental group containing GS4012, and the control group among the same days.

The analysis of CD31 that is a surface marker expressed by endothelial cells, gives an information about the amount of endothelial cells migrating to the scaffold. Results showed that at day 7, the fold difference of CD 31 expression between the experimental group and control group was higher compared to the fold difference at day 14 and day 21 (Figure 4.32B). Decrease in CD 31 expression was observed throughout 21 days of incubation. It was observed that GS4012 added group exhibited higher expression at day 7, compared to day 14 and day 21. In the graph of ALP (Figure 4.32C), at day 7, approximately 28.8 fold change in expression of ALP was also obtained between the experimental group and control group. This indicates that 28.8 fold higher ALP was expressed in the experimental group containing GS4012. From day 7 to day 21, the decrease in ALP expression was observed at GS4012 added group compared to control group (hydrogel without GS4012). In the Figure 4.32D, Runx2 expression was evaluated. It was observed that the expression of Runx2 reduced towards day 21. In the Figures 4.33E and 4.33F, the expressions of osteocalcin and collagen type I that are known as ECM proteins, were analyzed for differentiation. According to the results, the reduction of the expression of osteocalcin was observed from day 7 to day 21 (Figure 4.32E) and also 1.9 fold collagen type I expression was observed in the GS4012 added group at day 7 (Figure 4.32F). Despite a decrease in collagen type I expression at day 14, 3.75 fold increase in expression of collagen type I in GS4012 added group was obtained at day 21 compared to the control group.

4.7.5. VEGF Elisa Assay

At this part of the study, VEGF expression of the cells on the 20-60-40 PLGA scaffold during 21 days of incubation was evaluated by using Elisa method (Figure 4.33). The group consisting of PLGA-PEG-PLGA with GS4012 produced 7-fold VEGF at day 7, significantly ($*p < 0.05$).

The fold difference between GS4012 added group and control group was reduced to 1.3 at day 14. The amount of VEGF expressed in the group containing GS4012 was also reduced again at day 21 and the fold change became 1.2 between the experimental group and control group. The graph was compatible with the Real Time PCR graph as an up or down trend.
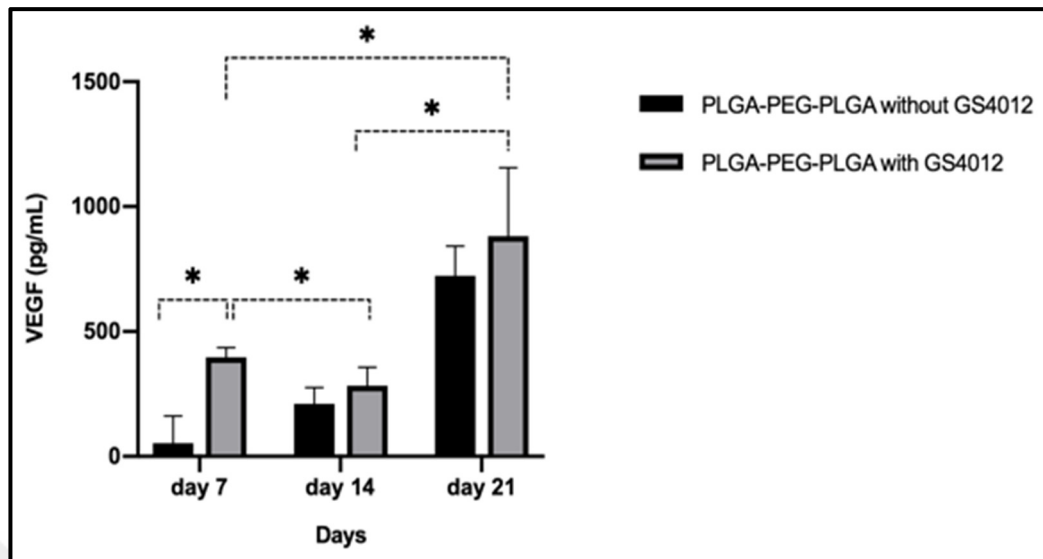
Figure 4.33. Evaluation of VEGF expression of cells during 21 days of incubation on 20-60-40 PLGA scaffold by Elisa method (*p<0.05).

4.8. *IN VIVO* STUDIES ON RAT MODEL: DETERMINATION OF BONE AND VASCULAR FORMATION

In five different groups, various combinations of fibrous PLGA scaffold base, rBMSCs, PLGA-PEG-PLGA hydrogel and GS4012 were applied on six different rats of each group (Figure 4.34a-d). After 4 and 8 weeks from the surgery, 3 rats from each group were sacrified. After the calvaria sections were stained with Masson's Trichrome Staining Techniques, histomorphometric analysis was applied to determine the volume of the bone and soft tissue.

Figure 4.34. *In vivo* studies on Rat Model a) 8 mm diameter cranial bone defect in rats b) PLGA scaffolds with or without rBMSCs in bone defects c) PLGA-PEG-PLGA hydrogel with or without GS4012 on the scaffold d) Sutured head after the operation.

4 weeks after surgery, vascularization and the new bone formation areas were increased in the cell seeded fiber + GS4012+ hydrogel groups compared with the control groups and other experimental groups (Figure 4.35). The difference between the control group and the fiber + GS4012 + hydrogel group also shows that GS4012 affected the formation of newly vascularized regions that led to the occurrence of new ossification sites (Figure 4.35). However, the cell seeded fiber + GS4012 + hydrogel group exhibited more remarkable results compared to the other groups which shows the effect of cells on bone formation.

After 8 weeks from the surgery, differences were clearly observed between the control group and the experimental groups. The formation of new vessels and new ossification areas were mostly found in the cell seeded fiber + GS4012 + hydrogel group. The same situation was also observed after 4 weeks from the surgery suggested that it continued its effect after 8 weeks in the experimental groups (Figure 4.35).
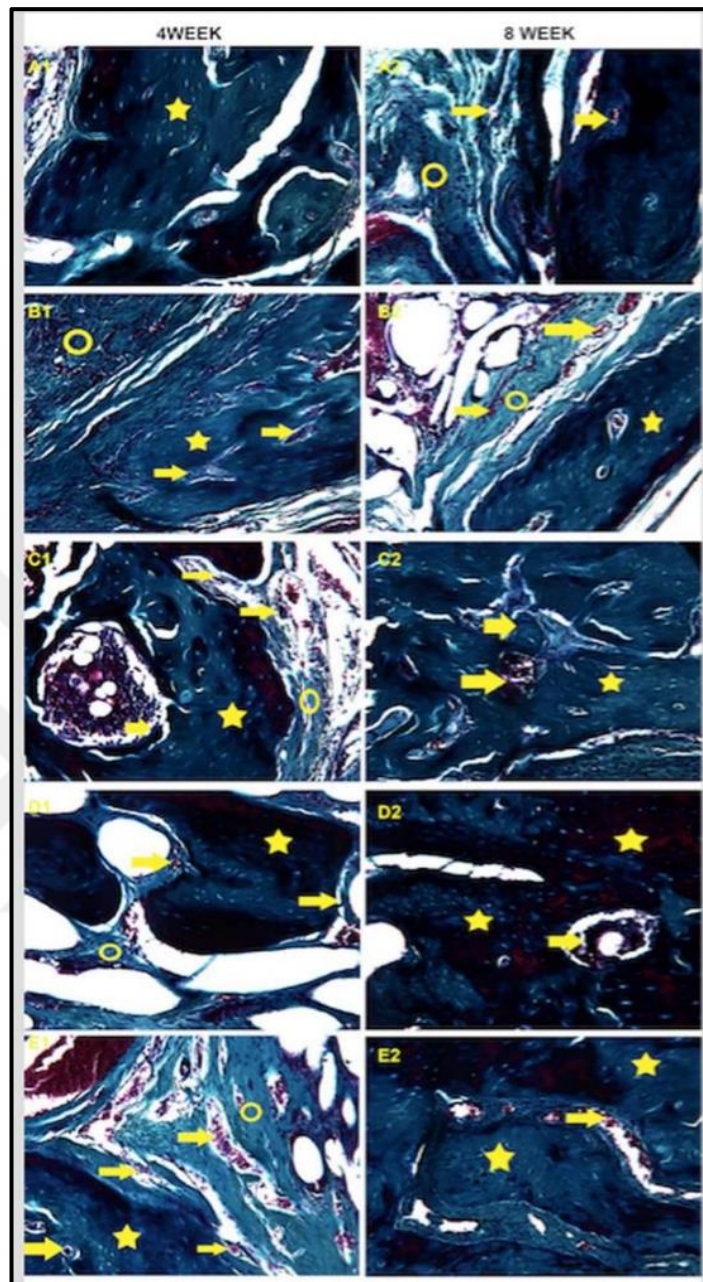
Figure 4.35. Photomicrographs demonstrating the sections from control and experimental groups. 4 weeks: A1; Control, B1; Fiber + Hydrogel, C1; Fiber+GS4012+Hydrogel, D1; Cell Seeded Fiber+Hydrogel, E1; Cell Seeded Fiber+ GS4012+Hydrogel. 8 weeks: A2; Control, B2; Fiber + Hydrogel, C2; Fiber+GS4012+Hydrogel, D2; Cell Seeded Fiber+Hydrogel, E2; Cell Seeded Fiber+ GS4012+Hydrogel. They were stained with Masson's Trichrome Staining Technique. New vascularization area (arrow) and connective tissue (circle) can be observed particularly in the groups after 4 weeks. These were shown using arrow and circles, respectively. Bone formation (star) was increased after 8 weeks. Original magnification is x20.

The results obtained from the histomorphometric measurements of the connective tissue volume ratio as well as the bone tissue volume ratio in the experimental groups are given in Tables 4.2 and 4.3 with the mean and standard deviation values.

Table 4.2. Comparision of calvaria bone tissue volume ratio values between 4 weeks and 8 weeks experimental groups. **p <0.5 and ***p <0.001.

Group Name	4 weeks (mean±stdev)	8 weeks (mean±stdev)
1	37,6867±4,3156	52,8333±7,14041
2	34,7267±3,69639	53,9±6,18297**
3	25,4733±10,55656	43,4867±1,60301
4	21,6267±7,54821	55,7333±6,44429***
5	33,70000±6,68356	53,8033±4,34261**

The ratio of the bone tissue volume to the total volume was analyzed histomorphometrically. Results shows that bone tissue volume ratio was significantly higher in group 2 after 8 weeks (53,9±6,18297) than the one after 4 weeks (34,7267±3,69639) (**p <0.5). The same result was also observed in group 4. The bone tissue volume ratio in group 4 was found significantly higher after 8 weeks (55,7333±6,44429) than the one after 4 weeks (21,6267±7,54821) (***p <0.001) (Table 4.2). Besides, the bone tissue volume ratio was higher in group 1 after 8 weeks (52,8333±7,14041) than the one after 4 weeks (37,6867±4,3156). In group 3, this ratio was found higher after 8 weeks (43,4867±1,60301) than the one after 4 weeks (25,4733±10,55656) (Table 4.2). However, in group 1 and 3, we could not observe any significant result of bone tissue volume ratio (Table 4.2) (Figure 4.36). The highest bone formation was observed in group 4 after 8 weeks whenever we compare it with the other groups.

Figure 4.36. Comparision of calvaria bone tissue volume ratio values between 4 weeks and 8 weeks experimental groups. **p <0.5, ***p <0.001.

Moreover, the ratio of the connective tissue volume to the total volume was analyzed histomorphometrically.

Table 4.3. Comparision of calvaria connective tissue volume ratio values between 4 weeks and 8 weeks experimental groups. **p <0.5 and ***p <0.001.

Group Name	4 weeks (mean±stdev)	8 weeks (mean±stdev)
1	62,3133±2,49161	47,1667±4,12252
2	65,2733±2,13411**	46,1±3,56974
3	74,5267±6,09483	56,5133±0,9255
4	78,3733±4,35796***	44,2667±3,72062
5	66,3±3,85876**	46,1967±2,50721

The ratio of connective tissue to total volume obtained from the tissues of the calvaria was found to be higher after 4 weeks in the groups 2 and 4. Results shows that connective tissue volume ratio was significantly higher in group 2 after 4 weeks (65,2733±2,13411) than the one after 8 weeks (46,1±3,56974) (**p <0.5). In group 4, the connective tissue volume ratio was found significantly higher after 4 weeks (78,3733±4,35796) than the one after 8 weeks (44,2667±3,72062) (***p <0.001) (Table 4.3). In addition, the connective tissue volume ratio was higher in group 1 after 4 weeks (62,3133±2,49161) than the one after 8 weeks (47,1667±4,12252). In group 3, this ratio was found higher after 4 weeks (74,5267±6,09483) than the one after 8 weeks (56,5133±0,9255) (Table 4.3). However, in group 1 and 3, we could not observe any significant result of connective tissue volume ratio (Table 4.3) (Figure 4.37). The highest vascularization was observed in group 4 after 4 weeks whenever we compare it with the other groups.
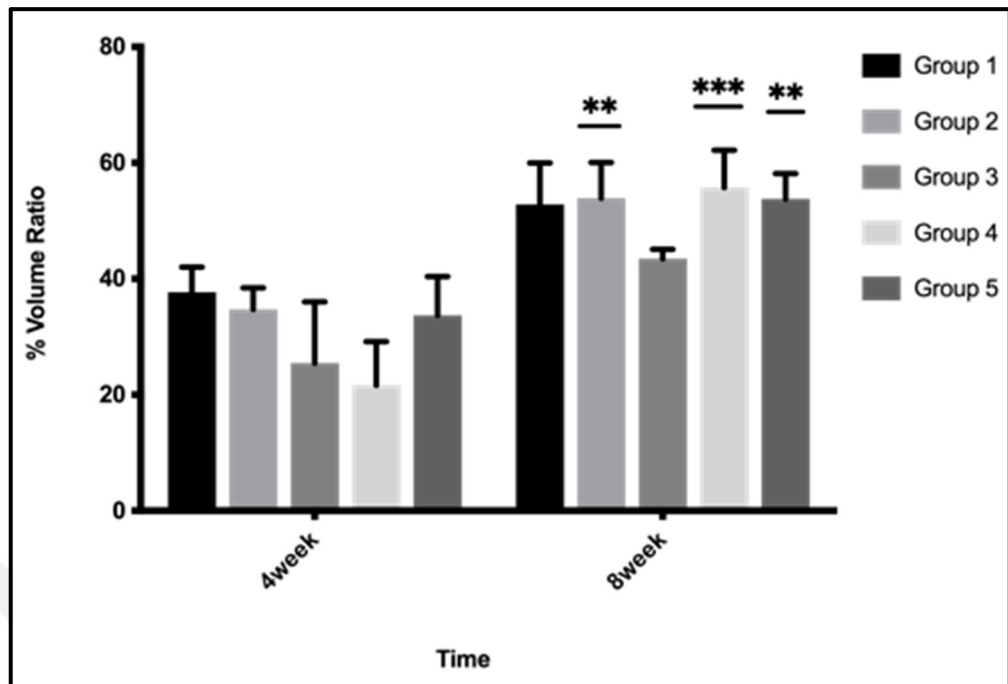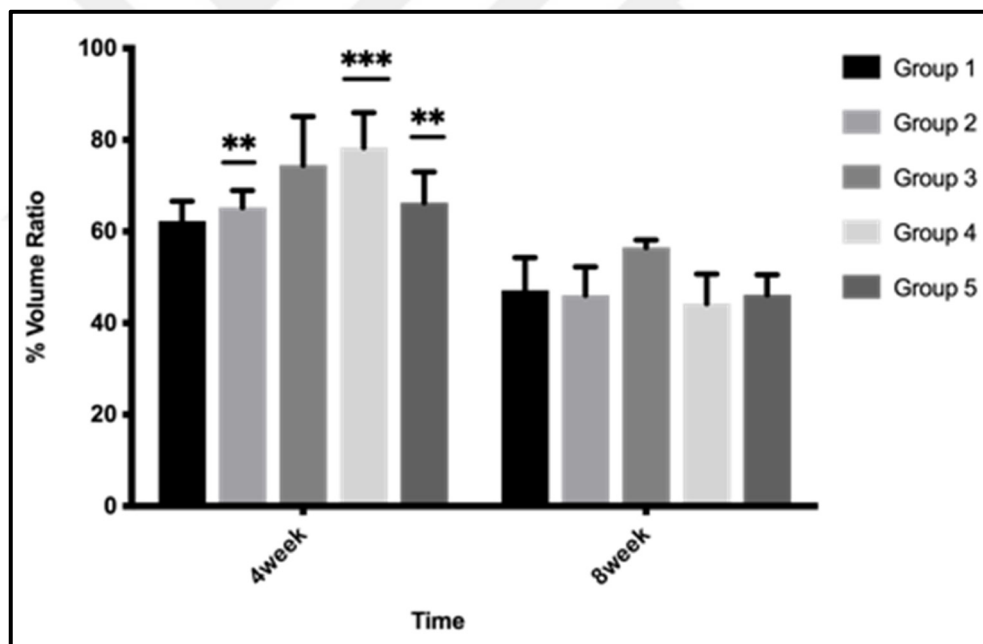

Figure 4.37. Comparision of calvaria connective tissue volume ratio values between 4 weeks and 8 weeks experimental groups. **p <0.5, ***p <0.001

5. DISCUSSION

Designing a biphasic scaffold are very important for the cells in bone tissue engineering studies. In this study, biphasic tissue engineering scaffold was composed of a fibrous PLGA scaffold base and PLGA-PEG-PLGA hydrogel which was responsible for the sustained release of VEGF inducer, GS4012 to induce vasculogenesis. This system was required to prevent insufficient vascularization in bone defect area.

In this study, we aimed to fabricate fibrous PLGA structure by using wet spinning technique and thus, prevent the problems related to both mechanical properties and biodegradation rates of PLGA. In one study, the effect of wet spinning method was analyzed for the production of polysulfonamide (PSA) fibers and compared with electrospinning method. The results displayed that improved mechanical properties could be observed when the PSA fiber was generated by wet spinning. Moreover, the molecular chain arrangement of the fiber prepared by wet spinning technique was more regular than the ones prepared by electrospinning [86].

Wet-spun fibrous PLGA scaffolds of 20, 25 and 30 per cent concentrations with 75:25, 60:40, 50:50 concentrations of isopropanol – dH$_2$O (IP:DW) coagulation baths were examined in this study for the future use of bone tissue engineering studies. First of all, scanning electron microscopy images of prepared scaffolds were evaluated. The external morphology of the fibers could be affected from the selected solvent system, polymer composition and concentration of the polymer solution. In addition, longitudinal grooves could provide contact guidance and it could result in the increase of surface area which could cause improvement in cell attachment [30, 87]. According to the SEM, 60:40 and 75:25 IP: DW coagulation baths were found more successful in wet spinning for 20, 25 and 30 per cent PLGA concentrations. However, 25 per cent PLGA concentration in 50:50 IP:DW coagulation bath resulted in the breaks in the fibers, therefore the process was ended up with spinning product. Due to reproducibility problems of 50-50 coagulation bath, it was decided to eliminate from further experiments. Reproducibility relies on the characteristics of diffusivity of the components used in coagulation baths and polymer solution in these samples.

The fabrication of materials can be affected by several factors that consist of polymer concentration, features of coagulation bath, nature of coagulants, injection rate of syringe pump, and diffusivity of components. Too much alcohol addition into coagulation bath can result in slower diffusion and reduction at the rate of precipitation of PLGA solution in coagulation bath can be obtained and precipitation rate can also be influenced by the solubility of PLGA in coagulation bath. The larger difference in solubility parameters between PLGA and the components of coagulation bath can generally indicate a faster precipitation rate. The precipitation rates follow the order: water > methanol > ethanol > IPA. Addition of isopropanol into the coagulation bath can lead to a decrease in precipitation rate [88, 89]. Therefore, 60:40 coagulation bath was chosen as an optimum coagulation bath, compared to 75:25 IP:DW coagulation bath since too much alcohol addition into coagulation bath can result in slower diffusion [90] and slower precipitation rate of PLGA solution in coagulation bath can be obtained. Also, increasing alcohol concentration causes slower diffusion and slower precipitation rates which can lead to lower mechanical properties of materials [88, 90]. Different concentrations of PLGA with 75:25 IP:DW coagulation bath, especially for the 20 per cent PLGA concentrations, couldn't be optimized to obtain a fiber formation by using wet spinning technique. Thus, 20-60-40, 25-60-40 and 30-60-40 samples were selected for the further usage.

Polymer concentration is one of the critical factors that have the effects on the mechanical properties of material. The critical polymer concentration should be decided to get an appropriate mechanical property [91]. Generally, increasing the polymer concentrations results in an increase in mechanical properties [88]. However, higher polymer concentration solutions beyond the critical viscosity are usually difficult for the fabrication of fibrous structure due to the problem with the penetration of the coagulant into the polymer matrix and also, weaker mechanical properties are detected at a polymer concentration lower than the critical viscosity [88, 91]. The 75-25 IP:DW coagulation baths could be thought as a weak coagulation baths due to their higher alcohol concentrations compared to the 60-40 IP:DW coagulation baths.

On the other hand, 75-25 IP:DW coagulation baths could show the same effect with 60-40 IP:DW coagulation bath in higher polymer concentrations such as 25 and 30 per cent. It is thought that the optimization problems of 20-75-25 could be related with this situation.

Contact angle measurements shows the the degree of wettability. Angles less than 90° exhibit highly wettable surfaces whereas angles greater than 90° induce lower wetting properties of the surfaces [92]. According to the results, each sample had a contact angle below 90°, indicating that wetting of the surface was favorable. Therefore, the fluid had the ability to spread over a large area on the surface. The moderate hydrophilicity is also required for cell proliferation and adhesion [92, 93].

Besides, the results of degradation studies showed that samples of 20-60-40, 25-60-40, 30-60-40, 30-75-25 and 25-75-25 maintained at least 80 per cent of their weight during the first 90 day. However, after day 90, rapid degradation of PLGA, especially for 30-75-25 and 25-75-25 samples, was observed. If the diffusion of water is not faster than the degradation of the polymer, it leads to the hydrolysis of bonds on the polymer surface. On the other hand, if the degradation of polymer is slower than the diffusion of water into the polymer, the polymer undergoes a bulk erosion [94]. Also, in our study, we observed bulk erosion of 30-75-25 and 25-75-25 samples after 90 days of incubation. Besides, whenever we investigated the pH changes in our samples, there was not too much pH change observed in the first 90 days except for the sample of PLGA 25-75-25.

While a phosphate buffered saline solution is used *in vitro* to resist the small pH changes due to degradation; *in vivo,* the blood buffer systems undertake the same task, and inhibit a rapid pH change due to degradation [95]. After 90 days incubation period, pH of the solution also decreased with increasing incubation period due to degradation of PLGA scaffold. It was due to the release of lactic acid and glycolic acid after the degradation of PLGA [28, 96, 97]. A significant decrease in pH was not desirable since it could result in necrosis in cells and tissues. The result of degradation of PLGA scaffolds showed that 60:40 bath composition with 20 per cent PLGA concentration was preferable for bone tissue engineering studies. In addition, when we observed the SEM images of degraded PLGA samples, instantaneous decrease in pH values was shown for 25-75-25 and 30-75-25, respectively, after 60 and 90 days of incubation periods.

It was due to the fact that the bulk erosion of the material may occurred earlier than the others. As a result of degradation analysis, the sample of 20-60-40 was found as the least degraded sample. These scanning electron micrographs supported the results of the degradation study.

In the second part of the study, rBMSCs and rPBECs were isolated. For the characterization of these cells, different tests were applied. According to the differentiation tests, cells isolated from bone marrow were found to exhibit mesenchymal stem cell properties. Their bone, cartilage and adipose cell differentiations were investigated. Also, cells isolated from peripheral blood were found to exhibit endothelial cell properties by examining LDL uptake capacity, CD31 expression, ability to form tubular structure and their migration capability.

After cell characterization, migration test was performed to observe the effect of GS4012 on rPBECs migration. In this assay, results showed that GS4012 was successful than the VEGF with respect to the migration of cells to the wells of cell culture plates. It was due to the fact that the medium containing GS4012 or VEGF were not be changed during 3 days of incubation and VEGF lost its effect due to its short half-life while GS4012 showed the effect for a long time on the migration of rPBECs.

In the third part of the study, *in vitro* cell-biomaterial interaction was investigated. For the cell proliferation, MTS assay was applied. In this assay, 20-60-40, 25-60-40, 30-60-40, 30-75-25, 25-75-25 samples were evaluated. The highest cell number at all time points was detected on TCP due to its larger surface area that was provided for cells to attach. Also, 20-60-40 sample showed the better characteristics for cell proliferation and it was selected as the best according to the MTS assay and degradation test. With respect to cell proliferation, 30 per cent PLGA sample also had good results. However, they were eliminated from the study since it showed a rapid degradation according to the degradation analysis. Sample of 20-60-40 PLGA was preferred to be used for further experiments.

Next, cell seeded 20-60-40 PLGA scaffolds were evaluated by using scanning electron microscope for cell adhesion. At day 10, spreading and proliferation of cells were observed on this scaffold, and the surfaces were completely covered with cells at day 20. It could be due to the appropriate pore size and porosity of the fibers produced by using wet-spinning technique [32].

Pore size provides an advantage for cells to penetrate inside the scaffolds and to supply efficient flow of O_2 and nutrients for supporting cell growth and cell spreading [98].

Also, 20-60-40 PLGA scaffolds were examined to observe cell viability by using MTS assay. According to the results, cell adhesion and proliferation were obtained on these scaffolds in osteogenic differentiation medium. From day 4 to day 14, the increase in cell number was observed even though they were grown in osteogenic differentiation medium. It was thought that MSCs have the ability to demonstrate repeated self-renewal for maintaining their stem cell characteristics, thus they can exhibit extended proliferation while keeping their differentiation capacity [99]. However, at day 21, the decrease in cell number was observed since they decreased the rate of proliferation while they were differentiating [98, 100].

In order to evaluate cell differentiation on 20-60-40 scaffold; ALP, von Kossa and Real Time PCR analyses were carried out. Osteogenic activity of rBMSCs was investigated by ALP assay first. ALP is known as an early marker of osteoblast differentiation [98]. Throughout 21 days of incubation, increase in the ALP activity was observed on 20-60-40 wet spun PLGA scaffolds. From day 7 to day 14, there was no significant increase in ALP activity since the proliferation of cells was still prevailed throughout day 14. At day 21, increase in ALP activity was shown. At this time point, decrease in cell number was observed depending on the differentiation. Also, our MTS result supported this finding.

Mineralization, which is one of the most important markers of bone differentiation in late stage, is also an important factor of forming a functional bone tissue. According to the results of von Kossa staining, mineralization was observed at high level on 20-60-40 wet spun PLGA fibers at the end of 21 days of incubation period. The homogeneous spreading of the mineralized nodules deposited by the cells was appeared on the scaffolds at days 14 and 21. By this way, nutrients and oxygen could be diffused to all inner parts of the scaffold due to its porous structure [98].

Furthermore, real time PCR analysis was applied for the determination of gene expression of VEGF, CD31, ALP, Runx2, osteocalcin and collagen type I. According to the results, firstly, VEGF expression that is responsible for the formation of vessel-like structure was evaluated [51, 56].

The expression of 1.3 fold VEGF was obtained in the experimental group containing hydrogel with GS4012 compared to the control group containing hydrogel without GS4012 at day 7. This difference was due to the effect of GS4012 on increase of VEGF expression [85].

In this experiment, rBMSCs seeded on the PLGA scaffold secreted more VEGF by the help of GS4012 released from the hydrogel that leads to endothelial cell migration from the pores of the insert to the scaffold. At day 14, VEGF expression decreased in the experimental group which was followed by an increase in VEGF expression after 21 days of incubation. At day 21, 2.6 fold VEGF expression was observed in the experimental group, compared to the control group. At the end of 21 days of incubation period, most of the endothelial cells migrated from the pores of the insert to the scaffold due to the effect of GS4012 [85, 51].

CD 31 is another marker used in this experiment and it exhibits the presence of endothelial cells. According to the results, from day 7 to day 21, there was a decrease between the experimental group containing hydrogel with GS4012 and the control group containing hydrogel without GS4012. At day 7, higher expression of CD 31 could be due to the fact that VEGF produced by the help of GS4012 led to the migration of endothelial cells in an early period. The decrease in VEGF expression from day 7 to 14 also affected the expression of CD31 and it led to decrease the amount of CD31 expression at day 14. At day 21, the lowest expression of CD31 was observed. It could be due to the fact that migration of endothelial cells was suppressed by an excessive amount of VEGF [101]. According to the graph of VEGF expression, we observed the high level of VEGF expression at day 21. However, at this time point, the low level expression of CD 31 was exhibited due to the excessive amount of VEGF.

The increase in ALP activity at the early stages is observed during osteoblast differentiation [98]. According to our results, the expression of 28.8 fold ALP was obtained in the experimental group containing hydrogel with GS4012 compared to the control group containing hydrogel without GS4012 at day 7. Throughout 21 days of incubation, the reduction of its expression was observed. This result was expected since the presence of the expression of ALP shows the presence of osteogenic cells in the culture in an early period [98].

Runx2 is one of the other transcription factors that plays role in differentiation. Its expression is observed at the early stages [98]. According to our results, at day 21, GS4012 added group showed a decrease in the expression of Runx2 compared to the ones at day 7 and day 14 due to the induction of Runx2 at the early stages.

Collagen type I and Osteocalcin (OCN) are known as ECM proteins of bone. Immature osteoblasts are responsible for the expression of Collagen type I while mature osteoblasts lead to the expression of osteocalcin [98]. In our results, the expression of osteocalcin was reduced from day 7 to day 21. Also, in one of the study, the expression of osteocalcin was observed at the early stages in bone differentiation [102]. Maximum level of osteocalcin is observed through the mineralization [98]. Thus, the presence of mineralized bone matrix and the differentiation of mesenchymal stem cells into mature osteoblasts were observed on PLGA scaffold. Also, the expression of collagen was decreased from day 7 to day 14 in the experimental group containing hydrogel with GS4012 compared to control group containing hydrogel without GS4012. Its expression is provided by immature osteoblasts, therefore, it was higher at day 7. However, reduction in the expression level of collagen was observed at day 14. It could be due to the bone remodeling cycle that shows the demineralization of the collagen by osteoclasts. It can also affect the osteoblast recruitment potential. Subsequently, bone matrix formation could be started [98]. Increase in the collagen expression was observed from day 14 to day 21 as the bone regeneration occurred in time.

According to the VEGF Elisa Assay, the results were found compatible with the Real Time PCR data in terms of an up or down trend. On the other hand, there was a difference in mRNA and protein levels after 21 days of incubation. Fold differences in this graph were not be same with the results of Real Time PCR due to the accumulation of VEGF protein in time. Also, the amount of VEGF production at day 7 indicated that GS4012 may have an effect on vascularity at the early stages.

GS4012, an activator of the vascular endothelial growth factor (VEGF), may have a positive and accelerating effect in an early period for induction of the formation of new vessels and also, the formation of new ossification sites may be facilitated by triggering the vascularization before bone mineralization. In our study, we expected to observe an increase in vascularization after 4 weeks and the replacement of this vascularization sites by new ossification after 8 weeks period.

According to the result of *in vivo* studies, in the 4 weeks experimental groups, the vascularity was increased and, in the 8 weeks period, formation of the newly ossified areas was observed, especially in group 4. This result was proved by the CD31 expression in Real time PCR analysis in terms of the effect of GS4012 on new vessel formation in an early period.

Also, the values of bone tissue volume ratio and connective tissue volume ratio supported the photomicrographs of these experimental groups. In addition, increase in bone formation from weeks 4 to 8 in group 2 was found less significant than the one in group 4. Here, it could be said that rBMSCs had a potential to accelarate bone formation. It was also thought that the vascularization that was provided by GS4012 in the 4 weeks period also facilitated the formation of bone tissue in the 8 weeks experimental period. Also, bone tissue volume ratio in group 4 was higher than the one in group 3 in the 8 weeks period. It may show the effect of GS4012 on bone formation by speeding up vascularization. On the other hand, in the group 1 and 3, we couldn't observe significant results for the formation of bone and vascularity. According to the results, it was said that the effect of rBMSCs and GS4012 was proved on both bone and vessel formation.

When the ratio of the connective tissue volume to the total volume was analyzed histomorphometrically, the values in connective tissue were more significant in group 4 in the 4 weeks period compared to the one in the 8 weeks period. Also, the decrease in connective tissue formation from weeks 4 to 8 in group 2 was found less significant than the one in group 4. This result shows the effect of cells on the formation of vessel in an early period. Also, connective tissue volume ratio in group 4 was higher than the one in group 3 in the 4 weeks period. It shows the effect of GS4012 on the vessel formation in an early period. In group 4, suitable environment required for bone formation was first achieved by the increase of connective tissue that was produced by the increase of vascularization and connective tissue fibers. It can also be said that rBMSCs and GS4012 accelerated the ossification by increasing vascularity. This result supports the result of bone tissue volume ratio.

6. CONCLUSION

This study was performed to create a tissue engineered biphasic scaffold that includes PLGA-PEG-PLGA hydrogel with or without GS4012 and PLGA scaffold base. Also, the effect of the extended release of GS4012 was investigated on insufficient vascularization of bone healing by the help of migration of endothelial cells to the defected area.

First of all, different concentrations of PLGA scaffold, which was the first phase of biphasic scaffold, was fabricated by wet spinning method and rBMSCs seeded scaffolds were investigated by SEM, contact angle analysis, degradation studies and cell proliferation assay. According to the results, sample of 20 per cent PLGA concentration in 60:40 IP:DW coagulation bath was selected as the best sample for their degradation properties and cell proliferation capacity. Secondly, the PLGA-PEG-PLGA hydrogel with GS4012 was prepared as the second phase of the scaffold to observe the release of GS4012 from the hydrogel. At this stage, the migration of endothelial cells was desired due to the induction of VEGF by the release of GS4012 and the acceleration of VEGF production by rBMSCs seeded on PLGA scaffold.

As a result of this study, it has been shown that GS4012 is capable of inducing endothelial cells to migrate, proliferate, and also provide the induction of vascularization due to its release from the hydrogel. *In vivo* studies, group 4 (rBMSCs seeded PLGA scaffold + PLGA-PEG-PLGA hydrogel with GS4012) demonstrated the better healing response of the defected tissue since adequate nutrition and oxygen requirements of the vascularized tissue were provided. It was determined that the scaffold was degraded in time and replaced by a bone tissue close to the natural tissue. The success of this material was proved with both *in vitro and in vivo* experiments by achieving sufficient vascularization that leads to bone regeneration.

This study will reduce the rate of failure due to insufficient vascularization in bone tissue engineering studies and will shorten the recovery period of the patient. The need for implants and prostheses will also decrease and it will also have an economical contribution to our country.

7. FUTURE PROSPECTS

In tissue engineering studies, the new biomaterials with better characteristics are always investigated and designed. In this study, biphasic scaffold was fabricated to solve the problem with insufficient vascularization in bone defect area by the help of sustained release of GS4012 from the hydrogel. In the future, other small molecules can be tried to induce vasculogenesis and be used with controlled delivery systems, instead of sustained delivery systems. Another type of hydrogel and different type of polymer can be selected for the delivery of small molecules and supplying mechanical strength to biphasic scaffold, respectively. Also, mechanical analysis should be done for these new biomaterials. Finally, *in vivo* studies can be carried out to prove the success of these new biomaterials in an experimental model.

REFERENCES

1. Clarke B. Normal bone anatomy and physiology. *Clinical Journal of American Society of Nephrology*. 2008;3: 131-9.

2. Bayliss L, Mahoney DJ, Monk P. Normal bone physiology, remodelling and its hormonal regulation. *Surgery*. 2012;30(2): 47-53.

3. Vernon L, Kaplan L, Huang CC. Stem cell based bone tissue engineering. *Bone Regeneration.* 2012: 11-33.

4. Zuo C, Huang Y, Bajis R, Sahih M, Li YP, Dai K, Zhang X. Osteoblastogenesis regulation signals in bone remodeling. *Osteoporos International.* 2012;23(6): 1653-63.

5. Mumford JE, Simpson AHRW. Management of bone defects: A review of available techniques. *Iowa Orthopaedic Journal.* 1992;12: 42-9.

6. Gan AWT, Puhaindran ME, Pho RWH. The reconstruction of large bone defects in the upper limb. *Injury.* 2013;44(3): 313-7.

7. Janicki P, Schmidmaier G. What should be the characteristics of the ideal bone graft substitute? Combining scaffolds with growth factors and/or stem cells. *Injury.* 2011;42: 77-81.

8. Oryan A, Parizi AM, Shafiei-Sarvestani Z, Bigham AS. Effects of combined hydroxyapatite and human platelet rich plasma on bone healing in rabbit model: radiological, macroscopical, histopathological and biomechanical evaluation. *Cell and Tissue Banking.* 2012;13(4): 639-51.

9. Hollinger JO, Uludag H, Winn SR. Sustained release emphasizing recombinant human bone morphogenetic protein-2. *Advanced Drug Delivery Reviews.* 1998;31(3): 303-18.

10. Parizi AM, Oryan A, Shafiei-Sarvestani Z, Bigham AS. Human platelet rich plasma plus Persian Gulf coral effects on experimental bone healing in rabbit model:

Radiological, histological, macroscopical and biomechanical evaluation. *Jornal of Materials Science: Materials in Medicine.* 2012;23(2): 473-83.

11. Li J, Wang HL. Common implant-related advanced bone grafting complications: classification, etiology, and management. *Implant Dentistry.* 2008;17(4): 389-401.

12. Moshiri A, Oryan A. Role of tissue engineering in tendon reconstructive surgery and regenerative medicine: Current concepts, approaches and concerns. *Hard Tissue.* 2012;1(2): 1-11.

13. Matassi F, Nistri L, Paez DC, Innocenti M. New biomaterials for bone regeneration. *Clinical Cases in Mineral Bone Metabolism.* 2011;8(1): 21-4.

14. Bakar ZA, Hussein BF, Mustapha NM. Cockle shell-based biocomposite scaffold for bone tissue engineering. *Regenerative medicine and tissue engineering – cells and biomaterials.* 2011: 365-391.

15. Sarkar D, Zhao W, Schaefer S, Ankrum JA, Teo GSL, Pereira MN, Ferreira L, Karp JM. Overview of tissue engineering concepts and applications. *Biomaterials science.* 2013: 1122-1137.

16. Liu Y, Wu G, de Groot K. Biomimetic coatings for bone tissue engineering of critical-sized defects. *Journal of The Royal Society Interface.* 2010;7(5): 631-47.

17. Yoruc ABH, Sener BC. Biomaterials. *Biomaterials Research Advances.* 1989: 53:160.

18. Subia B, Kundu J, Kundu SC. Biomaterial scaffold fabrication techniques for potential tissue engineering applications. *Tissue engineering.* 2010: 141-59.

19. Griffith LG. Emerging design principles in biomaterials and scaffolds for tissue engineering. *Annals of The New York Academy of Sciences.* 2002;961: 83-95.

20. Tabata Y. Biomaterial technology for tissue engineering applications. *Journal of The Royal Society Interface.* 2009;6(3): 311-24.

21. Schieker M, Seitz H, Drosse I, Seitz S, Mutschler W. Biomaterials as scaffold for bone tissue engineering. *European Journal of Trauma.* 2006;32(2): 114-24.

22. Mour M, Das D, Winkler T, Hoenig E, Mielke G, Morlock MM, Schilling AF. Advances in porous biomaterials for dental and orthopaedic applications. *Materials.* 2010;3(5): 2947-74.

23. Rezwan K, Chen QZ, Blaker JJ, Boccaccini AR. Biodegradable and bioactive porous polymer/inorganic composite scaffolds for bone tissue engineering. *Biomaterials.* 2006;27(18): 3413-31.

24. Pitt GG, Gratzl MM, Kimmel GL, Surles J, Sohindler A. Aliphatic polyesters II. The degradation of poly(DL-lactide), poly(e-caprolactone) and their copolymers in vivo. *Biomaterials.*1981;2: 215-220.

25. Tsuji H, Ikada Y. Properties and morphology of poly (L-lactide) 4. Effect of structural parameters on long term hydrolysis of poly(L-lactide) in phosphate- buffered solution. *Polymer Degradation and Stability.* 2000;67(1): 179-189.

26. Wu XS, Wang N. Synthesis, characterization, biodegradation, and drug delivery application of biodegradable lactic/glycolic acid polymers. Part II: Biodegradation. *Journal of Biomaterials Science, Polymer Edition.* 2001;12(1): 21-34.

27. Lu L, Peter SJ, Lyman MD, Lai HL, Leite SM, Tamada JA, Vacanti JP, Langer R, Mikos AG. In vitro degradation of porous poly (L-lactic acid) foams. *Biomaterials.* 2000;21(15): 1595-1605.

28. Engineer C, Parikh J, Raval A. Review on hydrolytic degradation behavior of biodegradable polymers from controlled drug delivery system. *Trends in Biomaterials and Artificial Organs.* 2011;25(2): 79-85.

29. Park PIP, Jonnalagadda S. Predictors of glass transition in the biodegradable polylactide and poly-lactide-co-glycolide polymers. *Journal of Applied Polymer Science.* 2006;100(3): 1983-1987.

30. Nelson KD, Romero A, Waggoner P, Crow B, Borneman A, Smith GM. Technique paper for wet-spinning poly(L-lactic acid) and poly(DL-lactide-co-glycolide) monofilament fibers. *Tissue Engineering.* 2003;9(6): 1323-1330.

31. Neves SC, Teixeira LSM, Moroni L, Reis RL, Blitterswijk CAV, Alves NM, Karperien M, Mano JF. Chitosan/poly(ε-caprolactone) blend scaffolds for cartilage repair. *Biomaterials*. 2011;32(4): 1068-79.

32. Pati F, Adhikari B, Dhara S. Development of chitosan-tripolyphosphate non-woven fibrous scaffolds for tissue engineering application. *Journal of Materials Science: Materials in Medicine*. 2012;23(4): 1085-96.

33. Puppi D, Dinucci D, Bartoli C, Mota C, Migone C, Dini F, Barsotti G, Carlucci F, Chiellini F. Development of 3D wet-spun polymeric scaffolds loaded with antimicrobial agents for bone engineering. *Journal of Bioactive and Compatible Polymers*. 2011;26(5): 478-92.

34. Fourne F. *Synthetic fibers: machines and equipment, manufacture, properties*. Ohio: Hanser/Gardner; 1999.

35. Gupta VB, Kothari V. *Manufactured fiber technology*. London: Chapman and Hall; 1997.

36. Arbab S, Noorpanah P, Mohammadi N, Soleimani M. Designing index of void structure and tensile properties in wet-spun polyacrylonitrile (PAN) fiber. I. Effect of dope polymer or nonsolvent concentration. *Journal of Applied Polymer Science*. 2008;109(6): 3461-3469.

37. Ooya T, Park K. Polymer solution properties, micelles, dendrimers, and hydrogels. *Biomaterials for delivery and targeting of proteins and nucleic acids*. 2005:102-110.

38. Alexander A, Ajazuddin, Khan J, Saraf S, Saraf S. Polyethylene glycol (PEG)-poly(N-isopropylacrylamide) (PNIPAAm) based thermosensitive injectable hydrogels for biomedical applications. *European Journal of Pharmaceutics and Biopharmaceutics*. 2014;88(3): 575-585.

39. Wu J, Zeng F, Huang XP, Chung JC, Konecny F, Weisel RD, Li RK. Infarct stabilization and cardiac repair with a VEGF-conjugated, injectable hydrogel. *Biomaterials*. 2011;32(2): 579-86.

40. Dhandayuthapani B, Yoshida Y, Maekawa T, Kumar DS. Polymeric scaffolds in tissue

engineering application: A review. *International Journal of Polymer Science*. 2011; 19.

41. Qiao M, Chen D, Ma X, Liu Y. Injectable biodegradable temperature-responsive PLGA–PEG–PLGA copolymers: Synthesis and effect of copolymer composition on the drug release from the copolymer-based hydrogels. *International Journal of Pharmaceutics. 2005;* 294(1-2): 103-112.

42. Zhang K, Tang X, Zhang J, Lu W, Lin X, Zhang Y, Tian B, Yang H, He H. PEG–PLGA copolymers: Their structure and structure-influenced drug delivery applications. *Journal of Controlled Release*. 2014;183: 77-86.

43. Ikada Y. Challenges in tissue engineering. *Journal of The Royal Society Interface*. 2006;3(10): 589-601.

44. Bonewald LF. The amazing osteocyte. *Journal of Bone and Mineral Research*. 2011; 26(2): 229-238.

45. Henriksen K, Bollerslev J, Everts V, Karsdal MA. Osteoclast activity and subtypes as a function of physiology and pathology - implications for future treatments of osteoporosis. *Endocrine Reviews.* 2011;32(1): 31–63.

46. Portal-Núñez S, Lozano D, Esbrit P. Role of angiogenesis on bone formation. *Histology and Histopathology.* 2012;27(5): 559-566.

47. Salgado AJ, Coutinho OP, Reis RL. Bone tissue engineering: state of the art and future trends. *Macromolecular Bioscience.* 2004;4(8): 743-65.

48. Fakhry M, Hamade E, Badran B, Buchet R, Magne D. Molecular mechanisms of mesenchymal stem cell differentiation towards osteoblasts. *World Journal of Stem Cells*. 2013;5(4): 136-148.

49. Goers L, Freemont P, Polizzi KM. Co-culture systems and technologies: taking synthetic biology to the next level. *Journal of The Royal Society Interface*. 2014;11(96).

50. Chong PP, Selvaratnam L, Abbas AA, Kamarul T. Human peripheral blood derived mesenchymal stem cells demonstrate similar characteristics and chondrogenic differentiation potential to bone marrow derived mesenchymal stem cells. *Journal of Orthopaedic Research*. 2012;30(4): 634-642.

51. Bai Y, Yin G, Huang Z, Liao X, Chen X, Yao Y, Pu X. Localized delivery of growth factors for angiogenesis and bone formation in tissue engineering. *International Immunopharmacology*. 2013;16(2): 214-223.

52. Vailhé B, Vittet D, Feige JJ. *In vitro* models of vasculogenesis and angiogenesis. *Laboratory Investigation.* 2001;81(4): 439-452.

53. Jabbarzadeh E, Blanchette J, Shazly T, Khademhosseini A, Camci-Unal G, Laurencin CT. Vascularization of biomaterials for bone tissue engineering: Current approaches and major challenges. *Current Angiogenesis*. 2012;1(3): 180-191.

54. Ennett AB, Kaigler D, Mooney DJ. Temporally regulated delivery of VEGF *in vitro* and *in vivo*. *Journal of Biomedical Materials Research Part A*. 2006;79(1): 176-184.

55. Levengood SK, Poellmann MJ, Clark SG, Ingram DA, Yoder MC, Johnson AJ. Human endothelial colony forming cells undergo vasculogenesis within biphasic calcium phosphate bone tissue engineering constructs. *Acta Biomaterialia*. 2011;7(12): 4222-4228.

56. Helmrich U, Di Maggio N, Güven S, Groppa E, Melly L, Largo RD, Heberer M, Martin I, Scherberich A, Banfi A. Osteogenic graft vascularization and bone resorption by VEGF-expressing human mesenchymal progenitors. *Biomaterials.* 2013;34(21): 5025-5035.

57. Tabata Y, Yamamoto M, Ikada Y. Biodegradable hydrogels for bone regeneration through growth factor release. *Pure and Applied Chemistry*. 1998;70(6): 1277-1282.

58. Forsythe JA, Jiang BH, Lyer NV, Agani F, Leung SW, Koos RD, Semenza GL. Activation of vascular endothelial growth factor gene transcription by hypoxia-inducible factor 1. *Molecular Cell Biology*. 1996;16(9): 4604-13.

59. Ceradini DJ, Kulkarni AR, Callaghan MJ, *et al*. Progenitor cell trafficking is regulated

by hypoxic gradients through HIF-1 induction of SDF-1. *Nature Medicine.* 2004;10(8): 858-64.

60. Skiles ML, Fancy R, Topiwala P, Sahai S, Blanchette JO. Correlating hypoxia with insulin secretion using a fluorescent hypoxia detection system. *Journal of Biomedical Materials Research – Part B Applied Biomaterials.* 2011;97(1): 148-55.

61. Tan W, Desai TA. Layer-by-layer microfluidics for biomimetic three-dimensional structures. *Biomaterials.* 2004;25(7-8): 1356- 64.

62. Hoeben A, Landuyt B, Highley MS, Wildiers H, Van Oosterom AT, De Bruijin EA. Vascular endothelial growth factor and angiogenesis. *Pharmacological Reviews.* 2004;56(4): 549-580.

63. Pecorino L. Growth factor signaling and oncogenes. *Molecular biology of cancer: mechanisms, targets and therapeutics.* 2012: 77-102.

64. Grellier M, Bordenave L, Amedee J. Cell-to-cell communication between osteogenic and endothelial lineages: implications for tissue engineering. *Trends in Biotechnology.* 2009;27(10): 562-71.

65. Bouletreau PJ, Warren SM, Spector JA, Peled ZM, Gerrets RP, Greenwald JA, Longaker MT. Hypoxia and VEGF up-regulate BMP-2 mRNA and protein expression in microvascular endothelial cells: implications for fracture healing. *Plastic and Reconstructive Surgery.* 2002;109(7): 2384-97.

66. Fiedler J, Brill C, BlumWF, Brenner RE. IGF-I and IGF-II stimulate directed cell migration of bone-marrow-derived human mesenchymal progenitor cells. *Biochemical and Biophysical Research Communications.* 2006;345(3): 1177-83.

67. Presta M, Dell EP, Mitola S, Moroni E, Ronca R, Rusnati M. Fibroblast growth factor/fibroblast growth factor receptor system in angiogenesis. *Cytokine Growth Factor Rev*iews. 2005;16(2): 159-78.

68. Deckers MML, van Bezooijen RL, van der Horst G, Hoogendam J, van der Bent C, Papapoulos SE, Löwik CW. Bone morphogenetic proteins stimulate angiogenesis

through osteoblast-derived vascular endothelial growth factor A. *Endocrinology*. 2002;143(4): 1545-53.

69. David L, Feige JJ, Bailly S. Emerging role of bone morphogenetic proteins in angiogenesis. *Cytokine Growth Factor Rev*iews. 2009;20(3): 203-12.

70. He C, Chen X. Transcription regulation of the VEGF gene by the BMP/Smad pathway in the angioblast of zebrafish embryos. *Biochemical and Biophysical Research Commun*ications. 2005;329(1): 324-30.

71. Resnicoff M, Ambrose D, Coppola D, Rubin R. Insulin-like growth factor-1 and its receptor mediate the autocrine proliferation of human ovarian carcinoma cell lines. *Laboratory Investigation*. 1993;69(6): 756-60.

72. Wang DS, Miura M, Demura H, Sato K. Anabolic effects of 1,25-dihydroxyvitamin D3 on osteoblasts are enhanced by vascular endothelial growth factor produced by osteoblasts and by growth factors produced by endothelial cells. *Endocrinology*. 1997;138(7): 2953-62.

73. Zhang G, Suggs LJ. Matrices and scaffolds for drug delivery in vascular tissue engineering. *Advanced Drug Delivery Rev*iews. 2007;59(4-5): 360-73.

74. Luginbuehl V, Meinel L, Merkle HP, Gander B. Localized delivery of growth factors for bone repair. *European Journal of Pharmaceutics and Biopharmaceutics*. 2004;58(2): 197-208

75. Wozney JM, Rosen V, Celeste AJ, Mitsock LM, Whitters MJ, Kriz RW, Hewick RM, Wang EA. Novel regulators of bone formation: molecular clones and activities. *Science*. 1988;242(4885): 1528-34.

76. Zara JN, Siu RK, Zhang X, Shen J, Ngo R, Lee M, et al. High doses of BMP2 induce structurally abnormal bone and inflammation in vivo. *Tissue Engineering Part A*. 2011;17(9-10): 1389-99.

77. Simons M, Bonow RO, Chronos NA, Cohen DJ, Giordano FJ, Hammond HK, et al. Clinical trials in coronary angiogenesis: issues, problems, consensus: an expert panel summary. *Circulation*. 2000;102(11): 73–86.

78. Lee SH, Shin H. Matrices and scaffolds for delivery of bioactive molecules in bone and cartilage tissue engineering. *Advanced Drug Delivery Rev*iews. 2007;59(4-5): 339-59.

79. Tang DW, Yu SH, Ho YC, Mi FL, Kuo PL, Sung HW. Heparinized chitosan/poly (γ-glutamic acid) nanoparticles for multi-functional delivery of fibroblast growth factor and heparin. *Biomaterials*. 2010;31(35): 9320-32.

80. Sokolsky-Papkov M, Agashi K, Olaye A, Shakesheff K, Domb AJ. Polymer carriers for drug delivery in tissue engineering. *Advanced Drug Delivery Reviews*. 2007;59(4-5): 187-206.

81. Nyberg E, Holmes C, Witham T, Grayson WL. Growth factor eluting technologies for bone tissue engineering. *Drug Delivery and Translational Research.* 2016;6(2): 184-194.

82. Lin CC, Metters AT. Hydrogels in controlled release formulations: network design and mathematical modeling. *Advanced Drug Delivery Reviews.* 2006;58(12-13): 1379-1408.

83. Blackwood KA, Bock N, Dargaville TR, Woodruff MA. Scaffolds for growth factor delivery as applied to bone tissue engineering. *International Journal of Polymer Science.* 2012;2012: 1-25.

84. Reinhart-King C. *Mechanical and chemical signaling in angiogenesis.* New York: Springer; 2012.

85. Peterson RT, Shaw SY, Peterson TA, Milan DJ, Zhong TP, Schreiber SL, MacRae CA, Fishman MC. Chemical suppression of a genetic mutation in a zebrafish model of aortic coarctation. *Nature Biotechnology*. 2004;22(5): 595-599.

86. Jin S, Chen Z, Xin B, Xi T, Meng N. An investigation on the comparison of wet spinning and electrospinning: Experimentation and simulation. *Fibers and Polymers*. 2017; 18(6): 1160-1170.

87. Salamian N, Irani S, Zandi M, Atyabi SM. Cell attachment studies on electrospun nanofibrous PLGA and freeze-dried porous PLGA. *Nano Bulletin.* 2013;2(1): 130103.

88.   Sukitpaneenit P, Chung TS. Molecular elucidation of morphology and mechanical properties of PVDF hollow fiber membranes from aspects of phase inversion, crystallization and rheology. *Journal of Membrane Science*. 2009;340(1-2): 192–205.

89.   Ahmad AL, Ramli WKW, Fernando WJN, Daud WRW. Effect of ethanol concentration in water coagulation bath on pore geometry of PVDF membrane for membrane gas absorption application in CO_2 removal. *Separation and Purification Technology*. 2012;88: 11-18.

90.   Ali N, Rahim NA, Ali A, Sani W, Nik W, Shiung LS. Effect of ethanol composition in the coagulation bath on membrabe performance. *Journal of Applied Sciences*. 2007;7(15): 2131-2136.

91.   Idris A, Man Z, Maulud AS, Khan MS. Effect of phase separation behaviour on morphology and performance of polycarbonate membranes. *Membranes*. 2017;7(2): 21.

92.   Yuan Y, Lee TR. Contact angle and wetting properties. *Surface Science Techniques*. 2013: 51.

93.   Yang Y, Qiu X, Sun Y, Wang Y, Wang J, Li Y, Liu C. Development of bioabsorbable polylactide membrane with controllable hydrophilicity for adjustment of cell behaviours. *Royal Society Open Science*. 2018;5(1): 170868.

94.   Burkersroda FV, Schedl L, Göpferich A. Why degradable polymers undergo surface erosion or bulk erosion. *Biomaterials*. 2002;23: 4221-4231.

95.   Verma NK, Khanna SK, Kapila B. *Comprehensive chemistry XI*. New Delhi: Laxmi Publications; 2010.

96.   Holy CE, Dang SM, Davies JE, Shoichet MS. In vitro degradation of a novel poly(lactide- co -glycolide) 75/25 foam. *Biomaterials*. 1999;20(13): 1177-1185.

97.   Zolnik BS, Burgess DJ. Effect of acidic pH on PLGA microsphere degradation and release. *Journal of Controlled Release*. 2007;122(3): 338-344.

98. Abay N, Gurel Pekozer G, Ramazanoglu M, Kose GT. Bone formation from porcine dental germ stem cells on surface modified polybutylene succinate scaffolds. *Stem Cells International.* 2016; 2016: 8792191.

99. Gharibi B, Hughes FJ. Effects of medium supplements on proliferation, differentiation potential, and in vitro expansion of mesenchymal stem cells. *Stem Cells Translational Medicine.* 2012;1(11): 771-782.

100. Cooper GM. *The cell: A molecular approach.* Sunderland (MA): Sinauer Associates; 2000.

101. Obi N, Toda H, Tabata Y. Human umbilical vein endothelial cells migration in matrigel by the concentration gradient of vascular endothelial growth factor. *Biotechnology and Biomaterials.* 2015;5: 4.

102. Nakamura A, Dohi Y, Akahane M, Ohgushi H, Nakajima H, Funaoka H, Takakura Y. Osteocalcin secretion as an early marker of in vitro osteogenic differentiation of rat mesenchymal stem cells. *Tissue Engineering Part C Methods.* 2009;15(2): 169-80.

APPENDIX A: ETHICAL APPROVAL FORM

YEDİTEPE ÜNİVERSİTESİ

T.C. YEDİTEPE ÜNİVERSİTESİ, DENEY HAYVANLARI ETİK KURULU (YÜDHEK)

ETİK KURUL KARARI

Toplantı Tarihi	Karar No	İlgi	Proje Yürütücüsü
11.03.2014	384	07.03.2014 Tarihli Yazı	Prof. Dr. Gamze TORUN KÖSE

"Damarlanmayı arttırıcı çift fazlı doku iskelesi ile kemik doku mühendisliği uygulaması" adlı bilimsel çalışma etik kurulumuzda görüşülmüş olup, çalışmanın etik kurallara uygun olduğuna oy birliğiyle karar verilmiştir.

Etik Onay Geçerlilik Süresi: 2 Yıl

GÖREVİ	ADI SOYADI	İMZA
Başkan	Prof. Dr. M. Ece GENÇ	
Başkan Yardımcısı	Prof. Dr. Erdem YEŞİLADA	
Raportör	Prof. Dr. Işıl Aksan KURNAZ	
Üye	Prof. Dr. Bayram YILMAZ	
Üye	Prof. Dr. Başar ATALAY	KATILMADI
Üye	Yard.Doç.Dr.Soner DOĞAN	
Üye	Yard. Doç. Dr. Ediz DENİZ	
Üye	Doç. Dr. C. Narter YEŞİLDAĞLAR	KATILMADI
Üye	Sumru KİRAZCI	